Exploring the implication of cholesterol in regulating pore-formation mechanism of *Vibrio cholerae* cytolysin, a β-barrel pore-forming toxin

A thesis submitted by

Reema Kathuria

In partial fulfilment of the requirements for the degree of

Doctor of Philosophy

Indian Institute of Science Education and Research (IISER)

Mohali

January 2021

Declaration

The work presented in this thesis has been carried out by me under the guidance of Dr. Kausik Chattopadhyay at Indian Institute of Science Education and Research Mohali. This work has not been submitted in part or in full for a degree, diploma or a fellowship to any other university or institute. Whenever contributions of others are involved, every effort has been made to indicate this clearly, with due acknowledgement of collaborative research and discussions. This thesis is a bonafide record of original work done by me and all sources listed within have been detailed in the bibliography.

Reema Kathuria

Place:

Date:

In my capacity as a supervisor of the candidate's PhD thesis work, I certify that the above statements by the candidate are true to the best of my knowledge.

Professor Kausik Chattopadhyay

Department of Biological Sciences

Indian Institute of Science Education and Research Mohali

Place:

Date:

Dedicated to my parents

Acknowledgements

My genuine gratitude goes firstly to my supervisor Dr. Kausik Chattopadhyay for his great support, consideration and guidance all the way through my project and also to his family whom I owe friendship and love. I would like to thank Dr. Chattopadhyay for giving me a chance to work in his lab, for his valuable timely advice, for being constructive and supportive with the preparation of manuscripts and establishing excellent and friendly environment to pursue challenging research. I owe my gratitude to my supervisor for sacrificing his time in teaching me all the experiments from scratch and for all the advice he gave me in overcoming various problems associated with my project. I am grateful to my supervisor for sharing all his knowledge, expertise and several stimulating discussions.

I owe sincere thanks to Dr. Arunika Mukhopadhaya for helping in different aspects of cell-based experiments, especially her tremendous help in Flow-cytometry based experiments. I am grateful to my Doctoral thesis committee members Dr. Mahak Sharma and Dr. Sudip Mandal for helpful advice and support during all the meetings and for providing valuable suggestions from time to time.

I sincerely thank Dr. Anand Kumar Rai for teaching me all the experiments during my initial days of PhD. I thank Dr. Barkha Khilwani for making me understand the mechanisms and basis of many experiments and techniques. I owe my gratitude to Krishna Prasad for being so generous in sharing his knowledge about various cell-based experiments. I would like to thank Dr. Samarjit Bhattacharya, Rohan Sharma and Anish Mondal for their much appreciated help in microscopy-based experiments for my project.

I express my heartfelt gratitude to all my lab members, comprising The Cytolysin Study Group, including Nidhi Kundu, Anish Mondal, Pratima Verma, Kusum Lata, Mahendra Singh, Shamaita Chatterjee and Riya Joseph for their constant help, friendship and support in the ups and downs of PhD, to all the time spent together during PhD experience and for providing a great environment in the lab. Thanks to all the labmates for all the chats and laughter and lunch time together. Huge thanks goes to all the staff in my department, who helped indirectly in accomplishment of this work. I would like to thank all the people from Dr.Arunika Mukhopadhaya's Lab who I had fruitful discussions with and who made this a good and enjoyable place to work at, including Aakansha Gulati, Deepinder Kaur, Vinica Dhar, Arpita Sharma, Shraddha Gandhi, Yogesh Saxena, Shashi Prakash Yadav,

I would extend my appreciation to past and present colleagues Dr. Karan Paul, Dr. Sanica Sakharwade, Dr. Shelly Garg, for their help and support.

I am grateful to IISER Mohali for providing financial support, for such great infrastructure and excellent research environment. I would like to thank Dr. P. Visakhi, Librarian and library facility of IISER Mohali for providing subscription to various journals. I am also

thankful to Deans, faculties and non-teaching staff of IISER Mohali for providing help and support whenever required.

At the end I want to thank my parents to be my life landmark, to comfort me in the difficulties, to tolerate my stress and madness moments. Thanks for all the beautiful moments that we had and hopefully will have. I feel thankful to my brother, my grand-parents and all other relatives that are so happy to see me. I really love knowing how much you support me. Last, but not the least I thank my Guruji and almighty for giving me the dedication and courage to complete my PhD.

Just to conclude…thanks you all, also the one I do not mention but present in my thoughts that have made a change (even smaller) in my life. I think I've grown a lot as a person. Thank you all!!!!!!

REEMA KATHURIA

List of Publications

i) **Kathuria R**, Mondal AK, Sharma R, Bhattacharyya S, Chattopadhyay K. Revisiting the role of cholesterol in regulating the pore-formation mechanism of Vibrio cholerae cytolysin, a membrane-damaging ß-barrel pore-forming toxin. Biochemical Journal. 2018 475(19): 3039-3055.

ii) **Kathuria R**, Chattopadhyay K. Vibrio cholerae cytolysin: Multiple facets of the membrane interaction mechanism of a β-barrel pore-forming toxin. IUBMB life. 2018 Apr; 70(4):260-6.

iii) Mondal AK, Sreekumar A, Kundu N, **Kathuria R**, Verma P, Gandhi S, Chattopadhyay K. Structural Basis and Functional Implications of the Membrane Pore-Formation Mechanisms of Bacterial Pore-Forming Toxins. InBiochemical and Biophysical Roles of Cell Surface Molecules 2018 (pp. 281-291). Springer, Singapore.

List of Figures

List of Tables

Abbreviations

BSA	Bovine serum albumin
CD	Circular dichroism
CDC	Cholesterol-dependent cytolysin
ClyA	Cytolysin A protein
DNA	Deoxyribonucleic Acid
DLS	Dynamic light scattering
EDTA	Ethylenediaminetetra-acetic acid
ELISA	Enzyme-linked immunosorbent assay
FITC	Fluorescein isothiocynate
FRET	Fluorescence resonance energy transfer
HEPES	N-2-Hydroxyethylpiperazine-N'-ethanesulphonic acid
HA/P	Haemagglutinin protease
HEK	Human embryonic kidney
HRP	Horseradish peroxidase
IPTG	Isopropyl-β-D-thiogalactosylpyranoside
Kb	Kilobase
kDa	Kilodaltons
LB	Luria broth
LUV	Large unilamellar vesicles
Ni-NTA	Nitrilotriacetic acid
OD	Optical density
OPD	Ortho-Phenylenediamine
PAGE	Polyacrylamide gel electrophoresis
PBS	Phosphate buffer saline

PBST	Phosphate buffer saline Tween-20
PC	Phosphatidylcholine
PCR	Polymerase chain reaction
PMSF	Phenylmethane-sulphonyl fluoride
PVDF	Polyvinylidene fluoride
SPR	Surface plasmon resonance
SDS-PAGE	Sodium dodecyl sulphate polyacrylamide gel electrophoresis
Tcp	Toxin co-regulated pilus
TEMED	N, N, N', N'-tetramethylethylene diamine
UV	Ultravoilet
VCC	*Vibrio cholerae* cytolysin

Content

CHAPTER 1

Introduction

Chapter 1

Introduction

1. Introduction and Literature Survey

1.1 Pore-forming toxins: disruptors of the cell membranes

The paramount requirement of a living cell is it's interaction with the external environment to carry movement of various essential molecules in and out of the cell, without which the life could not persist. Every cell is surrounded by a semi-permeable plasma membrane (1). This plasma membrane defines the contour of a living cell, separates the intracellular milieu from the extracellular environment, and regulates myriads of key biological processes (2). These biological membranes, composed of phospholipid bilayer, have proteins embedded in them that act to function as repositories of information for proper functioning of the cells and for controlling the signalling events within the cells (3,4). Many of these membrane proteins allow exchange of substances and information across the membrane lipid bilayer (5). Membrane lipid bilayer surface is decorated with carbohydrate molecules, which are linked via lipids and proteins, and they play significant roles in many processes that are critical for the functioning of the living cells (6). Cell membranes not only support and maintain the shapes of the cells, but also maintain integrity of the cells (7). As the plasma membranes are critical for the survival and proper functioning of the living cells, destruction of the cell membranes has evolved as one of the ancient forms of the cell-killing mechanisms in nature. Diverse life forms have evolved to produce a specific class of membrane-damaging proteins to achieve this pathophysiological functions, and they do so by producing a specific class of so-called pore-forming proteins (PFPs) or pore-forming toxins (PFTs) (8). These pore-forming protein toxins are produced by organisms from all kingdoms of life. They act by punching holes in the membrane lipid bilayer of the target cells, and they do so by forming

oligomeric transmembrane pores. PFPs/PFTs exhibit heterogeneity in terms of pore size, pore architecture, as well as in the mechanism of membrane pore formation (9). They perforate the target cell membranes, allowing free diffusion of ions, small molecules, and water across the plasma membranes. Most common outcome is the creation of osmotic imbalance in the cell that ultimately lead to killing of the cell (10).

PFTs have been shown to play important roles in promoting growth and dissemination of various pathogenic organisms (11). The most widely studied group of PFTs are those produced by the pathogenic bacteria. Wide range of bacterial pathogens employ PFTs as their major virulence factors (12). PFPs from the bacteria also constitute components of the type III and type IV secretion systems (13). Permeabilization of the target membranes involves multiple steps where PFTs assume specific structural states (14). PFTs display large diversity in terms of size, ranging from short peptides such as melittin from the honey-bee venom to the large oligomeric protein complexes as observed in the case of certain cholesterol-dependent cytolysins (CDCs) that are composed of 30-50 protomers (15). PFTs are not only confined to the bacterial systems. They are also produced by the eukaryotic organisms such as hydra, fungi, parasites, sea anemone, plants and human. PFPs/PFTs are not only contributing toward the pathogenicity of various organisms. They also play essential roles as the components of vertebrate immune system (16). PFPs and PFTs act as two-faced sword that play roles of virulence factors and toxins to attack the target cell, and also exhibit critical roles in the defence mechanisms of the vertebrate system (17). Based on their ability to form pores of defined stoichiometry in the cell membranes, PFPs/PFTs are being utilized in the development of new technologies for the purpose of DNA sequencing and drug delivery (18). Altogether, understanding the structure-function mechanisms of PFPs/PFTs are of enormous importance to elucidate some of the critical basic processes of biological systems starting from bacterial pathogenesis processes to vertebrate immune response generation.

Table. 1 PFTs are secreted by wide array of organisms across vast evolutionary distances

Kingdoms	Organism secreting the PFT	Pore-forming toxin	Target of PFT
Protists	Parasites: *Toxoplasma gondii*	PLP1	Parasitophorous vacuole
Fungi	Mushroom	Pleurotolysin	Eukaryotic cells
Plants	*Enterolobium contortisiliquum*	Enterolobin	Eukaryotic cells
Metazoans	Sea anemone: *Actinia equina*	Equinatoxin II	Eukaryotic cells
	Hydra: *Chlorohydra Viridissima*	Hydralysin	Eukaryotic cells
	Earthworm	Lysenin	Eukaryotic cells
Metazoans	Mammals: Human, mouse	Perforin Bax, Bak C9 proteins	Malignant or infected cells Mitochondria Bacterial and parasitic cells

Although large diversity is observed among the PFTs in terms of pore-size and intricate details of pore architecture, the journey of these toxins from the soluble monomeric secreted form to the membrane-inserted pore-forming states is similar for different PFTs. It involves specific steps for the generation of the trans-membrane pores (19). PFTs are usually secreted as water-soluble monomers, and then upon encountering the target membranes, these protein monomers either utilize specific receptors on the surface of host cells or associate non-

specifically to the membranes which can cause increase in the local concentration of the toxin monomers. When membrane-associated monomers come together, they tend to undergo oligomerization, whereas in case of some PFTs, oligomerization precedes membrane binding (20). Once the oligomeric assemblies are associated with the host cell membrane, pore-forming motifs tend to insert in the membrane lipid bilayer that permeate the membrane, generating the water-filled channel across the plasma membranes. This perturbs the membrane integrity and allows unregulated movement of ions, water and small molecules (15). Formation of such trans-membrane pores can lead to perturbation of the osmotic balance, ultimately causing lysis of the cell.

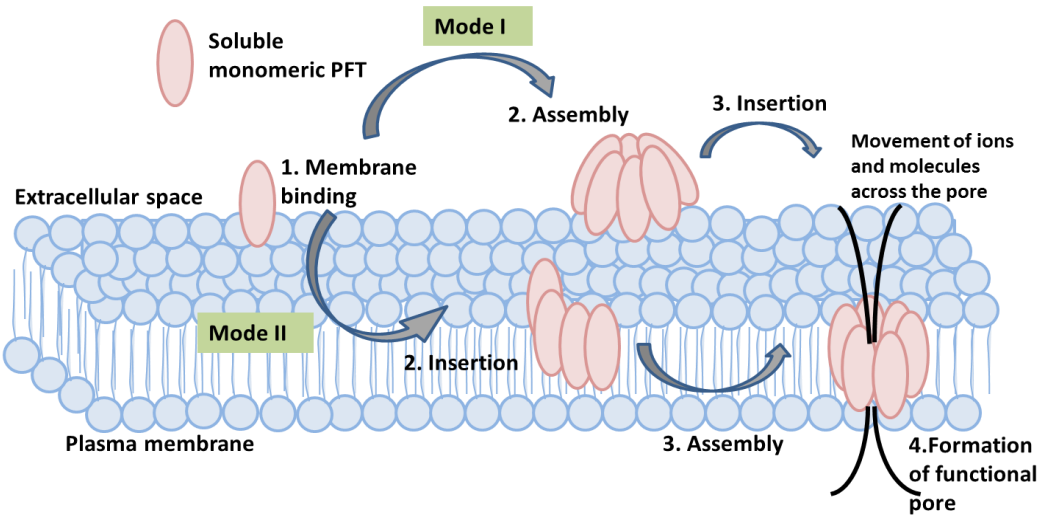

Fig. 1. Generalized mechanism of action of the PFTs. Schematic representation of pathways followed by the PFTs. PFTs initially interact with the cell surface receptors which could be proteins or lipids. Followingby binding, local concentration of the toxin on the membrane increases, leading to oligomerization of the bound monomers, generating a pre-pore. The pre-pore structure then gets converted to functional transmembrane pore by insertion of pre-stem loop that promote dissipation of ions and small molecules (Mode I). However, in case of α-PFTs, monomer insertion happens with oligomerization mechanism, generating active pores on the target membranes (Mode II).

1.1.1 Structural classification of PFTs

Structurally, PFTs can be classified into two broad categories, α-PFTs and β-PFTs, based on the secondary structural composition of their pore-forming region. When PFT spans the

target lipid bilayer using α-helices in order to generate pore, it is termed as α-PFT (21). In case of β-PFTs, β-sheets tend to permeabilize the target membrane to generate β-barrel pore that causes lysis of the target cell. In this case, β-sheets are contributed by monomeric subunits that together generate a barrel-like structure (22).

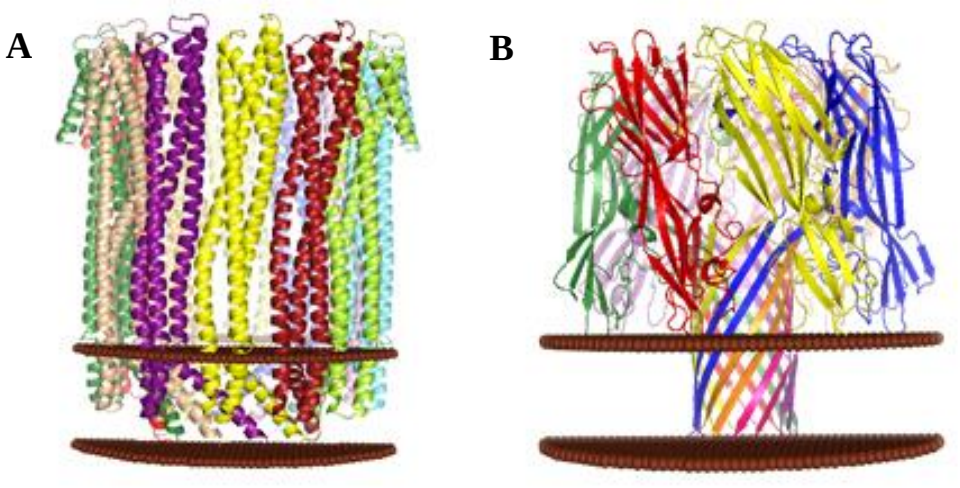

Fig. 2. Pore-architecture of α-PFT and β-PFT. Classification of PFTs is done majorly into two families based on the secondary structure of the transmembrane region: α-helical PFTs (A) and β-barrel PFTs (B).

Table.2 PFTs can be categorised as either α-PFTs and β-PFTs, based on secondary structure of membrane-permeating region

Bacteria secreting the PFT	**PFT**	**Pore stoichiometry**	**Class of PFT**
Escherichia coli	ClyA	13	α-PFT
Staphylococcus aureus	α-hemolysin	7	α-PFT
Bacillus cereus	Haemolysin BL	7-8	α-PFT
Actinia equina	Equinatoxin II	4	α-PFT
Staphylococcus aureus	Leukocidins	8	β-PFT

Clostridium perfringens	δ-toxin	7	β-PFT
Bacillus cereus	Non-haemolytic tripartite enterotoxin (Nhe)	-	α-PFT
Aeromonas hydrophila	Aerolysin	7	β-PFT
Clostridium perfringens	Perfringolysin O	>30	β-PFT
Bacillus anthracis	Protective antigen PA	7 or 8	β-PFT
Vibrio cholerae	VCC	7	β-PFT
Clostridium septicum	α-toxin	7	β-PFT
Escherichia coli	Colicin A	2	α-PFT
Eisenia fetida	Lysenin	3-6	β-PFT
Listeria monocytogenes	Listeriolysin O	>30	β-PFT
Stichodactyla helianthus	Sticholysin II	4	α-PFT
Staphylococcus intermedius	Intermedilysin	30-50	β-PFT
Actinia fragacea	Fragaceatoxin C	8-9	α-PFT
Clostridium perfringens	Necrotic enteritis toxin B (NetB)	7	β-PFT
Vibrio vulnificus	*V.vulnificus* hemolysin	7	β-PFT
Bacillus anthracis	Anthrolysin O	30-50	β-PFT
Laetiporus sulphureus	Hemolytic lectin	4-6	β-PFT
Streptococcus suis	Suilysin	30-50	β-PFT
Streptococcus mitis	Lectinolysin	30-50	β-PFT
Photorhabdus luminescens	Plu-MACPF	>30	β-PFT
Streptococcus pyogenes	Streptolysin O	30-50	β-PFT

1.1.2 α-PFTs

1.1.2.1 The colicin family

Colicins are characterized as PFTs, and are produced by *Escherichia coli*. They attack related species of the bacteria by formation of pores in the inner bacterial membrane (23). The primary requirement for functional pore-formation by colicins involves insertion of the hydrophobic hairpin helical structures into the bacterial inner membranes (24).

Three major domains have been identified in colicins that play important roles in receptor binding, transport and killing. As the name suggests, the binding and transport domains are used to associate with the target membrane and to transfer the toxic domain across the bacterial cells whereas the third domain is responsible for causing toxicity and killing the target cell by causing inhibition of protein or peptidoglycan synthesis by exhibiting nuclease or pore-forming activity (25). When colicin interacts with the host cell membrane, the amphipathic helices from its structure get inserted into the target membrane as they are driven away from hydrophobic helical hairpin. This causes generation of a distinct 'umbrella structure' (24). The formation of this 'umbrella model' has been proposed for Colicin A, though there have been no exact structure and stoichiometry known for these pores as these colicins do not generate stable oligomeric complexes which can provide structural insights upon analysis (26,27). This 'umbrella model' however, cannot alone support the formation of functional channel and it could be presumed that several other mechanisms could be playing important role. One of the possible mechanisms could be multimerization as a consequence of insertion of the hydrophobic hairpin structures (28). This has been observed in the case of Colicin A where dimers are formed, and in Colicin Ia where the trimers of dimers are observed. The complete structures of Colicins Ia, B and N have been determined and the structural features of pore-forming domains from Colicin A and E1 have been characterized

(29). The Cry toxins secreted by *Bacillus thuringiensis* possess colicin fold and play role as major insecticides (30). The presence of this colicin fold is also observed in translocation domain of Diptheria toxin in which the toxin's catalytic subunit is translocated across the endosomal membranes to inhibit protein synthesis in order to kill the cell (31). Moreover, the proteins of BAX and Bcl-2 family also have colicin-like fold (32).

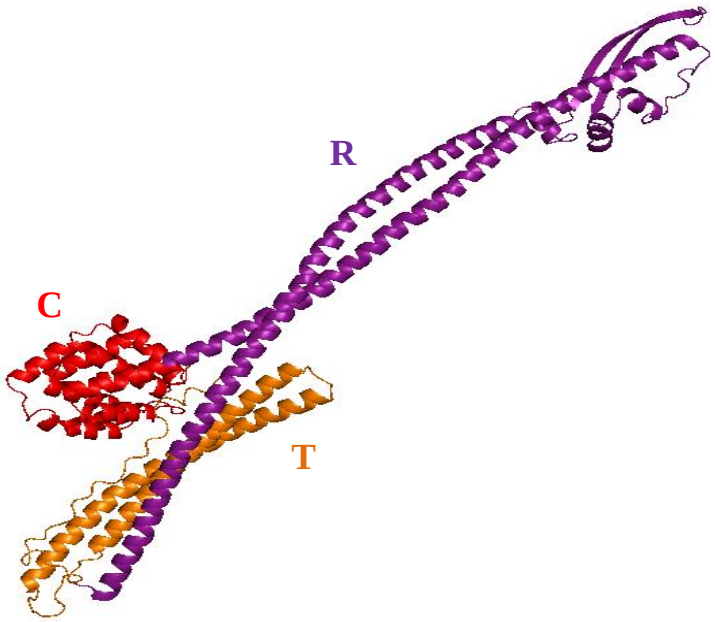

Fig. 3. Colicin Structure. Structural domains of Colicin Ia (PDB ID 1CII) represented in the crystal structure as R- the receptor-binding domain, T- Translocating domain and C- Channel-forming domain.

1.1.2.2 The ClyA family

The Cytolysin A (ClyA) family toxins have been studied in detail. Structures for both the soluble and the transmembrane forms have been determined (33). The Cytolysin A family of α-PFTs is comprised of several toxins that are secreted mainly by strains of *E. coli*, *Shigella flexneri* and *Salmonella enterica* (34). The B component of haemolysin BL enterotoxin (Hbl) and non-haemolytic tripartite enterotoxin secreted by *Bacillus cereus*also belong to ClyA family. ClyA monomer is comprised mainly of α-helices and also possesses some short

hydrophobic β-hairpins, called as β-tongue. When this ClyA monomeric units come in close proximity and bind the host cell membrane, the β-tongue structure moves away from the core structure of the protein and penetrates into the target cell membrane (34). Consequently, due to massive conformational change of the amino-terminal amphipathic α-helix, it comes in close proximity to the membrane. A lot of variations have been observed in the N-terminal amphipathic helix. The ClyA functional pore-formation involves formation of circular oligomeric assemblies which are similar to as observed in the actinoporin family. Here, α-helix containing barrel-like structure is formed which permeabilizes the membrane lipid bilayer and a ring-like structure is generated where amphipathic helices are bundled together (35).

However, another proposed mechanism of poreformation by ClyA family of toxins involves trapped soluble pre-pore oligomeric assemblies in the outer membrane vesicles (OMVs) of *E. coli* (36). These OMVs are of bacterial origin, and they lack cholesterol, and thus pore-formation cannot take place in the OMVs, as functional pore-formation requires presence of cholesterol in the target membranes.

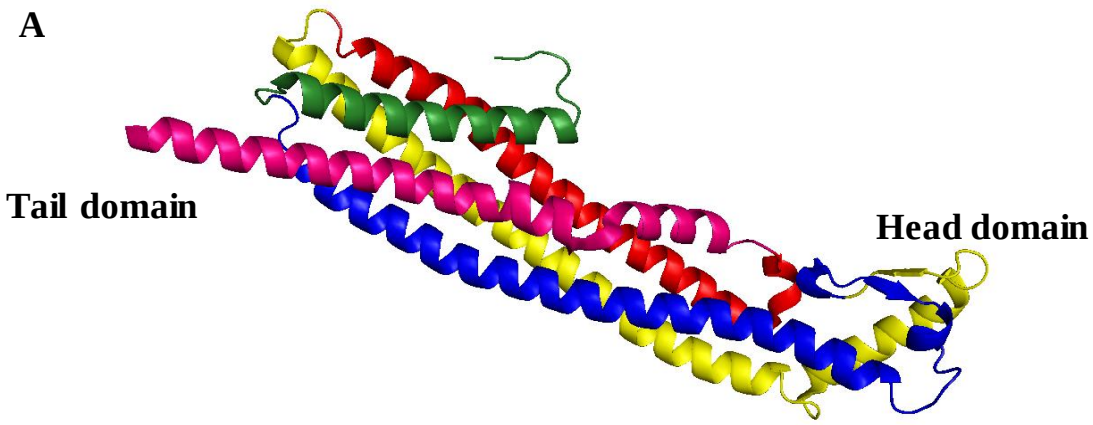

B

C

Fig. 4. ClyA structure. (A) Crystal structure of monomeric form of Cytolysin A (PDB ID 1QOY). Head domain is comprised of β-hairpin structure flanked by two short α-helical structures while four long α-helices and one small α-helix forms the tail domain. (B) The side-view of the transmembrane dodecameric pore structure of ClyA (PDB ID 2WCD) and (C) its Top view.

1.1.2.3 Cry toxin

Cry toxin is an insecticidal protein secreted by *Bacillus thuringiensis*. Cry toxin plays role as a biopesticide wherein it kills the insect by generating pores in the gut membrane upon ingestion (37). When the toxin is consumed by the insect, the protein toxin initially exists as protoxin, and upon reaching the midgut of insect, Cry toxin undergoes solubilisation followed by proteolytic removal of the carboxy terminal region due to high pH conditions of the midgut (38). The toxin then gets activated, interacts with cadherin-like receptor molecule and aminopeptidase N on the insect gut membrane, and forms pores ultimately leading to death of the insect (39).

Cry toxin is composedof three domains: N-terminal domain I harbouring 8 α-helical structures. It is predominantly involved in membrane-insertion and pore-formation event. Domain II is comprised of three anti-parallel β-sheets and two α-helical structures. Two

antiparallel β-sheets form domain III. The recognition of receptor and association to the target membrane is mediated by domain II and domain III (40).

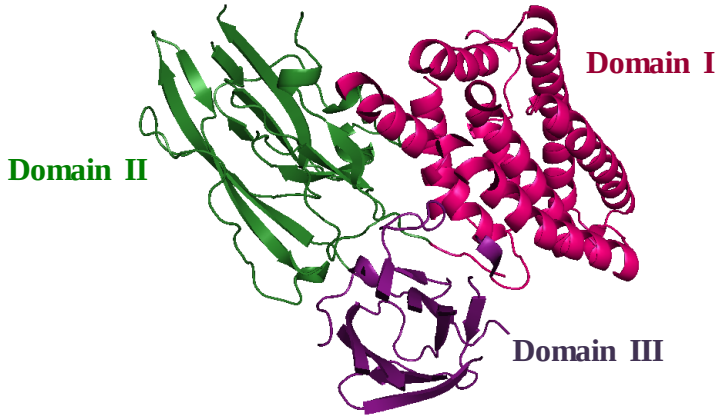

Fig. 5. Cry toxin structure. Crystal structure of Cry toxin (PDB ID 1CIY) indicating three structural domains. Domain I plays role in membrane-insertion and channel formation while domain II and domain III play role in binding and receptor recognition.

1.1.3 β-PFTs

1.1.3.1 The Aerolysin family

Aerolysin belongs to the β-PFT family of toxins produced by *Aeromonas hydrophila*. It promotes spread and dissemination of bacteria by disruption of the epithelial barrier functions, that lead to deep wound infections in some cases (41). Other bacterial toxins in the family, related in terms of structure and sequence, include α-toxin from *Clostridium septicum*, ε-toxin by *Clostridium perfringens*, hydralysins by cnidarian, enterolobin by Brazilian tree *Enterolobium contorliquum* and a haemolytic lectin by mushroom *Laetiporus sulphurous* (42).

Aerolysin is secreted as precursor toxin proaerolysin via type II secretion system into the extracellular medium. This proaerolysin associates with the host membrane as monomer or dimer via particular interaction with glycosyl phosphatidyl-inositol (GPI)-anchored proteins

(43). The specific interaction and binding of aerolysin is determined by the glycan core and N-linked sugars on proteinaceous receptors. In order to study the mode of action of aerolysin, certain aerolysin mutants that are trapped at different stages of pore-formation have been employed (44). The detailed study of aerolysin indicates that the assembled monomers generate heptameric pore structure which associates with the membrane, and a pocket is generated through which pre-stem loops can slide into the interior of the pre-pore. Upon transition of pre-pore to pore stage, there is formation of transmembrane β-barrel by refolding of the amphipathic β-hairpins, along with concerted swirling mechanism that causes flattening of the extracellular portion of the pore as the β-barrel forms and gets inserted into the membrane (45). In order to stabilize and restrain the potential movement of the amphipathic β-barrels in the membranes, the hydrophobic tips of the transmembrane β-hairpins adopt a rivet-like configuration (46).

The proaerolysin crystal structure demonstrates L-shaped elongated molecule having majorly two domains: a small globular domain and a huge lobular structure that are connected by a stretch of residues. The binding of the toxin to the carbohydrate moieties is mediated by globular domain I. The elongated domain is further divided into three domains where GPI-anchor-mediated binding is taking place by domain II, while the monomer-monomer contact in the heptameric structure is governed by domain III (47). The final domain IV is comprised of pro-peptide which needs to be proteolytically removed before the pore formation, as it has been observed that this pro-peptide prevents the oligomeric assembly formation in the case of Clostridial α-toxin (48).

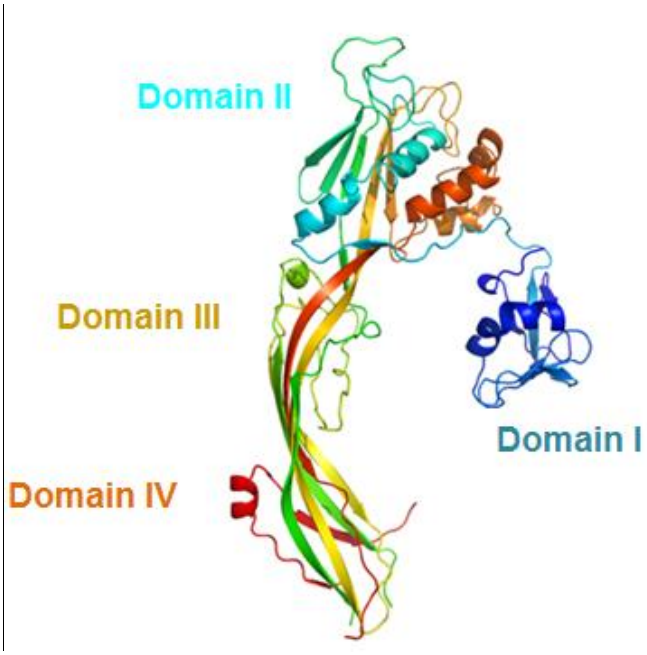

Fig. 6. Proaerolysin structure. Crystal structure of proaerolysin (PDB ID 1PRE) exhibited as L-shaped elongated molecule. Domain 1 represents N-terminal region. Domain 1 and 2 are essential for the membrane binding and interaction of the toxin. The oligomerization and insertion of toxin into lipid bilayer is carried by domain 3 and 4.

1.1.3.2 α-Haemolysins

The haemolysin family is comprised of α-hemolysin, Hlg, HlB, NetB and *Vibrio cholerae* cytolysin (VCC) for which structures have been determined for both water-soluble monomeric state and transmembrane pore states, making the haemolysin family as one of the best characterized bacterial pore-forming toxin families (49). One of the major roles played by haemolysins in *Staphylococcus aureus* pathogenesis is that they promote spread of infection by disruption of epithelial barrier functions. They also play roles in evasion of the host immune system (50). This family includes single component toxins such as α-haemolysin of *S. aureus* which generates heptameric pores, and also two component toxin Panton Valentine Leukocidin that assembles into octameric pores (51,52). Upon oligomerization of the toxins in this family, pre-pore ring-like structure is generated. Following this, the pre-stem motif detaches from the protein core, andrearranges into anti-

parallel β-hairpin to finally generate 14 or 16-stranded β-barrel structure with the neighbouring hairpins, and permeates the target membrane lipid bilayer (53,54).

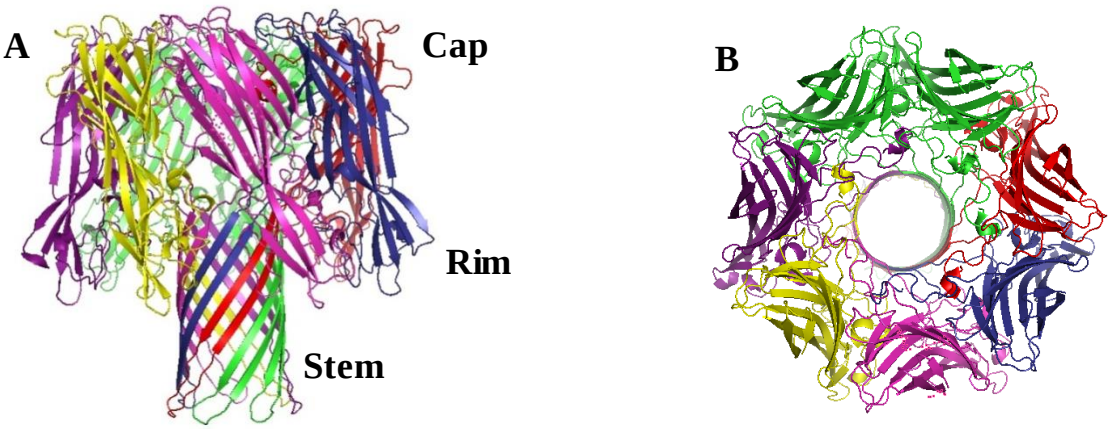

Fig. 7. α-hemolysin structure. Mushroom-shaped crystal structure of α-hemolysin toxin transmembrane oligomeric pore structure (PDB ID 7AHL) having three distinct domains, Cap domain, Rim domain and Stem domain, as represented in the side view (A). Top view is shown in (B). The transmembrane stem region is comprised of 14-strand β-barrel, contributed by seven protomers of the toxin molecule.

1.1.3.3 Cholesterol-dependent cytolysin family

Cholesterol-dependent cytolysins (CDCs) are a conserved family of toxins that have been identified in five different genera of Gram-positive bacteria such as Bacillus, Clostridium, Streptococcus, Listeria and Arcanobacterium (55). As the name suggests, the unique feature of CDCs is the absolute requirement of cholesterol in the target membrane for pore-forming activity. Intermedilysin is one exception in the CDC family that binds to specific receptor CD59 (56,57). The pores generated by CDCs are extremely large in size with pore diameter greater than 150 Å formed by 30-50 subunits (58).

Structural studies of CDCs show the presence of highly conserved undecapeptide, ECTGLAWEWWR, at the C-terminal end of the protein that appears to play role in the membrane binding (59). Several structural and mechanistic details are available for various CDCs that include Perfringolysin O from *Clostridium perfringens*, Lectinolysin produced

from *Streptococcus mitis*, Anthrolysin O produced by *Bacillus anthracis*, Streptolysin O by *Streptococcus pyogenes*, Intermedilysin produced by *Streptococcus intermedius*, Suilysin produced by *Streptococcus suis* (60).

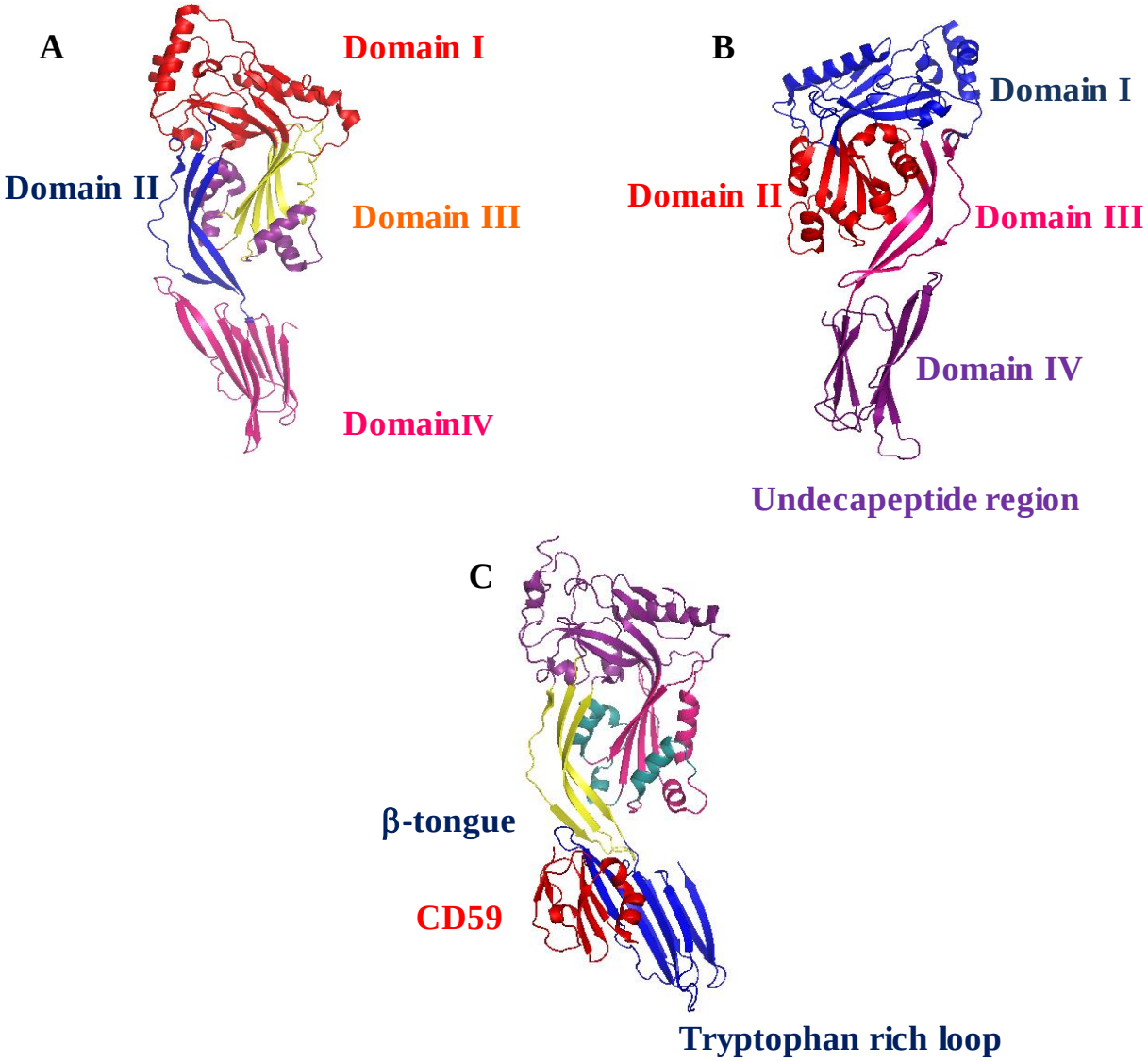

Fig. 8. Crystal structures of major CDCs. (A) Listeriolysin O (PDB ID 4CDB) secreted from *Listeria monocytogenes*, (B) Intermedilysin (PDB ID 1S3R) secreted from *Streptococcus intermedius*, and (C) Vaginolysin secreted from *Gardnerella vaginalis* (PDB ID 4BIK).

Perfringolysin O is one of the extensively studied CDCs that unravelled the mechanistic details of pore-formation by the CDCs. Generally, there is structural rearrangement in several PFTs that causes generation of the transmembrane pore whereas CDCs are the only class of toxins that are able to switch secondary structures (61). The soluble form of CDCs possess α-

helical bundle that gets transformed into β-hairpin during pore formation. In contrast to haemolysin and aerolysin, where single β-hairpin is contributed for the pore-formation, two amphipathic β-hairpins are contributed by each CDC molecule for the formation of the final β-barrel structure (62). In monomeric soluble form of CDC, there is presence of two pairs of short α-helices flanking a central β-sandwich structure. CDCs exhibit α-helix to β-strand transition upon oligomeric pore formation (63). During oligomerization event, a sequential mode is observed for monomer addition that can sometimes generate arc-like structures in the pre-pore state (64). Upon insertion process, β-sheets generate a large β-barrel pore, consisting of 80-200 β-strands by concerted arrangement of two β-hairpins, that get partially unfolded and then assembled into slightly curved β-sheet by interaction with the neighbouring β-sheets, and finally generate a locked β-barrel conformation (65,66). During the conversion of the pre-pore to pore state, there is elongation of CDCs on the surface of the target membrane, leading to orchestrated disruption of monomeric interface for which the energy is provided by the salt bridge formation between monomeric subunits (67). Finally the core domain of the toxin undergoes simple rotation which is similar to the swirling mechanism as observed for the aerolysin pore formation.

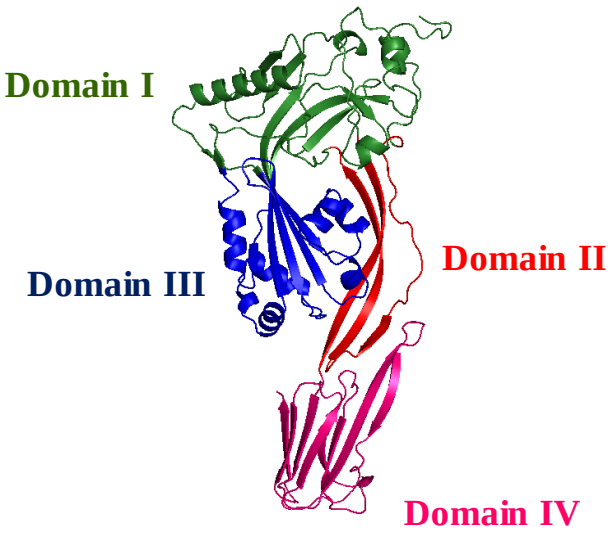

Fig. 9. Perfringolysin O Structure. Crystal structure of Perfringolysin O (PDB ID 1PFO) indicating four distinct structural domains

CDCs have been shown to exhibit multiple ways to assist in pathogenesis mechanism for different pathogens. Pneumolysin plays important role in tissue invasion by *Streptococcus pneumonia*e by developing inflammation and activation of the complement cascade, while Perfringolysin O contributes to the gangrene formation during *C. perfringens* infections (68).

1.2 Host cell membranes: primary interaction site for the PFTs

In order to execute permeabilization of the target membrane lipid bilayer and formation of functional pore, PFTs have to interact with the target cell membranes (69). For generation of the functional membrane pore, PFTs must establish efficient interaction with the membrane lipids as well as other membrane components that would allow subsequent pore-formation event (70). Several studies have been carried out to understand the mechanistic details of pore-formation by the diverse class of PFTs (71). Association with the target membranes is the critical first step in the pore-formation mechanism. Association and binding of these PFTs tend to increase the localized concentration of toxin on the host cell membrane surface (72). Binding of the PFTs to the target membranes increases the possibility of protomer-protomer interactions due to limited diffusion of the PFT upon binding to the membrane surface. Binding of the PFTs can occur via specific cell surface receptors, or certain non-specific interactions can also govern the association of these proteins to the membrane lipid bilayers (73). Toxin-membrane interaction can further drive the subsequent oligomerization event leading to generation of arc or ring-shaped structures that will insert into the membrane allowing functional pore-formation (19). The interaction of the PFTs with their cognate receptors may also trigger the signalling cascades within the cellular system, eliciting a variety of host responses (74). Hence, interaction and binding of the PFTs to the target membranes appear to be critical initial event to generate an array of downstream responses and events implicated in the pore-formation mechanism and associated pathophysiological responses in the target cells. It has been observed that the pore-forming activity is

significantly affected by the physicochemical properties of the target lipid membranes, such as (i) the membrane fluidity and hydrophobic mismatch, (ii) membrane line tension at domain boundary that determines lateral membrane organization, and (iii) liquid-ordered domain formation that defines the availability of the receptors (75). The lipid membranes are decorated by several molecular components suchas lipids, protein molecules and glycans that PFTs utilize in order to associate specifically with the target membranes (76). The huge diversification in the target membrane recognition and receptor identification by different families of PFTs can be attributed to the specific structural folds and domains that the PFTs possess (77). All these factors are the major determinants of the target cell specificity, which can collectively provide insights for the development of therapeutics for arresting the pore-formation mechanism.

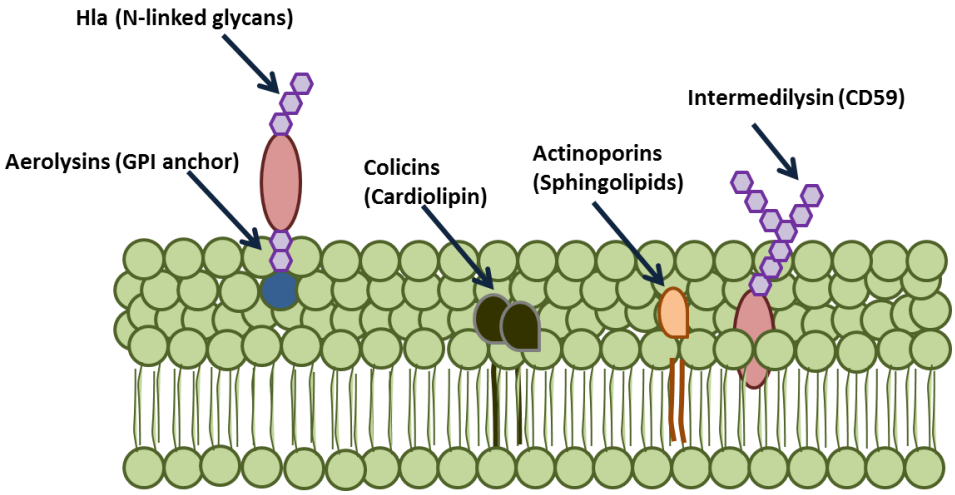

Fig. 10. Biomolecules which are binding targets for the PFTs. Membranes are endowed with multiple components that play crucial roles in the interaction mechanism of several PFTs.

1.2.1 Protein receptors as the determinants for interactions of the PFTs with the target cell membranes

In case of several PFTs, presence of specific receptor(s) determines the association and interaction of the toxin to the target cell membrane. As observed in case of *S. aureus* LukED,

the interaction with macrophages, T-cells and dendritic cells appears to be mediated by presence of cognate receptor C-C chemokine receptor type 5 (CCR5), also known as CD195, while the interaction of this bi-component LukED with neutrophils or monocytes is mediated by interaction with CXC-Chemokine receptor type-1 (CXCR1) and (CXCR2) (78,79). In case of *Staphylococcus aureus* α-hemolysin, the interaction with the epithelial cells is mediated by the protein receptor disintegrin, and metalloproteinase domain-containing protein-10 (ADAM-10), together with the phosphocholine headgroups of the membrane phospholipids (80,81). *Aggregatibacter actinomycetemcomitans* produces a toxin known as Leukotoxin (LtxA), which is a member of repeat-in toxin family that specifically binds to alpha-L/beta-2 integrin, and lymphocyte function-associated antigen-1 (LFA) (82).

The Panton-Valentine Leukocidin binds to neutrophils, monocytes and macrophages via interaction with C5a receptors on the target cell membrane (83). The presence of the chemokine receptors, particularly CXCR1, CXCR2 and CCR2 and complement receptors C5aR and C5L2 determine the binding propensity of the γ-bi-component haemolysins AB and CB towards neutrophils and monocytes, respectively (84). Glycophorin B, a sialoglycoprotein has been indicated as an important molecule associated with receptor for the *Vibrio cholerae cytolysin* (VCC), a β-PFT secreted by the cholera pathogen *V. cholerae* (85).

Cytotoxins secreted by *Bacillus thuringiensis* (Cry toxins) generate pores in the midgut epithelial cells of insects and is employed as biological insecticide. The binding of Cry toxins to the target cells is mediated by interaction with specific receptors that include aminopeptidase N (APN) and cadherin-like proteins that are sensed by domain II and III of the toxin (86).

Cholesterol-dependent cytolysins (CDCs) exhibit obligatory requirement of cholesterol in the target membranes for pore-formation mechanism. Apart from cholesterol, CDCs such as Intermedilysin (ILY) shows interaction with human CD59 receptor for its binding to the target membrane (87). Interaction of ILY with it's cognate receptor CD59 causes structural rearrangements in the PFT to trigger proper alignment of the toxin molecule for efficient interaction with the cholesterol-containing membranes, and proper protomer-protomer interaction for the generation of the pre-pore structure (88,89).

1.2.2 Carbohydrate moieties in binding of PFTs to the target membranes

Apart from the cell surface receptors, sugar moieties have also been reported to regulate the association of certain PFTs with the host membranes. The PFTs, which permeabilize the eukaryotic cell membranes, tend to bind via glycan moieties attached to either proteins or lipids, present as glycoproteins and glycolipids, respectively, on the cell surface. PFTs that target bacterial membranes exhibit very strong affinity toward covalently-attached sugars with the lipids in bacterial membranes (90). The well-studied example of this is the bacterial outer membrane lipopolysaccharides (LPS), which constitute high-affinity receptor for Colicin N, secreted by *E. coli* (91). Also, it has been observed that eukaryotic PFPs exhibit binding to carbohydrates in bacterial membranes. For example, bactericidal C-type lectins of human gut can generate hexameric pores in Gram positive bacteria by associating with peptidoglycan carbohydrates (92). Apart from binding with cholesterol, some of the CDCs have also been found to interact with the cell surface glycan moieties (93).

Aerolysin employs its N-terminal domain for binding to the host membranes where this domain exhibits interaction with N-linked sugars as well as to glycan-anchor of the GPI-linked proteins, causing interaction to be of very high affinity (94). In case of *C. perfringens*, ε-toxin binds to the target membrane via O-linked glycoprotein, Hepatitis A virus cellular

receptor 1 (HAVCR1), where the exact binding site is comprised of carbohydrate moiety of this glycoprotein (95).

The C-terminal β-prism domain of VCC has been shown to exhibit specific high affinity towards β1-galactosyl-terminated glycoconjugates that plays critical role in the pore-formation mechanism in the erythrocyte membrane (96). *Vibrio vulnificus* haemolysin employs N-acetyl-D-lactosamine and N-acetyl- D-galactosamine moeities for interaction with the host membrane (97).

1.2.3 Membrane lipid interactions defining binding of PFTs

Several studies have reported that many PFTs exhibit strong binding tendency for specific lipids in the target membrane. Lysenin, a PFT that is produced by earthworms, belonging to the aerolysin family, exhibits specific interaction towards sphingomyelin in the host membrane. As sphingomyelin forms a part of the lipid rafts, lysenin tends to translocate to the raft domains also (98,99). Pleurotolysin A also exhibits strong binding towards sphingomyelin-rich membranes (100). Pore-forming activity of colicins is promoted by the anionic lipids, such as cardiolipin, present in the target bacterial membranes (101). Hla from *S. aureus* belonging to the haemolysin family, and NetB toxin from *C. perfringens* show presence of phosphocholine binding pockets within their structures, suggesting binding propensity toward membrane lipids (102).

Equinatoxin II associates with the target membrane via two-step mechanism, which involves interactions of different regions of the molecule with sphingomyelin in the target cell membrane. Initially, the attachment of the toxin is promoted by exposed aromatic cluster having tryptophan 112 and 116. Subsequently, the N-terminal amphiphilic helix is translocated across the lipid bilayer (103).

1.2.4 Membrane cholesterol governing binding of PFTs

Cholesterol represents a key component of the cell membranes, constituting nearly 30% of the total membrane lipid composition (104). However, the distribution of cholesterol in membranes is not uniform. Structurally, cholesterol can adopt multiple conformations due to it's flexible isooctyl chain (105). Further, cholesterol exhibits asymmetric nature due to planar α-face and rough β-face (106). These structural features generate a huge possibility of interactions between cholesterol and many proteins.

Cholesterol have been shown to regulate channel formation and appear to be critical for pore-formation mechanism of various PFTs (107). The basis for regulation of pore-forming activity and critical requirement of cholesterol in the target membrane could be attributed to the way cholesterol interacts with the PFTs. Presence of cholesterol enhances formation of specialized membrane structures, such as generation of inverted hexagonal phases. Presence of cholesterol in the membrane of the host cell could assist the insertion of the trans-membrane motifs for functional pore-formation. This process can potentially be facilitated by filling of interstitial spaces surrounding the PFTs/PFPs by cholesterol to strongly promote protein-lipid interactions (108).

Studies enlightening the critical roles of cholesterol in the modes of action of certain PFTs have revealed the implication of specific sequence motif(s), termed as CRAC (Cholesterol recognition/interaction amino acid consensus sequence), in the interaction of these PFTs with cholesterol (109). The sequence determined for this CRAC motif is L/V-(X_{1-5})-Y-(X_{1-5})-R/K, comprising of leucine or valine, tyrosine residue and an arginine or lysine, having intervening 1-5 arbitrary residues (110). This CRAC motif was first studied in the peripheral benzodiazepine receptor that regulates cholesterol transport within the steroid-synthesizing

cells (111). NAP-22, a neuronal membrane protein also have this motif in it's structure (112). Further, pneumolysin also harbours this CRAC motif which could be responsible for it's interaction with multiple cholesterol molecules (113). The CARC motif represents sequence similar to that of CRAC but in opposite orientation, forming an "inverted CRAC" motif (114). Tilted peptides represent smaller helical fragments of protein that induce disturbances and distortions in the target membrane, hence playing significant role in the membrane fusion phenomenon by the viral glycoproteins (115).

Cholesterol has been reported to induce formation of 'liquid-ordered' state which possesses fluidity of intermediate level between gel and liquid-crystalline state (116). α-hemolysin from *S. aureus* tends to generate pores in the phosphatidylcholine-containing membranes above gel-to-liquid phase transition temperatures (117). In this case, if the target membrane is supplemented with 20% molar concentration of cholesterol, liquid-ordered state is formed and pore-formation mechanism can be easily executed (118).

Cholesterol is a 'cone-shaped' lipid molecule, similar to phosphatidylethanolamine and diacylglycerol (119). Substantial experimental studies suggest major role of cone-shaped lipids in the conversion of lipid bilayers to the inverted hexagonal phase (120). The presence of cone-shaped lipids in target membrane exhibits enhancement in cholesterol-dependent pore-formation mechanism of certain PFTs, such as Streptolysin O (121). The reason behind this could be the increase in free energy of cholesterol by the cone-shaped lipids due to their competition with cholesterol for the headgroup coverage, which can be borrowed from the neighbouring polar lipids, hence promoting the interaction of cholesterol with the toxin molecules.

A distinct class of toxins, identified in various species of Gram-positive bacteria, is termed as Cholesterol-dependent cytolysin (CDCs). Cholesterol plays a major role in the pore-

formation mechanism of the CDCs (122). As the name indicates, CDCs necessarily require cholesterol in the target membrane to display cytolytic activity. Interaction and association of Streptolysin O, a cholesterol-dependent cytolytic protein, to target bilayer is regulated by the presence of cholesterol molecules which is mediated by the C-terminus of the toxin (123). In case of Perfringolysin and Pneumolysin also, C-terminus has been shown to play major role (124,125). Listeriolysin O is another CDC produced by *Listeria monocytogenes* whose interaction with host membrane is determined by presence of membrane cholesterol (126). This toxin exhibits strong affinity towards membranes supplemented with cholesterol.

Vaginolysin (VLY) also belongs to the CDC family. It is produced by *Gardnerella vaginalis* which causes bacterial vaginosis pathogenesis (127). VLY absolutely requires presence of cholesterol to exert pore-formation mechanism, and human CD59 acts as assisting molecule for the activity (128). Cholesterol in the membrane can independently lead to formation of oligomeric species of the toxin. VLY appears to interact with the membranes via two alternative pathways: one is the interaction with the target membrane causing conformational changes leading to pore-formation, and, via interaction with CD59 that leads to generation of pre-pore complex on the host membrane (129).

Perfringolysin O, another CDC produced by *Clostridium perfringens*, exhibits critical requirement of cholesterol in the target cell membrane. Optimal level of cholesterol is needed in membrane for interaction of the toxin. Loops of domain IV in PFO mediates cholesterol-dependent interactions of the toxin (130). Presence of surface exposed cholesterol is necessary for binding of PFO to the membranes (131). Pneumolysin, a CDC secreted by *Streptococcus pneumonia*, exhibits slight deviation from the conventional mechanism of CDCs in that it not only requires just the presence of cholesterol in the lipid bilayer but also binds to carbohydrate moiety on the target membrane for generation of conductive channels in the target lipid bilayer.

1.3 Lipid rafts

1.3.1 Floating icebergs of cholesterol and sphingolipids in membranes

Over the last decades, extensive studies have demonstrated non-random distribution of lipids, giving rise to the concept of lipid microdomains in 1983 by Van Meer and Simons and by Klausner and Colleagues in 1980, that have been conceptualized as islands floating in the cellular membranes (132). The cell membranes enclosing the living cells do not appear to be a homogeneous passive entity; rather it is comprised of dynamic nanoscale assemblies generated by the coalescence of sterols, sphingolipids andproteins (133). The explanation for the formation of these lipid rafts could be attributed to self-associative properties of sphingolipids and cholesterol (134). The fatty acyl chains of phospholipids constituting the raft domains are more saturated than the surrounding membrane that render tight packing of the acyl chains of sphingolipids, forming less fluid liquid-ordered domain (135). Lipid rafts generate liquid-ordered domains in the plasma membrane which exhibit resistance to solubilisation using non-ionic detergent (136). Historical definitions suggest rafts to be of low density and to exhibit insolubility in 1% Triton-X 100. Rafts have been known as DRMs (Detergent resistance membranes), TIM (Triton-insoluble membranes) and TIFF (Triton-insoluble floating fraction). Presently a variety of detergents are employed for isolation of these raft domains, that include detergents such as CHAPS, NP-40, octyl-glucoside, Lubrol and Brij98 or the traditional Triton-X100 (137).

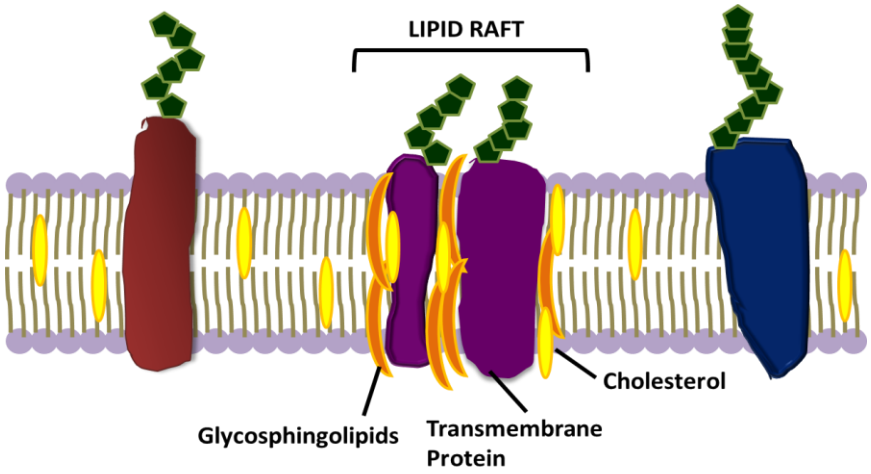

Fig. 11. Lipid rafts. Lipid raft domains represent highly-ordered, nano-structural, fluctuating assemblies of cholesterol and sphingolipids in the plasma membranes.

1.3.2 Lipid Rafts define functional platforms

Lipid rafts generate architectures in the membrane lipid bilayer in order to define membrane functionality. These rafts exhibit dynamic compartmentalization within membranes, generating platforms to exhibit functions involved in membrane trafficking and signalling (138). Number of proteins which are involved in cell signalling events are sequestered in lipid rafts. The proteins which are highly enriched in lipid rafts include Flotillins, Caveolins, GPI-linked proteins, EGF receptors, Src family kinases, hetero-trimeric G-proteins, MAP kinases, the phosphotyrosine phosphatase syp, Grb2, Shc, protein kinase C, platelet-derived growth factor receptors, p85 subunit of PI-3 kinase (139,140). These microdomains tend to get sorted in cells as observed in the polarized epithelial cells where there is enrichment of glycosphingolipids at the apical surface (141). The DRMs are also highly enriched in glycolipids, such as gangliosides and sulfatides (142,143). Lipids enriched in the raft domains tend to be localized mostly in the exofacial leaflet of the membrane, whereas ethanolamine glycerophospholipids are localized mainly in the cytofacial leaflet of the cell membrane. The

heterogeneity generated by these ordered-domains serves to coordinate and functionalize the activity of the cellular membranes.

1.3.3 Do lipid rafts really exist?

The existence of raft domains has suffered questions on being considered as a membrane artefact (144). The methods involving isolation of the DRMs using 'cold detergent extraction method' can induce artefacts. To overcome this, certain methods involving detergent-free preparations are now being employed for the isolation of the lipid rafts (145). One method employs sodium carbonate buffer of pH 11 for whole-cell lysis, as the basic pH assists in removing the peripheral membrane proteins (146,147). The lysate prepared is then sonicated and subjected to discontinuous sucrose gradient. Another method involves lysing the cells in isotonic sucrose buffer and preparing plasma membrane fractions by sedimentation of thepost-nuclear supernatant using the Percoll gradient, where the modifications of pH and ionic composition of gradient would help in the separation of the raft fractions (145). There is also a possibility of induction of heterogeneity in the membranes while observing them. Light-microscopy-based imaging suggests presence of homogeneously-distributed putative raft components on the cellular surface. In order to study and observe the native organization of lipid rafts, advances in spectroscopy-based experiments and in microscopic imaging is required. Several techniques that involve measuring the rate of lateral diffusion of GPI-linked proteins segregated in the raft domains suggest these domains to be of 200-300 nm in diameter. Single particle studies and FRET-based assays also suggest transient occurrence of lipid rafts (148).

1.3.4 Lipid rafts in governing the cellular signalling events

Lipid raft domains play significant roles in the cell signalling events. Rafts tend to bring together the molecular components in close proximity and serve to facilitate their interaction

in order to carry out a signalling event by generating ordered-phase platforms (149). In some cases, fusion of the lipid domains could be observed when the cell is stimulated with a receptor molecule. It has also been observed that the components required in a signalling cascade could be localized together in a raft domain and the signalling pathway is executed upon the recruitment of receptor or activator as the interaction of various components would be promoted (150).

1.3.5 Lipid rafts efficiently mediate host-pathogen interactions

Lipid rafts have also been shown to play critical roles in phagocytic mechanisms as well as in adhesion and interaction of pathogens. Several pathogens employ host-membrane lipid domain machinery for transduction of signalling events and as platforms for gaining access into the host cells during the invasion process (153). Pathogenic organisms like viruses, protozoa and bacteria utilize lipid rafts of host cells to gain entry and to employ strategies to disrupt raft-mediated signalling, assisting in replication of pathogens and to subvert immune responses generated by the host cells (154).

Table.3 Categorisation of different kinds of infections based on the type of pathogens responsible

Viral Infections	Bacterial Infections	Other pathogens
HIV-1	*Vibrio cholera*	Leishmania
Epstein-Barr Virus	*Campylobacter jejuni*	Trypanosoma
Measles Virus	*Clostridium tetani*	*Toxoplasma gondii*
Influenza Virus	*Salmonella, Shigella*	Plasmodium
Filoviridae (Ebolavirus, Marburg Virus)	*Mycobacteria tuberculosis and bovis*	Prions (Creutzfeldt-Jacob disease, Kuru)
Echovirus-1	*Escherichia coli*	
Respiratory syncytial cell virus	*Clostridium difficile*	

1.4 PFTs and the rafts

An array of cytolytic pore-forming toxins has been shown to associate with the membrane lipid raft-domains. PFO and many other CDCs associate with the host membrane lipid raft domains, enriched in cholesterol and sphingolipids (172). FRET-based studies demonstrate association of PFO to the DRMs (173). *Vibrio parahaemolyticus* produces thermostable direct haemolysin (TDH) as the major virulence factor. TDH exhibits strong tendency to associate with the DRMs. This association is majorly governed by sphingomyelin, although TDH could not directly interact with the sphingomyelin (174). The haemolysin of *Vibrio vulnificus* have also been observed to segregate into the lipid raft domains (175). Aerolysin also exhibits strong affinity to translocate to the lipid rafts by utilizing GPI-anchor protein as it's receptor (176).

The aegerolysin family of proteins is comprised of two mushroom proteins, Ostreolysin (Oly) and Pleurotolysin (Ply) that exhibit strong affinity towards sphingomyelin(SM)/cholesterol membranes. Oly from *Pleurotus ostreatus* (oyster mushroom) interacts with SM/cholesterol and DPPC/cholesterol membranes (177). The cytotoxicity of Oly is observed in SM membranes. PlyA generates complex with PlyB that exhibit affinity towards SM membranes, supplemented with cholesterol (178). Shiga toxin has also been observed to bind to the lipid rafts in order to generate oligomeric assemblies for functional pore-formation (179).

The Staphylococcal two-component PFT, comprising of LukF and LukS, causes lysis of human and rabbit PMNLs (Polymorphonuclear leukocytes). It interacts with the host cell membrane using protease-sensitive LukS receptors and GM1, that are enriched in the lipid rafts (180). Hence, the pore-formation takes place in the raft domains of the target membrane by formation of hetero-oligomeric pores. The vacuolating cytotoxin A from *H. pylori*, which

is also a PFT, tends to partition in the raft domains of the target cell membrane for exerting it's cytotoxic and other cellular effects (181).

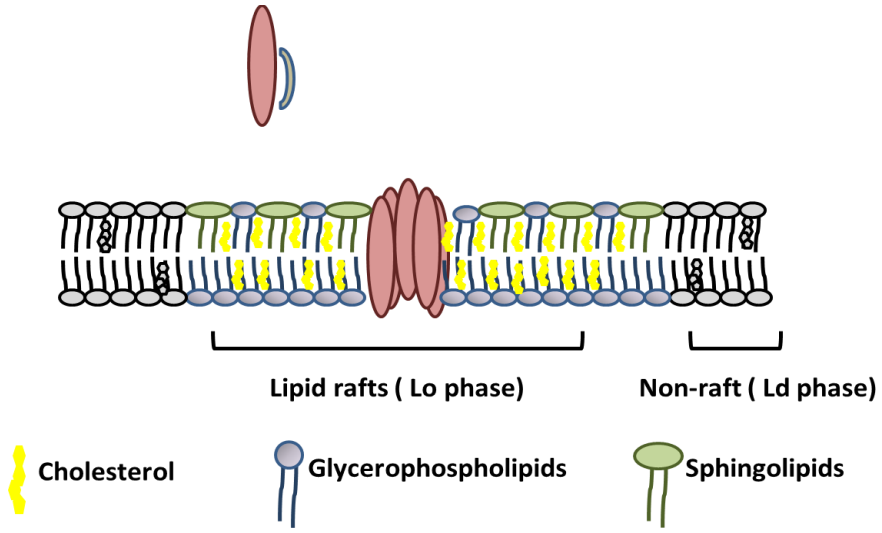

Fig. 12. PFTs sequesteration in lipid rafts. Several PFTs exhibit marked tendency to selectively sequester into cholesterol and sphingolipid-rich raft domains of host membrane.

1.5 *Vibrio cholerae*

1.5.1 Microbiology and Physiology

Vibrio cholerae is a member of the *Vibrionaceae* family, which is a motile, curved rod-shaped, Gram-negative flagellated bacterium (182). The enteropathogenic mechanism and virulence of *V. cholerae* is mediated by the expression of virulence factors, interactions with the mucosal membranes and secretion of cholera toxin (CT) (183). Out of the total 63 species of *Vibrio* genus, *V.cholerae* (O1 and O139), *V. vulnificus, V. parahaemolyticus, V. mimucus, V. hollisae, V. fluvialis, V. alginolyticus, V. damsela, V. metschnikovii, V. cincinnatiensis and V. furnissii* are known to be highly pathogenic for humans (184). The LPS in the outer membrane, majorly heat-stable O antigen forms the basis of classification of *V. cholerae*. Out of 206 identified O serotypes, O1 and O139 are known to cause the epidemic breakdown of cholera (185). Both of these serogroups have two major regions responsible for imparting the

virulence. These are CTX genetic region and VC-pathogenicity island (VPI) (186). When the non-virulent strains of *V.cholerae* acquires CTXϕ (lysogenic filamentous bacteriophage) and VPIϕ that possess the operon genes for cholera toxin and for toxin-coregulated pilus (TCP), they can get transformed into new toxigenic strains (187). The classification of O1 serogroup can be done into two biotypes: classical and El Tor, possessing distinct phenotypic markers. In 1961 in Indonesia, the seventh cholera pandemic occurred that was caused by the serogroup O1 biotype 'El Tor'.

Classical Cholera Toxin (CT) is the major exotoxin produced by enteropathogenic *V. cholerae*. *It* also produces accessory cholera toxin and zonula occludens toxin (188). The production of the former toxin is dependent on the CT gene and a 'virulence cassette' region bears the latter two toxins (189). *Vibrio cholerae* cytolysin (VCC) is another exotoxin which is independent of the expression of CT. Hence, in *V. cholerae* several genes form a cluster which exhibit coordinated interaction to efficiently carry out the enteropathogenic mechanism (190).

1.5.2 Major Virulence factors of *Vibrio cholerae*

1.5.2.1 Cholera Toxin

Cholera toxin is a heterodimeric protein that is encoded by the *CtxAB* gene, and it belongs to the AB5 type of toxins. It is comprised of pentameric B subunit and A subunit (191). The A-subunit (CTA) has an ADP-ribosyl transferase activity that causes increase in the levels of intracellular cyclic AMP. The pentameric B subunit (CTB) is involved in mediating the binding of the holotoxin to the ganglioside GM1, which is localized primarilyin the lipid rafts and constitutes the major receptor molecule on the eukaryotic cells (192).

Upon endocytosis, CT follows the retrograde transport pathway and reaches endoplasmic reticulum (ER), where the dissociation of CTA from CTB takes place (193). The CTA then causes ADP-ribosylation, resulting in Adenylate Cyclase (AC) to be in the GTP-bound form, thus increasing the AC activity that causes intracellular cAMP levels to go up (194). The enhanced levels of cAMP causes reduced uptake of sodium, simultaneously causing the decrease in the water influx, and the associated efflux of anion tends to cause the outflow of sodium. This results in the net loss of fluid from the enterocytes, exhibiting diarrhoeal disease in the affected individuals (195).

1.5.2.2 Toxin co-regulated Pilus (TCP)

In order to efficiently execute the pathogenesis mechanism, *V.cholerae* requires colonization of bacteria. This processis governed by the toxin co-regulated pilus (TCR). This colonization factor is critical for the adhesion and assembly of *V. cholerae* (196). Many other accessory factors have been identified that comprise the additional pilus structure, as fucose-binding and mannose-binding hemagglutinins (197).

1.5.2.3 Mannose-sensitive haemagglutinin (MSHA)

The mannose-sensitive hemagglutinin pilus appears to mediate the adhesion of *V. cholerae* to *Daphnia pulex*, a crustacean copepod. MSHA shows association of *V. cholerae* with the glycosylated S-IgA, though only limited roles of MSHA have been reported in the virulence mechanism (198,199).

1.5.2.4 RTX Toxin

The RTX (repeats-in-toxin) represents multifunctional toxin, the gene cassette for which is present in the virulent strains of *V. cholerae*, O1 El Tor and O139. The molecular weight of the toxin is nearly 485 kDa and the N- and C-terminal of this toxin harbours a series of

glycine-rich repeat regions. This RTX toxin causes the crosslinking of the actin filaments, contributing towards the cholera pathogenesis (200). It is encoded by *rtx A,B,C,D* and *E* gene cassette where the toxin is encoded by *rtxA* gene.The putative toxin activator acyltransferase is encoded by *rtxC, rtxB* and *rtxE* code for the putative secretory ATPases and the periplasmic linker of typeI secretion system is encoded by *rtxD* (201).

1.6 Vibrio cholerae cytolysin (VCC)

1.6.1 *Vibrio cholerae* cytolysin (VCC): a β-barrel PFT

Vibrio cholerae cytolysin (VCC) is a potent pore-forming toxin (PFT), which is secreted by *V. cholerae*. It is secreted in the form of an inactive precursor termed as Pro-VCC. Pro-VCC gets activated upon proteolytic removal of the Pro-domain, converting the toxin into the mature, active form (202). VCC acts as a major virulence factor in the strains of *V. cholerae* that lacks cholera toxin and exhibit very high epidemic potential (203). VCC is primarily secreted by O1 biotype El Tor, O139 and non-O1/non O139 *V.cholerae* isolates. Purified form of VCC has been shown to cause fluid accumulation in the ligated rabbit ileal loops that defines it's role in potentiating the enteropathogenic activity of the cholera pathogen (204). VCC generates water-filled channels in the planar lipid bilayer that is commonly believed to attribute to the enterotoxicity (205). VCC belongs to the family of β-PFTs and exhibits cytolytic as well as cytotoxic activity by generating transmembrane 14-stranded β-barrel pores in the host membrane, leading to colloid-osmotic lysis of the cells (206). VCC evokes damage at the cellular and tissue level by induction of autophagy, apoptosis, necrosis, cellular vacuolization and cell lysis (207,208). VCC has been shown to cause hemolysis of erythrocytes. It exhibits cytotoxic activity in cultured cells and induces lethality in mice. *Caenorhabditis elegans* has also been employed as a host model system where the lethality evoked by VCC, governed by LuxO-regulated genes in the quorum sensing pathway, has

been studied (209). VCC inflicts delay in the developmental stages and induces vacuolation of intestines in *C. elegans*.

VCC is synthesized in *V. cholerae* as ~82 kDa Pre-pro-VCC molecule, comprised of a signal peptide, a pro-region and a mature region. This molecule then undergoes cleavage of 25-residue long N-terminal signal sequence to allow for the proper transport of VCC across the bacterial membrane (210,211). The secreted form of the toxin, termed as Pro-VCC, of ~79 kDa have to further undergo the proteolytic removal of the N-terminal Pro-domain by endogenous or exogenous proteases to generate mature, functionally active form of the toxin (212). The secreted monomeric form of VCC then follows the β-PFT mode of action to generate oligomeric assemblies for the functional pore-formation, disrupting the integrity of target membrane lipid bilayer (213). The binding of VCC to the target cell membranes happens in a temperature-independent manner. However, the oligomeric pore-formationgets arrested at low temperatures below 15 ^{o}C. VCC, like any other bacterial PFT exhibits dimorphic nature, as it is secreted as inactive, water-soluble monomers and gets converted into the membrane-inserted oligomeric form during the pore-formation event (214). In monomeric form, the pore-forming pre-stem-motifis remain folded against the core cytolysin domain to prevent energetically expensive exposure of the hydrophobic regions to the aqueous environment. The pore-forming motif then undergoes structural rearrangements to generate the transmembrane β-barrel stem during the oligomeric pore-formation in the membrane (215,216). It has been estimated that even less than 10,000 molecules of VCC can be lethal towards the cultured intestinal cells (207).

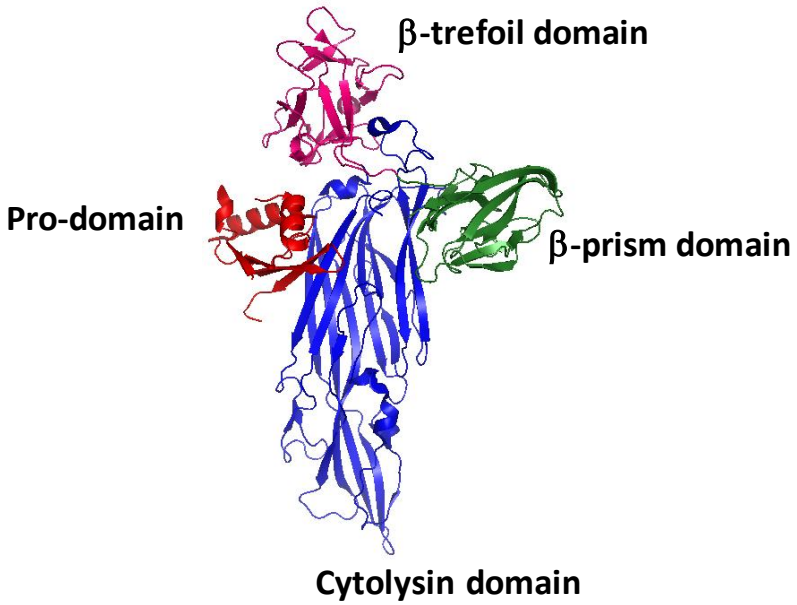

Fig. 13. Crystal structure of VCC. Monomeric form of VCC (PDB ID 1XEZ) consists of clover-leaf structure harbouring four distinct structural domains: N-terminal Pro-domain, Central cytolysin domain and the two lectin-like domains, β-trefoil and β-prism domains.

1.6.2 Mode of action of VCC

Being a prototype member in the bacterial β-barrel PFT family, VCC pore-formation involves the following distinct steps (206):

i) Interaction and binding of the water-soluble monomeric form of the toxin with the target cell membranes, mediated by an array of receptor-like entities on the target membrane surface (217).

ii) Formation of the metastable transient pre-pore oligomeric species by self-assembly of the membrane-bound monomeric units, governed by the protomer-protomer and lipid-protein interactions (218). β-prism domain undergoes the structural re-alignment relative to the cytolysin domain during oligomerization (219,220).

iii) This is followed by the insertion of the pre-stem motif from each monomer involved in the pore-formation event, generating the functional heptameric, 14-

stranded β-barrel pores of diameter ~1.2 nm. These pores modify the permeability barrier function of the plasma membranes, causing colloid-osmotic lysis of the mammalian erythrocytes and exhibiting toxicity as well as apoptosis of the epithelial cells (221,222).

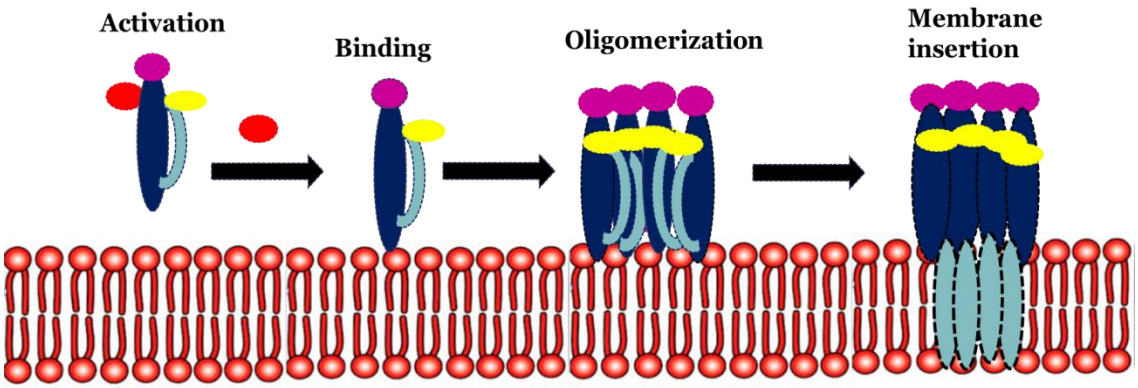

Fig. 14. Mechanism of VCC pore-formation. VCC is secreted as water-soluble monomer which then undergoes the proteolytic removal of N-terminal Pro-domain (indicated in red). Mature form of the toxin then binds to the target membrane, followed by oligomerization event, where seven monomers generate the heptameric assembly. Finally the insertion of pore-forming stem loop leads to the formation of the transmembrane β-barrel pore.

1.6.3 Structural features of VCC

The high-resolution structures for both the monomeric and the transmembrane oligomeric form of VCC have been described. These structures provide insights for the changes undergone in the protein structure, thus providing details of the structural and conformational rearrangements during the transition. The Pro-form of VCC exhibits clover-leaf-like structure comprising of four distinct domains (212). The N-terminal pro-domain allows efficient secretion of VCC through the bacterial membrane periplasm to the extracellular medium. This Pro-domain renders the toxin inactive and in doing so it exerts intra-molecular chaperone-like activity, assisting in the proper folding of the toxin (211). This Pro-domain exhibits sequence-homology to the Hsp90 family of heat-shock proteins. The pro-domain is connected to the cytolysin domain that harbours proteolytic cleavage sites where the site of

cleavage is determined by the specificity of proteases (210). The Pro-domain can be cleaved by exogenous, endogenous or extracellular proteases.This domain traps the toxin as a monomer, to prevent oligomerization event by masking the protomer-protomer interaction regions, and also imparts stability to the toxin. The subsequent ~250 residue cytolysin domain is structurally similar to the other members of the β-PFT family. It shows ~16.5% similarity to the *Staphylococcus aureus* α-haemolysin and ~12.9% similarity to the Staphylococcal LukF toxin. There is presence of a cluster of conserved amino acid residues within the hydrophobic core of protein. This cytolysin domain forms the central domain of VCC, hence determining the structure and function of this PFT. It defines the oligomeric assembly formation and membrane permeabilization ability of VCC. VCC also harbours two additional C-terminal lectin-like domains that may help in the interaction with the cell-surface glycan receptors. β-trefoil domain pertains to the carbohydrate-binding domain B of plant toxin ricin, while the β-prism domain shows relatedness to the sugar-interacting domain of the plant lectin jacalin with β-prism fold (223). β-prism-fold have been observed in many plant lectins such as *Griffithsia coralloides* Griffithsin, *Artocarpus integrifolia* artocarpin and *Maclura pomifera* agglutinin (224). Ricin-like lectin domains are associated with the binding to the cell-surface carbohydrate moieties, and are commonly found in A-B type plant toxins. These domains exhibit pseudo 3-fold symmetry with three QxW (glutamate x tryptophan) ligand-interacting sites that probably arose from the ancestral gene triplication (225). It is important to note that the exact physiological implication of the β-trefoil domain of VCC still remains unknown. β-prism domain forms an autonomously folding unit and can be attributed to the interaction of the toxin to the β1-galactosyl-terminated cell-surface glycoconjugates. β-prism domain exhibits preferential binding of ~100 nM affinity towards the complex N-glycans having a heptasaccharide $GlcNAc_4Man_3$ core (NGA-2) (226). This domain assists in generation of the heptameric β-barrel pores by contributing towards the entropy of

oligomerization (227). However, the removal of β-prism domain doesn't bring about any significant change in the toxin molecule, whereas if present, it enhances the lytic activity of VCC by ~1000-folds, indicating the improved activity being the result of efficient communication of different domains in a multi-domain protein. This β-prism domain is however absent in cytolysins from *Aeromonas hydrophila*, *Aeromonas salmonicida* and *Vibrio vulnificus* (97). Apart from the specific defined roles, these domains also play roles in determining the global properties of VCC.

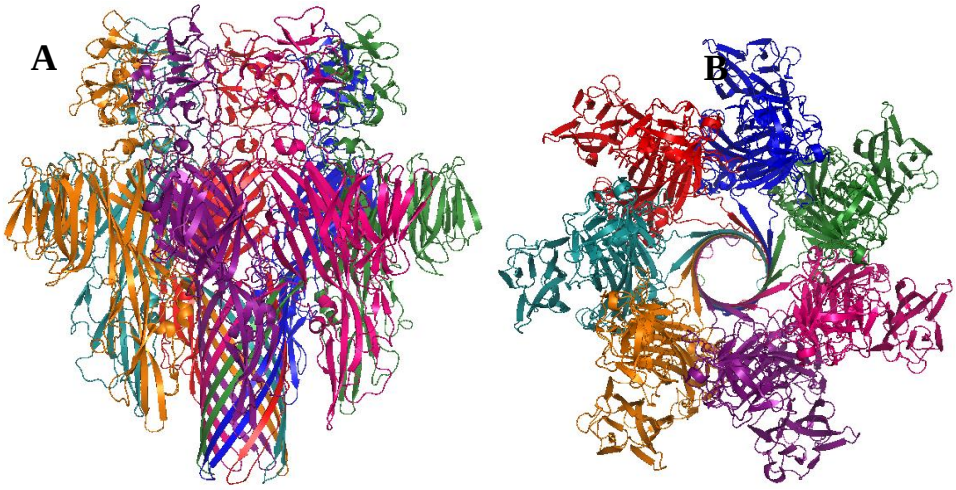

Fig. 15. VCC transmembrane oligomeric structure. The heptameric pore structure generated by the seven protomers of VCC (PDB ID 3O44) in the target membrane lipid bilayer, causing permeabilization of the host cell membranes. (A) represents side-view of the VCC oligomeric pore and (B) represents the top-view of the transmembrane oligomeric structure.

1.6.4 VCC and its interaction with the target membrane components

The target membrane forms the primary interaction site to provide a platform for the pore-forming activity of several PFTs, hence favouring structural rearrangements for the generation of the functional pores (228). The association and binding of PFTs with the target membrane lipid bilayer significantly enhances the local concentration of the PFTs on the cellular surface by confining the interaction in the two-dimensional milieu, which strongly favours the pore-formation mechanism (229).

The interaction and association of VCC is governed by the concerted interplay of diverse interactions that leads to the association and pore-formation event on the target membrane (230). The multiple interactions of the toxin with various cellular components greatly enhance the efficacy of pore-forming activity. Hence the pore-formation event is much more favoured in case of biomembranes, as compared to the liposome membranes. However, VCC can still generate heptameric pores on the lipid bilayer membranes of the liposomes, indicating non-requirement of any specific proteinaceous receptor molecule on the target membrane for the pore-formation by VCC (231).

1.6.4.1 Interaction of VCC with the lipid components of the target membrane

The pore-forming activity of VCC is affected greatly by the lipid composition of the host membrane. VCC has been shown to generate functional pores in the artificial lipid membrane system, devoid of any proteinaceous or sugar moiety, suggesting that the lipid-only platform is sufficient to allowexecution of thepore-formation process (232). The pore-formation mechanism of VCC is more efficient in case of liposomes constituted from asolectin, which is comprised of mixture of phospholipids, as compared to phosphatidylcholine liposomes (232). Further, presence ofsphingolipids or ceramides in the liposomesenhances pore-forming efficacy of VCC (233). The cone-shaped structure of the sphingolipids tend to enhance the exposure of the membrane cholesterol, hence effectively mediating VCC-sterol interaction (121). Upon careful observation of the VCC monomeric structure, it has been demonstrated that the three distinct loop structures at the bottom of cytolysin domain in the membrane proximal region of VCC would make intimate interactions with the target membrane lipid head-groups (217). This interaction forms an essential requirement for the action of VCC, as the mutation in these loop regions tend to abrogate pore-forming activity of VCC, resulting into abortive membrane-bound oligomeric assemblies.

1.6.4.2 Amphipathicity-driven association of VCC with the target lipid bilayer

Several reports have demonstrated selective partitioning of VCC into the amphipathic phases. VCC has been observed to selectively partitionto the detergent-rich phase formed by the detergent TritonX-114 with water (234). The compact 3-D structure of the water-soluble VCC monomer does not exhibit any surface-exposed hydrophobicity, which is otherwise observed in the membrane proteins. Still, VCC exhibits tendency to non-specifically partition into the amphipathic membrane lipid bilayer, which can be attributed to the intrinsic amphipathicity displayed by VCC monomers, though the exact reason for this behaviour is not yet known (234).

1.6.4.3 Interaction of VCC with the cell-surface carbohydrates

The detailed analysis of the monomeric structure of VCC indicates that it harbours two lectin-like domains, a β-trefoil domain followed by a β-prism domain. Deletion, or introduction of mutations in the β-prism domain, inhibit the binding with the cell surface and block pore-formation mechanism of VCC (96). VCC exhibits very high binding efficacy towards the heptasaccharide core of complex N-glycans (226). VCC interacts with the target cells using β1-galactosyl moiety of complex glyco-conjugates present on the cell surface (235). Hence, these glycan-mediated interactions act to potentiate the binding of the toxin to the host membranes.

1.6.4.4 Interaction of VCC with other probable cellular receptors

The presence of several other accessory receptor-like entities has been indicated that may assist in the interaction of VCC to the biomembranes. A sialoglycoprotein, Glycophorin B has been shown to be a possible receptor-like molecule for the activity of VCC, since Glycophorin B-lacking human erythrocytes display significantly reduced sensitivity towards

the pore-forming activity of VCC (85). Furthermore, upon pre-incubation of human erythrocytes with the monoclonal antibody against Glycophorin B, the binding and pore-formation by VCC tends to be completely abrogated. VCC has also been observed to bind to the TLR2/TLR6 complex in order to evoke the cellular responses in the innate immune cells (236). Hence several interactions come into play for the efficient binding and pore-formation process of VCC.

1.6.4.5 Interaction of VCC with membrane cholesterol

Similar to the obligatory requirement of cholesterol in the target membranes for pore-formation exhibited by the CDCs, cholesterol forms the essential component in the host membrane for the permeabilization ability of VCC (233). It has been demonstrated that only in the presence of cholesterol in the liposomes, execution of the pore-formation mechanism by VCC takes place (237). Furthermore, VCC displays direct interaction with cholesterol in a stereo-selective fashion. An enantiomeric form of cholesterol known as ent-cholesterol does not allow pore-formation, though this ent-cholesterol might be providing the similar fluid consistency to the membranes (238). There appears to be a fine recognition of the specific structural features of cholesterol, as the β-hydroxyl group in A-ring at C-3 position and the presence of C-C double bond between C-5 and C-6 in the B-ring of cholesterol appear to be critical for its recognition by VCC (239). Moreover, formation of VCC oligomeric species on the microcrystals of cholesterol in the aqueous suspension indicates direct interaction of the toxin with cholesterol (240).

It has been observed that introduction of a single point mutation in VCC critically affects cholesterol-dependent membrane-interaction mechanism of VCC with the cholesterol-containing artificial membranes (241). VCC exhibits similar functional pore-formation process as CDCs, in terms of the critical requirement of cholesterol in the target membranes.

However, the intricate details of the pore-formation mechanism, pore size, and architecture of VCC excludes it from the CDC family of toxins.

Earlier experimental data have suggested that the presence of cholesterol in the target membranes is crucial for the pore-formation mechanism of VCC. However, the exact mechanism by which cholesterol governs the mode of action of VCC is still not known. The details of how particular steps in the pore-forming activity of VCC are being regulated by cholesterol have not been explored yet. Furthermore, the critical requirement and implications of cholesterol in VCC pore-formation mechanism against the biomembranes have still not been elucidated.

1.7 Specific Objective of the study

Present thesis work explores the critical role(s) of cholesterol in the target membranes in regulating the pore-forming functionality of VCC. Our specific objectives are:

i) To investigate the implications of membrane cholesterol in the distinct steps of the membrane pore-formation mechanism of VCC.

ii) To examine the role of cholesterol-rich microdomains in the biomembranes for the mode of action of VCC.

CHAPTER 2

Material and Methods

Chapter 2

Material and Methods

2.1 Protein purification

The nucleotide sequence encoding Pro-VCC was introduced into the pET-14b bacterial expression vector. The recombinant plasmid harbouring Pro-VCC gene was transformed and expressed in *Escherichia coli* Origami cells. *E. coli* Origami cells transformed with recombinant plasmid were grown in LB broth containing ampicillin (50 μg/ml) at 37 $^{\circ}$C to mid-log phase (A_{600}= 0.5). Induction of protein expression was done in the presence of 1 mM IPTG (BR Biochem) by incubation at 30 ^{o}C for 3 hours. Cells were harvested and resuspended in Phosphate buffer saline (PBS) and the bacterial protease inhibitor cocktail (Sigma) was added. Cells were then lysed using ultrasonic waves by performing sonication for 15 minutes at amplitude 20, keeping 30 second pulse on and 10 second pulse off. After centrifugation at 12,000 rpm for 30 minutes, the supernatant having soluble protein was taken and equilibrated with 20 mM imidazole in PBS. Cell lysate was passed through the Ni-NTA column and then with 20 mM imidazole in PBS, washing was done to remove loosely bound protein molecules from the column. The desired protein from column was eluted by 300 mM imidazole. Protein fractions were collected and the presence of protein in eluted sample was checked by Bradford's reagent (Sigma). Eluted protein was diluted four times with 10 mM Tris-HCl and 1 mM EDTA buffer (pH 8.0), which was then loaded onto Q Sepharose anion-exchange column. Bound protein was eluted using 500 mM sodium chloride in 10 mM Tris-HCl buffer (pH 8.0). The eluted protein fractions were analysed by SDS-PAGE and Coomassie staining. The concentration of the eluted protein was measured

spectrophotometrically using the calculated extinction coefficient according to the amino acid composition.

2.1.1 Maturation of purified Pro-VCC

The Pro-domain was cleaved by the trypsinization of Pro-VCC with 1:2000 ratio of VCC: trypsin at 37 $^{\circ}$C for 5 minutes, followed by the addition of 1 mM phenyl methyl sulphonyl fluoride (PMSF) to cease the trypsinization reaction. The protein was then passed through Q-sepharose column to obtain the mature form of the toxin, free from trypsin and PMSF. SDS-PAGE and coomassie staining was done to assess purification of the toxin. Protein concentration was determined by measuring the absorbance at 280 nm, utilizing the extinction coefficient value of 1.4 for Pro-VCC and 1.6 for mature form of the toxin corresponding to the protein concentration of 1 mg/ml.

2.1.2 Purification of variants of VCC having point mutation

Point mutations were introduced in the wild-type nucleotide sequence of VCC. The purification protocol employed was same as mentioned above for the wild type VCC protein purification. The protein concentration for mutant protein was determined by measuring the absorbance at 280 nm using theoretically calculated extinction coefficient, based on the amino acid composition of particular mutant.

2.2 Experiments with the artificial membrane systems

2.2.1 Preparation of asolectin-cholesterol Liposomes

Six different asolectin-cholesterol liposomes were prepared, having varied percentage of cholesterol as 0%, 10%, 20%, 30%, 40% and 50% by weight. The final concentration of liposome was kept to be 1 mg/ml. For this, the calculated amounts of asolectin (from soybean) and cholesterol were weighed, dissolved in chloroform (Sigma) and transferred to

the round bottom flask. The chloroform was allowed to evaporate at room temperature, purged with the stream of nitrogen and kept in the dessicator for 2 hours under vacuum for lipid film formation. Following that, the lipids were hydrated to 1 mg/ml in phosphate buffer saline (PBS). Large unilamellar vesicles (LUVs) were formed by repeated extrusion of the liposome suspension for 11 times through polycarbonate membranes (100 nm pore size).

2.2.2 Light scattering measurement

In order to characterize the difference in size of LUVs, differing in cholesterol levels, Malvern Zetasizer Nano ZS90 was employed, which measures the extent of scattering of incident light to indicate the liposome size. For this, different liposomes, having varying amount of cholesterol were extruded through 0.1 μm pore size polycarbonate membrane 11 times and 200 μl of this sample was taken in a quartz cuvette. Using Zetasizer software, the appropriate cell and measurement type was chosen for the sample. Three replicate measurements were taken for each sample and the average was obtained that indicates Intensity and volume-based Particle size distribution (PSD). This data revealed the unimodal size distribution.

2.2.3 DPH (1, 4 Diphenyl 1, 3, 5 hexatriene) anisotropy measurement

To monitor the changes in fluidity of the membrane, with increasing levels of cholesterol in liposome membranes, DPH anisotropy measurement was carried out. Being a hydrophobic molecule, DPH gets sequestered in the non-polar region of liposome membrane and can provide the measure of fluidity of constituted liposomes. For this, 1 mg/ml stock of DPH was prepared in 1, 4 dioxane and 5 μl of this was added to lipids dissolved in chloroform in a round bottom flask and evaporated at room temperature, keeping DPH: liposome ratio of 1:200. Lipid film prepared was dried under the vacuum for 2 hours and resuspended in PBS for 2 hours at 37 $^{\circ}$C in dark. LUVs having DPH incorporated were prepared by repeated

extrusion of liposomes through the polycarbonate membranes of 0.1 μm pore size using mini-extruder apparatus.

Single point anisotropy values measurement was done on Horiba Fluoromax-4 equipped with polarizers in excitation and emission path lengths. Fluorescence intensities using excitation and emission wavelength of 350 nm and 452 nm respectively, having slit width of 2.5 nm for both were measured at perpendicular and parallel orientation of polarizers. Unlabelled liposomes served as control for the experiment. Fluorescence anisotropy was calculated as:

$$r = (I_{VV}-GI_{VH})/ (I_{VV}+2GI_{VH}) \quad [G=I_{HV}/I_{HH}]$$

In a total reaction volume of 2 ml of 10 mM Tris-HCl buffer (pH 8.0), 50 μg/ml of liposome was added and anisotropy was obtained as single point values at 25°C.

2.2.4 Calcein release assay

2.2.4.1 Asolectin-cholesterol liposomes: kinetic Method

To study the functional pore-formation by VCC, release of calcein-entrapped in the liposomes was monitored by incubating 25 μg of calcein-containing liposomes with 1 μM VCC, and measuring the fluorescence intensity of released calcein over a period of 15 minutes time having integration time of 1 second. Liposome film was prepared by dissolving the weighed amount of asolectin and cholesterol and then hydrating the film in filtered calcein (100 mM), prepared in 20 mM Tris-HCl and 150 mM NaCl buffer (pH 8.0) after purging nitrogen stream through the film. 1 ml of the resuspended liposome was taken and extruded 11 times to get unilamellar vesicles. Extruded liposomes were loaded onto the G-50 Sephadex (Sigma) size-exclusion column for the separation of free dye from the liposomes having entrapped calcein. Eluted fractions containing liposomes were collected and the assay was performed in a 2 ml reaction volume on Fluoromax-4 (Horiba Scientific, Edison, NJ,

USA) spectrofluorimeter by performing excitation at 488 nm, having excitation slit width of 2.5 nm and monitoring emission at 520 nm, having slit width of 5 nm, keeping integration time of 1 second and the time increment of 20 seconds, unless mentioned otherwise. The kinetics of calcein release upon addition of 1 μM VCC to 25 μl of prepared liposomes was measured for 15 minutes. The addition of 6 mM deoxycholate (Sigma) to liposomes was used to monitor the complete lysis of liposomes, acting as the positive control. Percent calcein release was plotted for each liposome differing in cholesterol concentration taking into account the deoxycholate-treated liposomes indicating 100% lysis.

2.2.4.2 Calcein-release assay employing phosphatidylcholine (PC) liposomes

The membrane permeabilization and functional pore-formation by VCC was investigated further using calcein-containing phosphatidylcholine (PC) liposomes having different levels of added cholesterol, ranging from 0 to 50% by weight, as described above.

2.2.5 Pull-down based assay for binding of VCC to liposomes

1 μM of VCC was incubated with 65 μl of extruded liposomes in 500 μl reaction volume for 1 hour at 25 $^{\circ}$C, then subjected to ultracentrifugation at 1,05,000 x g for 30 minutes, the supernatant was collected, pellet was washed twice with PBS and then finally the pellet was resuspended in 500 μl of PBS. 20 μl of both supernatant and pellet fractions were taken and examined via SDS-PAGE/Coomassie staining to analyse the binding of VCC to different liposomes.

2.2.6 Surface Plasmon Resonance (SPR)

For analysing the binding of VCC to different cholesterol-containing liposomes, L1 chip was used on Biacore 3000 (GE Healthcare) platform, which was preconditioned with Hepes buffer saline (20 mM Hepes, 150 mM Nacl, pH 7.5), and the liposomes were coated one by

one over the chip. Then, five different concentrations of VCC, starting from 200 nM to 1000 nM were used to study the binding efficacy of protein with these coated liposomes. Starting with the detergent (40 mM β-octyl glucoside), passed at the rate of 10 µl/minutes, followed by coating of the chip with extruded liposomes (8-fold diluted) at 2 µl/minute, then sodium hydroxide (20 mM) was injected at 100 µl/minute to remove the loosely bound lipids, then flown BSA (0.1 mg/ml) at 10 µl/minute to block the non-specific binding of protein and finally five different concentrations of protein were passed at the rate of 5 µl/minute for 10 minutes. The L1 chip was regenerated by flowing 40 mM β-octyl glucoside, passed at the rate of 10 µl/minutes. So, the flow rate and total amount per injection was set and continuous programme was run by repeating these cycles. Sensorgram plots were generated using the BIA evaluation 4.1.1 software (GE Healthcare Life Sciences). The average SPR signal at the end phase of protein flow (over 40 seconds) represents near-steady-state binding, whereas the stabilized SPR signals obtained upon washing with the buffer without protein defines the end-point data.

2.2.7 Enzyme-linked immunosorbent assay (ELISA)

Association of VCC with the liposome membranes differing in cholesterol-content was quantitated by ELISA, where the liposomes were incubated in triplicate in 96-well ELISA plate (Nunc, Rochester, NY, USA) at 4 $^{\circ}$C overnight. Three washings were done with TPBS and then blocking with 200 µl of 3% non-fat dry milk powder was done for an hour. Then liposomes were subjected to VCC treatment by incubation with different concentrations of VCC for 2 hours at 25 ^{o}C. Subsequently after washing thrice with TPBS, incubation with Anti-VCC antibody (1: 5000) was done for 90 minutes followed by the incubation with HRP-conjugated secondary antibody (1: 10,000) for an hour at 25 $^{\circ}$C, followed by three washings with TPBS. Development was done by the addition of OPD (Fluka analytical) in citrate

buffer containing H_2O_2, followed by addition of H_2SO_4 to stop the colour development. Absorbance was then measured at 490 nm.

2.2.8 FRET from tryptophans in VCC to dansyl-PE in liposomes

To study the intimate interaction of VCC with liposome membrane, qualitative FRET-based assay was employed where the intimate interaction of VCC with phospholipid head-groups was monitored. Earlier reports have indicated that VCC forms close interactions with membrane lipid head-groups during the process of functional pore-formation. For this, the asolectin-cholesterol liposomes having Dansylated-PE (Sigma) incorporated in the membrane lipid bilayer were prepared. Calculated amount of asolectin and cholesterol were weighed, dissolved in chloroform and to it, 1% dansylated-PE was added. The flask was swirled and the chloroform was evaporated. The flask was then kept in dessicator for 2 hours under vacuum. The lipid film was then resuspended in Phosphate buffer saline for 2hrs at 37°C. FRET between the tryptophan in VCC and dansyl moiety in the liposome membranes was assessed by incubating 1 μM VCC with 50 μg/ml of dansylated liposomes in a 2 ml reaction mixture using Fluoromax-4 spectrofluorimeter. FRET was monitored at the emission wavelength of 512 nm, upon excitation at 290 nm. The end-point data represented relative change in fluorescence intensity upon addition of VCC to liposomes with respect to the buffer-treated sample.

2.2.9 Pull-down based assay for oligomerization

In order to study the oligomerization efficiency of VCC with liposomes differing in cholesterol-content, pull-down assay was done by incubating 1 μM of VCC with 65 μl of extruded liposomes for 1 hour in 500 μl reaction volume at 25 °C, then subjected to ultracentrifugation at 1,05,000 x g for 30 minutes. Supernatant was discarded, pellet was washed twice with PBS and then finally the pellet was resuspended in 40 μl of PBS and 10 μl

of SDS-PAGE sample buffer was added to it, of which, one half was taken as boiled fraction that was boiled for 15 minutes at 100 °C, while the other half was taken as unboiled fraction that was kept at 25 °C. Both the fractions were analysed by SDS-PAGE/Coomassie staining to check the difference in oligomer formation in liposomes differing in cholesterol content.

2.2.10 Diphenylhexatriene-FRET (DPH-FRET)

For studying the insertion of the pre-stem loop of VCC into the lipid membrane and for analysing the effect of cholesterol in membranes for regulating the efficacy of insertion of pre-stem loop, this assay was performed. The assay qualitatively determines the membrane-insertion step of the pre-stem motif of VCC as upon insertion of this motif, Trp318 residue within this motif will form FRET pair with DPH incorporated in the liposome. Liposomes having 0%, 10%, 20%, 30%, 40%, and 50% cholesterol were prepared. Lipid film was prepared by adding the weighed amount of asolectin and cholesterol to get these mentioned desired ratios. After solvation of lipid film in PBS for 2 hours at 37 °C, prepared liposomes were extruded 11 times through 0.1 μm polycarbonate membrane (Avanti Polar lipids). 1 mg/ml DPH (Sigma) stock was made in 1, 4 Dioxane (Sigma) and DPH:liposome ratio was kept 1:200 for DPH-labelled liposome preparation. DPH was incubated for one hour with extruded liposomes in dark at room temperature. DPH being hydrophobic in nature, it will be incorporated in the hydrophobic core of lipid bilayer. Horiba fluoromax-4 equipped with peltier-based system was used to measure FRET from tryptophan in the pre-stem region of VCC to DPH at 25 °C. Excitation wavelength of 290 nm with slit width of 2.5 nm and emission wavelength of 470 nm with slit width of 5 nm was used, keeping data interval of 20 seconds and integration time of 1 second. Liposome concentration of 50 μg/ml was used in a reaction volume of 2 ml in the experiment and monitored for 30 minutes to study the efficiency of insertion of pre-stem loop into synthesized liposomes. The relative change in the

fluorescence intensity of liposomes upon addition of VCC with respect to buffer-treated control at the end of 30 minutes is represented by the end-point data.

2.2.11 Steady-state tryptophan fluorescence anisotropy

Tryptophan fluorescence anisotropy was performed on Fluoromax-4 (Horiba Scientific, Edison, NJ) spectrofluorimeter equipped with a peltier-based temperature controller using 1 cm path length and keeping excitation and emission wavelength of 295 nm and 340 nm, respectively, with slit widths of 5 nm and 10 nm respectively. 0.25 μM VCC was incubated with 700 μg/ml of extruded liposomes consisting of asolectin and having varied amount of cholesterol for 30 minutes at room temperature (~25°C). Following incubation, the final volume was made to 2 ml by addition of phosphate buffer saline. Anisotropy measurement was done for multiple sets of samples in triplicate, keeping excitation wavelength of 295nm and emission wavelength of 340 nm and finally the average anisotropy values were calculated as:

$$r = (I_{VV}-GI_{VH})/\ (I_{VV}+2GI_{VH}) \quad [G=I_{HV}/I_{HH}]$$

where I_{VV} and I_{VH} represents measured fluorescence intensities (after appropriate background subtraction) with the excitation polarizer vertically oriented and emission polarizer vertically and horizontally oriented respectively. G forms the grating correction factor that defines the ratio of the ability of detection system for vertically and horizontally polarized light.

Further, the anisotropy values of all liposomes were plotted together to observe the changes in anisotropy values corresponding to changing cholesterol levels. The experiments were carried out with multiple sets of samples and the average values were taken into consideration.

2.2.12 Acrylamide Quenching

The quenching of intrinsic tryptophans fluorescence of VCC by acrylamide in the free form of protein, on binding to membranes devoid of cholesterol and the cholesterol-enriched membranes was studied using the excitation wavelength of 295 nm and emission wavelength of 340 nm. The extent of tryptophan fluorescence quenching by acrylamide provides the insight upon accessibility of the tryptophans in VCC by the acrylamide quencher, when VCC binds and partitions into the liposome membrane, compared to their accessibility in the free-form of the protein. Thus, the quenching of tryptophan fluorescence will indicate the interaction and association of VCC with the liposome membranes. For this, 5 M stock of acrylamide (Sigma Aldrich) was prepared. In a 2 ml reaction mixture, 0.5 μM of protein was incubated with 100 μg/ml of liposomes containing cholesterol, and in the other set of experiment incubation was done with the liposomes lacking cholesterol for 30 minutes at room temperature (25 $^{\circ}$C). Acrylamide from the prepared stock was added after incubation of VCC with liposomes to get the final desired acrylamide concentration, as 100 mM, 200 mM, 300 mM, 400 mM and 500 mM. Fluorescence intensity was recorded for three independent sets of experiment, each having triplicate reading. Single point fluorescence measurements were carried on Horiba Fluoromax-4 at 25 $^{\circ}$C. The data was analysed using Stern-Volmer equation:

$$F_o/F = 1+ K_{SV} [Q]$$

Where F_o and F refers to the fluorescence intensities in the absence and presence of quencher respectively, K_{SV} being the collisional quenching constant and [Q] denotes the concentration of quencher, acrylamide in this case.

2.2.13 Time-correlated Single photon counting (TCSPC)

Freshly prepared 0% cholesterol and 50% cholesterol-containing asolectin liposomes were taken and extruded 21-times to obtain the unilamellar liposomes. Firstly, 0.5% ludox i.e colloidal silica that acts as a scatterer is taken for measuring prompt for the experiment, for studying the instrument response factor. Experiment was set up by incubating 1 μM VCC with 1600 μg/ml liposomes for thirty minutes. Following this, the lifetime measurement was done in 1 cm path length quartz cuvette. Lifetime measurement was done thrice for each set, comprising of only VCC, VCC incubated with 0% cholesterol-containing liposome, and VCC with 50% cholesterol-containing liposome. The count rate was set at 10,000. Time-resolved fluorescence intensity decay with data analysis software in time-correlated single photon counting mode was used to measure the fluorescence lifetimes. The excitation source used was nano LED-295. For optimizing the signal to noise ratio, a total of 10,000 photon counts were collected in the peak channel. After completion of taking the decay measurements, it was analysed in DAS6 software and fitted in tri-exponential decay to get the Chi-square value around 1, and three lifetime components were obtained for each sample. Counts were then plotted against channel to get lifetime decay of each sample. The prompt and lifetime values for free protein and protein incubated with 0% and 50% cholesterol-containing liposomes were plotted.

2.3 Experiments with pure cholesterol

2.3.1 Lysis inhibition Assay

To study whether the prior interaction of VCC with cholesterol competes with its binding ability with erythrocytes and to monitor how this interaction of VCC with cholesterol affects

the functional pore-forming activity of VCC i.e how haemolytic activity is affected, lysis-inhibition assay was performed. The stock solution of cholesterol was prepared by dissolving 1.3 mg cholesterol in 100 µl of chloroform. Further, four different stocks of cholesterol were prepared by serial dilution of the prepared cholesterol stock solution. Reaction volume of 500 µl was set up by the addition of 200 nM VCC and 1 µl of cholesterol stock solution in PBS, keeping the VCC: cholesterol ratio 1:2, 1:1, 1:0.5 and 1:0. This reaction mixture was incubated at 25 °C for an hour. Then 500 µl of erythrocytes were added in a way so as to make the volume 1 ml, having $O.D_{650}$ of ~0.9, and the final VCC concentration would be 100 nM. Haemolytic activity of VCC was tested for a period of 60 minutes. VCC incubated with the identical volume of chloroform i.e 1 µl chloroform in the reaction mixture served as a control.

2.3.2 Cholesterol pull-down Assay

The binding efficacy of VCC and its variant, Ala425Val to pure cholesterol in suspension was monitored using the pull-down based assay. For this, cholesterol stock was prepared by dissolving 26 mg of cholesterol in 1 ml of chloroform and the two serial dilutions of cholesterol were prepared using this stock. Reaction mixture of 1 ml PBS having 1 µM VCC and 5 µl of cholesterol from the prepared stock was set up. This reaction mixture was incubated at 25 °C for an hour and then centrifuged at 16,000 × g for 20 minutes. The pellet was dissolved in 25 µl of PBS and boiled for 15 minutes after the addition of SDS-loading dye. The pellet fraction was tested for the presence of VCC by SDS-PAGE/Coomassie staining.

2.3.3 Lipid dot blot assay

Lipid dot blot assay was employed to demonstrate the interaction of VCC and its variant, Ala425Val to pure immobilized cholesterol. For this, stock solution of cholesterol was prepared by dissolving 38.6 mg cholesterol in 1 ml of chloroform. Further, three more concentrations of cholesterol were prepared by serially diluting this prepared stock in chloroform. The nitrocellulose membrane was taken, wetted with MQ water and air dried, but kept moist. Cholesterol in different concentrations was spotted onto the nitrocellulose membrane by adding 20 µl of each prepared cholesterol concentrations. Membrane was then blocked using 3% BSA, prepared in PBS for 2 hours. 100 nM VCC was then added and the membrane was incubated for an hour. Membrane was then washed for an hour using PBS having 0.05% Tween 20. Membrane was then incubated with Anti-VCC primary antibody (1:10,000), followed by the washing with PBS- Tween 20 (PBST). Further, the incubation of membrane was done with HRP-conjugated secondary antibody for an hour, followed by washing with PBST. Dot blot was finally developed by the method of chemiluminescence, using Clarity Western ECL substrate (Bio-rad). Imaging was done with ImageQuant LAS 4000 (GE Healthcare Life Sciences).This assay was performed to assess the interaction efficacy of VCC and VCC mutant Ala425Val with immobilized cholesterol.

2.4 Erythrocytes Experiments

2.4.1 Assay of lytic activity against human erythrocytes upon cholesterol depletion

Working with human erythrocytes was approved by the Institutional Ethics Committee of IISER Mohali. The assay of haemolytic activity by VCC was monitored by measuring the decrease in turbidity of erythrocytes cell suspension in Phosphate Buffer Saline (20 mM sodium phosphate buffer containing 150 mM NaCl, pH 7.4). For this, the optical density of erythrocytes in PBS was adjusted to 0.9 at 650 nm. To examine the regulatory role of cholesterol (Sigma Aldrich) on the pore-forming ability of VCC, erythrocytes were firstly

treated with methyl-β-cyclodextrin (Sigma Aldrich), a class of sugar molecule that can sequester the cholesterol in its ring-like structure, hence reducing the cholesterol content in the cells. So, for this assay four different reactions were set up, each of 1 ml PBS, having erythrocytes suspended in that so as to have the optical density of suspension to be 1.4, 1.2, 0.9 and 0.9 at 650 nm. Then, 100 mM of methyl-β-cyclodextrin (mβCD) is prepared in PBS, which is used to sequester the cholesterol from cells. In four RBC suspensions, mβCD was added to get the final concentrations of 5 mM, 2.5 mM, 1 mM and no mβCD, in order to deplete the erythrocyte membrane cholesterol. Thus, the erythrocytes suspension was treated with these four different concentrations of mβCD and incubated at room temperature for 30 minutes. Then, two washings of erythrocytes were done with PBS by centrifugation at 2200 rpm for 15 minutes. RBCs were suspended in fresh 1 ml PBS. Erythrocytes were then treated with 100 nM VCC and haemolysis was observed for 60 minutes by measuring $O.D_{650}$ to monitor the decrease in turbidity over time. Erythrocytes treated with mβCD only, to deplete cholesterol but with no protein treatment served as control in the experiment.

2.4.2 Cholesterol replenishment in erythrocytes

Upon depletion of membrane cholesterol as described above, the set of erythrocytes to be replenished with cholesterol was incubated with mβCD: cholesterol complex in a 10 mM: 1 mM ratio, prepared in PBS, for 30 minutes at room temperature (25 $^{\circ}$C). The mβCD: cholesterol complex was then washed off by centrifugation of cells at 2200 rpm and the erythrocytes were then resuspended in PBS. $O.D_{650}$ was measured again which should be 0.9. After replenishment back of cholesterol to erythrocytes membrane, haemolytic activity assay was carried out as stated above using 100 nM VCC for a period of one hour.

2.4.3 Cholesterol estimation in depleted and replenished erythrocytes membranes

2.4.3.1 Erythrocytes cell membrane preparation

For quantification of membrane cholesterol, the cell membranes were prepared from untreated, cholesterol-depleted and cholesterol-replenished cells. For preparation of erythrocytes membranes, after the required treatment, cells were centrifuged, and to the cell pellet which is resuspended in 100 µl of PBS, 1000 µl of ice-cold 5 mM phosphate buffer, 1mM EDTA was added. Cells were then incubated on ice for 30 minutes to cause complete lysis of erythrocytes. Then the cells were centrifuged at 15,000 × g for 20 minutes. The pellet was finally resuspended in 200 µl of PBS. Quantification of membrane cholesterol was done by the Amplex red cholesterol estimation assay kit (invitrogen), upon following the manufacturer's protocol.

2.4.3.2 Amplex red cholesterol assay kit

The kit is designed to detect both free and cholesteryl esters in the membrane.

2.4.3.3 Standard curve preparation

2 mg/ml stock of cholesterol was given in the kit to be used for preparation of standard curve by serial dilution using 1 x reaction buffer provided in the kit. Only reaction buffer served as the negative control, while H_2O_2 provided in the kit served as positive control to monitor the proper detection of cholesterol by kit components.

2.4.3.4 Preparation of working solution for the assay

To prepare working solution for the assay, 20 mM stock solution of amplex red reagent, prepared in DMSO (provided in the kit) was added to the calculated volume of reaction buffer (based on number of samples). 2 U/ml HRP and 2 U/ml cholesterol oxidase were added to it, and finally 0.2 U/ml cholesterol esterase was added. 50 µl of this solution was used for each sample. Hence, to 50 µl of cell lysate, 50 µl of working solution for the assay

was added in black 96-well plate and the fluorescence intensity was determined for each sample using Fluostar Optima Plate reader, keeping the excitation wavelength of 544 nm and emission was measured at 590 nm. Concentration of cholesterol in each sample was calculated using the standard curve obtained.

2.4.3.5 Protein quantification in prepared erythrocytes cell membranes

Further to quantify the amount of total protein in prepared membranes of erythrocytes, subjected to cholesterol depletion, replenishment and in untreated samples, Bradford assay was employed. For this, BSA stock of 1 mg/ml was prepared in PBS. Eight different dilutions of BSA were prepared by serial dilution of the stock. In a 96-well microtiter plate, 90 µl of Bradford's reagent was taken and 10 µl of sample for the protein quantification was added. After incubation for 5 minutes at room temperature, the absorbance was measured at 595 nm. Finally, the cholesterol content for each sample was normalized with respect to the protein equivalent for it.

2.4.4 Flow cytometry-based assay with human erythrocytes

The quantitative estimation of VCC binding to human erythrocytes was done using the flow-cytometry based assay. For this, the human erythrocytes cell suspension was taken, washed with PBS and the cells were counted using haemocytometer. Then, in 96-well V-bottom plate, 100 µl reaction was set up by adding that much volume of blood so as to get ~$1.1x10^6$ cells in each well. Three different reactions were set in triplicates as: only RBCs in PBS, RBCs to be treated with VCC without prior treatment of mβCD, RBCs treated with 5.0 mM mβCD, for the depletion of membrane cholesterol, prior to VCC treatment. Firstly, erythrocytes were treated with 5 mM mβCD to sequester membrane cholesterol along with the control having no mβCD for 30 minutes at 4 $^{\circ}$C. Then, the two washings were done with

100 µl PBS to remove mβCD by centrifugation of 96-well plate at 2200 rpm for 5 minutes. The cells were then suspended in 100 µl PBS, counted again using the hemocytometer and treated with 75 nM of VCC for 30 minutes at 4 °C. After that, the cells were treated with rabbit anti-VCC antiserum for 30 minutes at 4 °C, followed by FITC-conjugated goat anti-rabbit antibody again for 30 minutes at 4 °C, along with the negative control where the cells were not treated with protein but stained with anti-VCC and FITC-conjugated antibody only. Cells were then analysed by FACSCalibur (BD Biosciences) flow cytometer by measuring the FITC fluorescence at excitation wavelength of 488 nm and emission wavelength of 530 nm. Data obtained from the flow-cytometry experiments was analysed using FlowJo software.

2.4.5 Pull-down assay with human erythrocytes to study oligomerization propensity of VCC

In order to assess the oligomeric assembly formation by the membrane-bound fraction of VCC on the erythrocyte membrane after treatment with mβCD, pull-down based assay was performed. For this, 1 ml reaction was set up where the erythrocytes corresponding to $O.D_{650}$ of 0.9 was adjusted before the VCC treatment. Two reactions were set up of 1 ml each having $O.D_{650}$ corresponding to 1.4 and 0.9, since 5 mM mβCD treatment causes mild lysis of the cells and slight decrease in turbidity. So, $O.D_{650}$ should be 0.9 while subjecting erythrocytes to the protein treatment. Firstly, 5 mM of mβCD treatment was given to RBCs for 30 minutes at 25 °C. Then, two washings with PBS were done to remove mβCD and $O.D_{650}$ was measured after mβCD treatment which was around 0.8-0.9. Erythrocytes were then treated with 100 nM VCC for an hour at 25 °C, and then subjected to the ultracentrifugation at 1,05,000 × g for 30 minutes. Two washings with PBS were done again for 30 minutes by the same ultracentrifugation condition of 1,05,000 × g. The supernatant was discarded and the pellet was resuspended in 40 µl PBS, dividing it into two fractions, one being boiled fraction

which was heated at 100 ^{o}C for 15 minutes and the other fraction was kept unboiled to examine whether the bound fraction of the toxin is capable of forming oligomeric species onto the membrane of erythrocytes. Both boiled and unboiled fractions were subjected to SDS-PAGE and western blotting, where blocking was done by 5% non-fat dry milk (Santa cruz), followed by the treatment with Anti-VCC rabbit antiserum (1:10,000), followed by HRP-conjugated secondary antibody (1:10,000). Clarity Western ECL substrate (Bio-rad) was employed to visualize oligomeric species formed by VCC on erythrocytes membrane, upon development of the blot by chemiluminiscence. The unboiled fraction would allow the detection of oligomeric assemblies generated by VCC.

2.4.6 Recovery of haemolytic activity of VCC upon replenishment back of cholesterol in the erythrocytes membrane

In order to study whether VCC could induce pore-formation mechanism upon replenishing back the cholesterol in cholesterol-depleted erythrocytes, a special experimental strategy was employed. Here, 5 ml of human erythrocytes were taken in PBS having OD_{650} of 1.4, which were then subjected to 5 mM mβCD treatment for 30minutes at room temperature. Following washing with PBS, the erythrocyte pellet was resuspended in 5 ml PBS and 1 ml was taken in two sets having $O.D_{650}$ of 0.9, where one set was used as control and kept at room temperature for an hour while the other set was incubated with 100 nm VCC for an hour. Both sets of erythrocyte suspension were then centrifuged at 2200 rpm, followed by treatment with cholesterol-replenishment mixture, comprising of mβCD: cholesterol mixture in a ratio of 10 mM: 1 mM for half an hour at room temperature. The erythrocytes were then washed with PBS, resuspended and then the OD_{650} was measured for an hour to observe if any haemolytic activity of VCC is regained back for both the untreated and VCC-treated samples.

2.5 Lipid Raft Isolation

Lipid raft fractions of the erythrocytes membranes were isolated and probed using the lipid raft isolation kit (Sigma-Aldrich Caveolea/Rafts Isolation kit), as per the manufacturers protocol.

2.5.1 Lysis buffer Preparation

To 1 ml of lysis buffer (provided in the kit), 1% of Triton-X100 and 1% of protease inhibitor cocktail was added, vortexed and kept on the ice.

2.5.2 CTB reconstitution and dilution

To the lyophilized CTB-HRP, provided in the kit, 50 µl of water was added to the vial and stored at 4 ^{o}C. CTB was diluted in a ratio of 1:500 in PBS. Hence, to 2 ml of PBS, 4 µl of reconstituted CTB was added.

2.5.3 Preparation of cell lysate after VCC treatment

5 ml of washed human blood having OD_{650} of 2.8 was taken. To it, 100 nM VCC was added and incubated on the ice for 30 minutes. The sample was then subjected to ultracentrifugation at 1,05,000 × g for 30 minutes. The pellet was washed twice with the PBS by ultracentrifugation at 1,05,000 × g for half an hour. Finally, the pellet was resuspended in 1 ml of lysis buffer and incubated on ice for 30 minutes.

2.5.4 Preparation of cell lysate after cholesterol depletion using mβCD, followed by the VCC treatment

5 ml of concentrated human blood having OD_{650} of 3.2 was taken and the washing of blood was done by centrifugation at 2200 rpm for 5 minutes. 100 mM stock of mβCD was prepared in PBS. 5 mM mβCD was added to 5 ml of washed blood and the incubation was done at

room temperature for 30 minutes. The blood sample was then centrifuged twice at 2200 rpm for 5 minutes to remove mβCD after the treatment. The OD_{650} was measured again which was 2.7 for the blood sample. The cholesterol-depleted erythrocytes were then treated with 100 nM VCC, incubated on the ice for 30 min and then subjected to ultracentrifugation twice at 1,05,000 × g for half an hour. Finally, the cell pellet was resuspended in 1ml of prepared lysis buffer and incubated on ice for 30 minutes.

2.5.5 Preparation of cell lysate after CTB treatment

Cell lysate prepared upon the treatment of human erythrocytes with CTB will allow the identification of isolated raft fractions, whether the lipid rafts has been efficiently extracted from the human erythrocytes or not. For this, 5 ml of washed blood was taken having OD_{650} of 2.7. Erythrocytes were pelleted by the centrifugation at 2200 rpm for 5 min to obtain the cell pellet. To this pellet of erythrocytes, 2 ml of diluted CTB-HRP solution was added and incubated on the ice for an hour. The sample was centrifuged after incubation at 450 × g for 5 minutes at 4 $^{\circ}$C and the diluted CTB-HRP solution was aspirated. Cells were then washed twice with ice-cold PBS by centrifugation at 450 × g for 5 minutes at 4 $^{\circ}$C. Cell pellet was finally resuspended in 1ml of prepared lysis buffer and incubated on the ice for 30 minutes.

2.5.6 Density gradient preparation for the isolation of Lipid rafts from human erythrocytes membrane

Density gradient is composed of 5 layers OptiPrep with different concentrations as: 35%, 30%, 25%, 20% and 0%. The lowest 35% OptiPrep layer contains the cell lysate. Five solutions were prepared that will form the OptiPrep gradient layers by mixing the required amount of lysis buffer and OptiPrep density gradient solution given in the kit. Each solution was vortexed and kept on the ice. Each OptiPrep gradient layer was placed over the other very gently and subjected to ultracentrifugation at 2,00,000 × g for four hours at 4 $^{\circ}$C. After

the ultracentrifugation, 500 µl fraction each was collected from top to bottom of the ultracentrifuge tube. The total number of fractions collected were 18 were stored at -20 °C.

2.5.7 Gradient fraction analysis by the dot blot

2.5.7.1 CTB-HRP detection

A strip of nitrocellulose membrane was cut, marked and soaked in the milliQ water. A wet Whatman paper was soaked in water and the nitrocellulose membrane was placed over it to keep the membrane moist. 2.5 µl of each isolated gradient fraction as well as the original lysate was loaded onto the membrane. Sample drops and nitrocellulose membrane were air dried and washed once with the PBS. Chemiluminescent peroxidase substrate solution was applied on the nitrocellulose membrane. The membrane was then exposed for different time durations for imaging using the ImageQuant LAS 4000 (GE Healthcare Life Sciences).

2.5.7.2 Detection of VCC, Transferrin receptor and flotillin-1 in gradient fractions using the dot blots

For this, nitrocellulose membrane was marked and soaked in water. 2.5 µl of each gradient fraction and original input lysate were loaded onto the membrane. After air drying the sample and nitrocellulose membrane, the membrane was incubated with 3% BSA blocking solution for an hour at room temperature. The membrane was then incubated with Anti-VCC (1:10,000) or Anti-flotillin-1 (1:2,000) or Anti-TfR (1:10,000) primary antibody diluted in PBS for an hour. Washing of the membrane was done for an hour using TPBS (PBS having 0.05% Tween-20). The membrane was then incubated with HRP-conjugated secondary antibody (1:10,000) for an hour. The nitrocellulose membrane was finally washed with TPBS for an hour. The blot was then exposed to different time intervals and developed for

visualization by the method of chemiluminescence, using Clarity Western ECL substrate (Bio-rad).

2.5.7.3 Detection of VCC in the isolated raft fractions using immunoblot

In order to detect the presence of VCC in isolated raft fractions, 2 µl of lysate was taken and diluted with 18 µl of 10 mM Tris-Cl (pH 8.0). The sample was boiled at 100 $^{\circ}$C for 10-15 minutes, loaded onto 10% SDS-PAGE and then transferred onto the PVDF membrane. The membrane was blocked by incubation with 3% BSA for an hour. Then the membrane was treated with Anti-VCC (1:10,000) antiserum for an hour. Washing was done for an hour using TPBS (PBS with 0.05% Tween20) to remove the loosely and non-specifically bound primary antibody, followed by the incubation with HRP-conjugated secondary antibody for an hour. Finally, upon washing the blot for an hour, the blot was developed and the band size for VCC was verified.

2.5.7.4 Cholesterol estimation in isolated membrane fractions from human erythrocytes

Next we wanted to measure the levels of cholesterol in isolated membrane fractions from the human erythrocytes, without pre-treatment with mβCD and also in the distinct raft fractions isolated from human erythrocytes, upon 5 mM mβCD pre-treatment for depletion of membrane cholesterol. For this, 50 µl of each fraction, out of total 18 isolated fractions was taken and mixed with the reaction mixture for cholesterol estimation prepared as described above. These were incubated for half an hour at 37 ^{o}C and then the fluorescence intensity was measured for each sample at excitation wavelength of 544 nm and the emission wavelength of 590 nm to finally calculate the content of cholesterol using the standard curve prepared.

2.5.7.5 Confocal microscopy

Human erythrocytes (10^6 cells in PBS) were incubated for 1 hr at 4 °C with VCC. The erythrocytes were washed with ice-cold PBS, followed by treatment with 3% BSA in PBS for an hour on ice. Then the cells were incubated with rabbit anti-VCC antiserum (1:1000 dilution) again for an hour on ice. Following washing, the blocking of cells was done with 2% goat serum for 30 minutes on ice and then the staining of cells was done using Alexa-488-conjugated goat anti-rabbit secondary antibody (1:1000 dilution) for an hour on ice. Then, followed by washing with ice-cold PBS, cells were resuspended in ice-cold PBS containing 2 μg/ml of Alexa-594-conjugated CtxB and incubation was done on ice for 30 minutes. Upon washing, the cells were incubated in 1ml ice-cold PBS containing rabbit anti-CtxB antibody (5μl) for 30 minutes on ice. The cells were washed with ice-cold PBS and plated onto poly-D-lysine-coated (50 μg/ml) coverslips for 30 min on ice. Then the fixation of cells was done with 2% PFA on ice for 10 minutes, followed by washing with PBS and the coverslips were mounted on glass slides using a fluoromount mounting medium (Sigma).

The imaging of cells was done on an Olympus confocal laser scanning microscope using 60× oil immersion objective with 1.35 numerical aperture. In each experiment, the images were obtained from all the conditions using identical parameters. For analysis purpose, raw images were used and colocalization was determined by estimating the Mander's coefficient using the Fiji software. In three independent experiments, total of 61 erythrocytes were scanned. The extent of VCC colocalization with CtxB, the cells were thresholded with identical values for a particular channel and subsequently measuring the extent of colocalization of VCC with CtxB. For each experiment, the imaging and analysis of cells was done from two coverslips for the same condition of a particular experiment.

2.6 Statistical Analysis

Data was represented as mean +/-SEM. Statistical analysis was performed using the GraphPad/ QuickCalc t-test calculator. Two group comparisons were performed using the Student's Two-sided unpaired t-test. All p-values less than 0.05 were considered as statistically significant. Here, $P < 0.05$, $P < 0.01$ and $P < 0.001$ are marked by *, ** and *** respectively.

CHAPTER 3

Results

Chapter 3

Results

3.1 Characterization of the liposomes by dynamic light scattering (DLS) measurement.

The effect of gradually increasing the cholesterol content on the size of asolectin liposomes was studied by DLS. Different liposomes were prepared with asolectin containing cholesterol at various weight percentages (from 0% to 50% cholesterol levels; by weight). These asolectin-cholesterol liposomes were characterized for their size. The size distribution of liposomes is commonly studied by DLS by determining the mean cumulative radii. The DLS measurements, performed on the Nano-zetasizer instrument, clearly suggested that all the liposomes prepared were of approximately 100 nm diameter, as indicated in the Fig. 16.

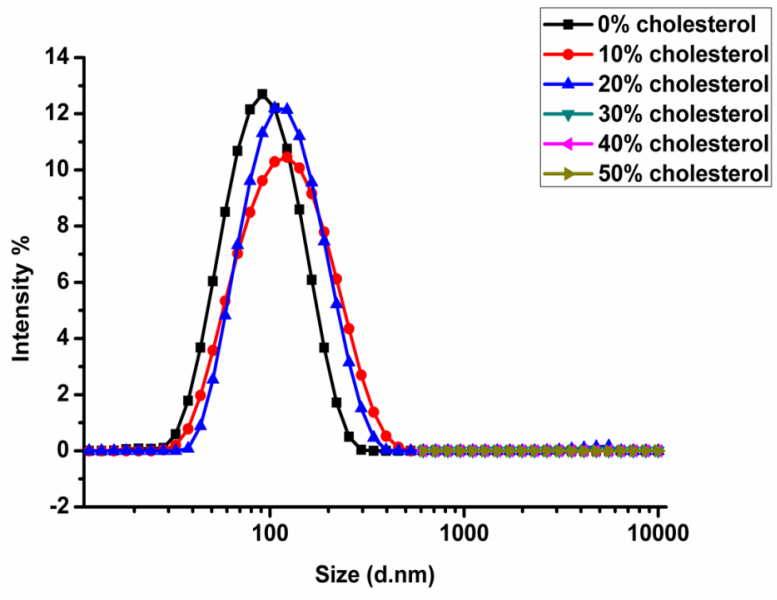

Fig. 16. Dynamic light scattering technique employed to analyse the size of the Asolectin-cholesterol liposomes. Nanozetasizer-based DLS experiment demonstrated that all the liposomes containing varying levels of cholesterol were of nearly similar size.

3.2 Gradual increase in the cholesterol levels induces decrease in the fluidity of the membrane lipid bilayer.

The changes in membrane fluidity of the asolectin liposomes, containing varying levels of cholesterol were determined by employing the diphenyl hexatriene (DPH) anisotropy measurement assay. DPH was incorporated in all the six different types of liposome containing varying amount of cholesterol (having 0, 10, 20, 30, 40 and 50% cholesterol content; by weight), and the anisotropy measurement of the incorporated DPH was carried out. The results indicated that there was a gradual increase in the anisotropy values of DPH upon increasing the levels of membrane cholesterol, which reflects to the decreasing fluidity of the liposome membranes. Upon incorporating increasing amount of cholesterol in the liposomes, the fluidity is expected to reduce, thus causing the increment in the DPH anisotropy values from ~0.13 in the asolectin liposomes lacking cholesterol to 0.26 in 50% cholesterol-containing liposomes (Fig. 17).

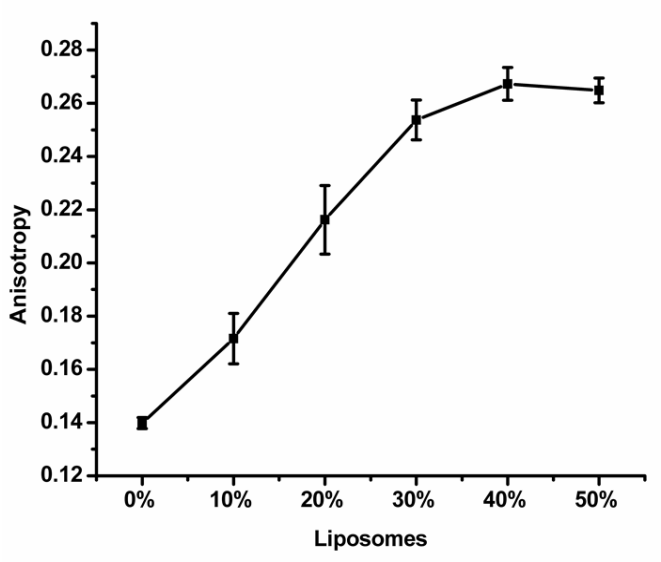

Fig. 17. DPH fluorescence anisotropy measurement to monitor the fluidity of the membrane lipid bilayer of the asolectin liposomes containing varying levels of cholesterol. The DPH anisotropy was measured to analyse the fluidity of the liposome membranes containing varying levels of cholesterol. Fluorescence anisotropy data shown here represents the average of the three independent sets of experiments. %Cholesterol content in the Asolectin liposomes is indicated in the x-axis.

3.3 Presence of cholesterol is essential for the functional pore-forming activity of VCC in the membrane lipid bilayer of liposomes.

We explored the role of cholesterol in the membrane-damaging pore-forming activity of VCC against the synthetic lipid vesicles constituted from asolectin and varying amount of cholesterol. For this, different liposomes having stepwise increase in the cholesterol content were prepared. For exploring any role of cholesterol in the functional pore-formation mechanism of VCC, we employed the conventional calcein-release assay. In our study, we constituted asolectin liposomes with varying levels of cholesterol, and having trapped calcein fluorophore. The disruption of the liposome membranes by VCC, via pore formation, was then assessed by monitoring the release of calcein. Release of calcein from the liposomes relieves the self-quenching of calcein fluorescence, ultimately resulting in the increased calcein fluorescence emission intensity. We observed a gradual stepwise increase in the pore-forming ability of VCC upon stepwise increment in the cholesterol level in the asolectin liposomes. Release of entrapped calcein was monitored from the liposomes upon treatment with VCC**.** Protein concentration of 1 μM, when monitored for 15 minutes time period at 25 $^{\circ}$C, induced nearly 85% calcein release from the liposomes having 50% (weight ratio) cholesterol (Fig. 18). However, limited cholesterol content in the liposome membranes allowed marginal calcein release. For example, a nominal 30% calcein release was observed when the cholesterol content was 20% (weight ratio). The end-point averages of the calcein release data, measured from three independent experimental sets, showed significant release of entrapped calcein from the liposomes composed of 30, 40 and 50% cholesterol (by weight) upon addition of 1 μM VCC. In contrast, lower cholesterol content allowed drastically reduced calcein release. Hence, calcein-release assay of pore-forming activity showed progressive increase in the pore-forming activity with increasing levels of cholesterol in the

liposome membrane, suggesting the presence of an optimal level of cholesterol to be critical for the pore-formation mechanism of VCC.

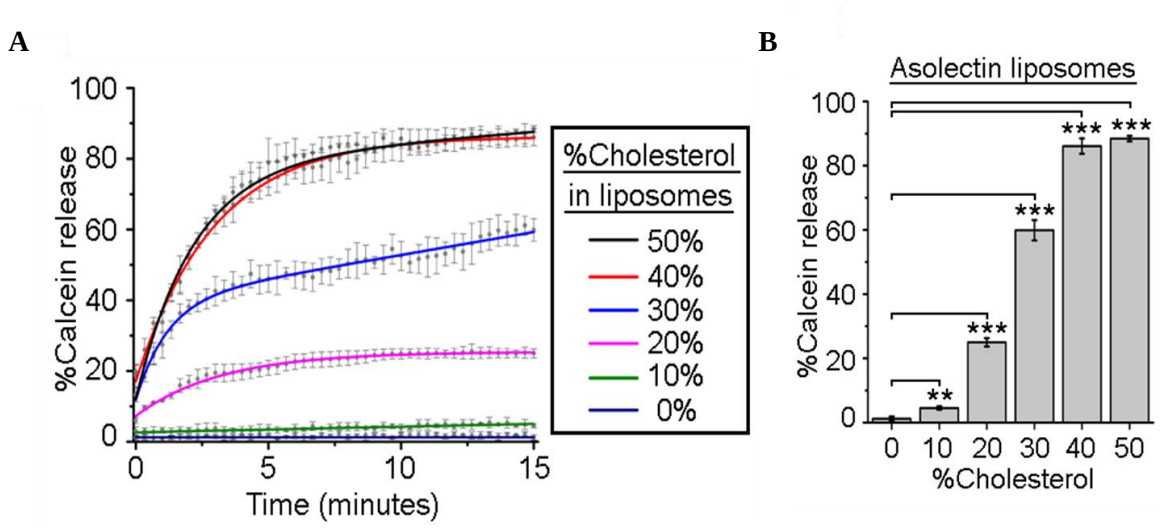

Fig. 18. Calcein-release assay to examine the membrane-permeabilization ability of VCC towards asolectin liposomes, having varying levels of cholesterol. A. Functional pore-forming activity of VCC appears to increase gradually with the increasing levels of membrane cholesterol as observed by the calcein-release assay. B. The end-point analysis also confirms increased pore-forming ability of VCC with increase in the levels of membrane cholesterol. Data shown is a representative average ± standard deviation of three independent experiments.

Calcein-leakage assay was also performed using the phosphatidylcholine (PC) liposomes, supplemented with cholesterol in a similar way as performed with the asolectin liposomes. Here, the pore-forming ability is significantly less as compared to the asolectin liposomes, when using the same concentration of VCC. This is due to less susceptibility of the PC liposomes toward VCC. Whatsoever, upon monitoring the pore-forming activity of VCC against the PC liposomes, similar effect of cholesterol was observed, though they exhibit very less susceptibility compared to the asolectin-cholesterol liposomes. The trend of functional pore-formation was found to be similar in both the asolectin and PC liposomes, thus indicating the progressive increase in pore-forming activity of VCC with the increasing levels of cholesterol in the liposome membranes (Fig. 19).

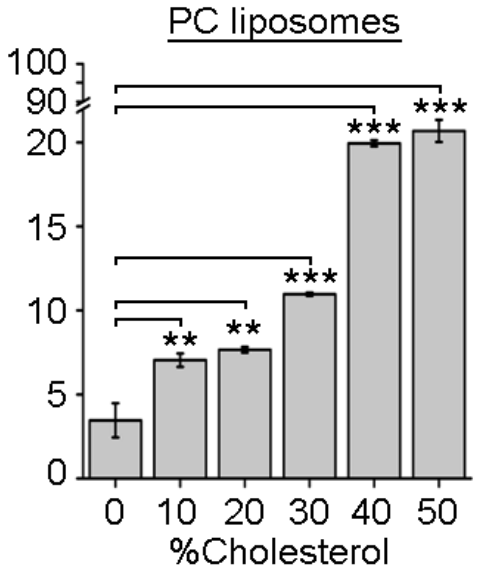

Fig. 19. Calcein-release assay employing PC liposomes to assess the membrane-permeabilization ability of VCC. The pore-forming ability of VCC monitored over time using PC liposomes, containing stepwise increase in the cholesterol levels clearly suggests the increase in the membrane pore-formation activity with increasing levels of cholesterol. The data is represented as the average end-point calcein release from three different treatments.

3.4 Pull down-based assay showing the association of VCC with liposome membrane containing varying levels of cholesterol.

Binding of VCC to the asolectin-cholesterol membrane was also monitored by pull down-based assay. VCC was incubated with different liposomes having varying levels of cholesterol and then the reaction mixture was ultracentrifuged. The SDS-PAGE/Coomassie staining analysis of the pellet and supernatant fractions collected upon the ultracentrifugation showed that VCC migrated to the liposome-bound pellet fractions as the levels of cholesterol in the membranes increased from 0 to 50%. VCC did not exhibit any prominent interactions with the membranes composed solely of asolectin or supplemented with 10% and 20% cholesterol (by weight) as only a basal level interaction was observed. In contrast, in the membranes constituted of 30% or more cholesterol content, VCC localized into the liposome-bound pellet fraction more efficiently, indicating the association of the toxin to these

cholesterol-rich liposome membranes (Fig. 20). Hence, an optimal level of cholesterol is required in the target liposome membranes for the efficient association and binding of VCC.

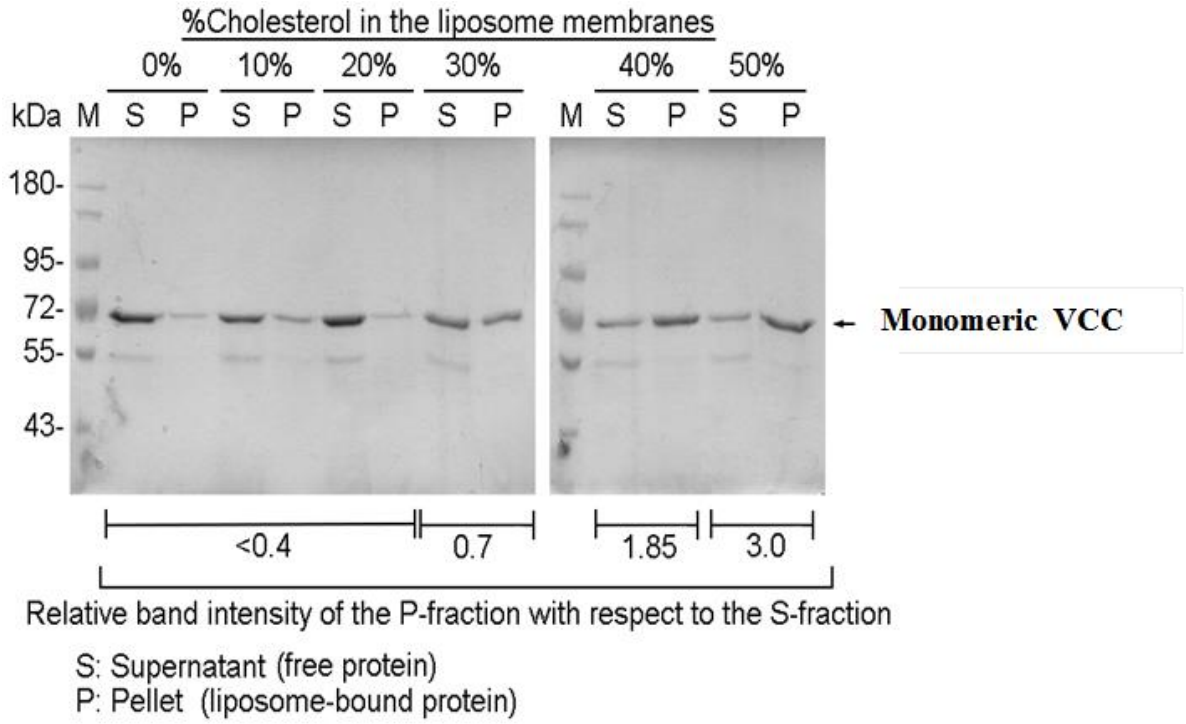

Fig. 20. Pull down-based assay to examine the association of VCC to different liposomes containing varying levels of cholesterol. SDS-PAGE/Coomassie staining analysis showing pellet fractions, that contained the liposome-bound protein and the supernantant fractions that contained the unbound free protein. This data clearly suggest enhanced binding of VCC upon increasing the membrane cholesterol levels as indicated by the increased amount of VCC in the pellet fractions in the higher cholesterol-containing liposomes.

3.5 Surface-plasmon resonance (SPR)-based binding assay showed compromised binding of VCC towards cholesterol deficient liposomes membranes.

We employed SPR-based study to monitor binding of VCC with the asolectin liposomes containing varying amount of cholesterol. Liposome membranes (having varying cholesterol content; in the range of 0-50%, by weight) were coated onto the surface of the SPR sensor chips, and then VCC (at various concentrations) was flown over the sensor chips (revealing the steady-state binding phase). At the end of the protein flow, buffer was passed to achieve the end-point response units that represented the irreversibly-bound fraction of VCC. The sensograms generated from the SPR-based assay showed inefficient binding of VCC with the

membranes containing no or marginal level of cholesterol. Membranes containing less than 30% cholesterol (by weight) exhibited compromised binding of VCC indicating the crucial role of cholesterol in the efficient membrane-interaction mechanism of VCC with the membrane lipid bilayer of liposomes. Near steady state binding phase of the real-time sensograms obtained from SPR based assay showed that VCC associated with all the liposome membranes with nearly similar efficacy, despite whether the liposome membranes lacked or had progressively increasing levels of membrane cholesterol (Fig. 21A). However, the end-point data analysis showed that the irreversible anchoring of VCC to the liposome membranes occurred efficiently, only when the membrane cholesterol levels were 30% or more. Upon the removal of the loosely-bound toxin molecules by the buffer flowing, only the tightly-associated molecules of VCC remained anchored and were reflected in the end-point data (Fig. 21B). This data suggest that there is a critical role of the membrane cholesterol that serves the important purpose of the binding of the VCC protein to the membrane lipid bilayer of the liposomes. End-point data analysis also revealed the necessity of cholesterol in the target membrane for the efficient membrane anchoring of the toxin.

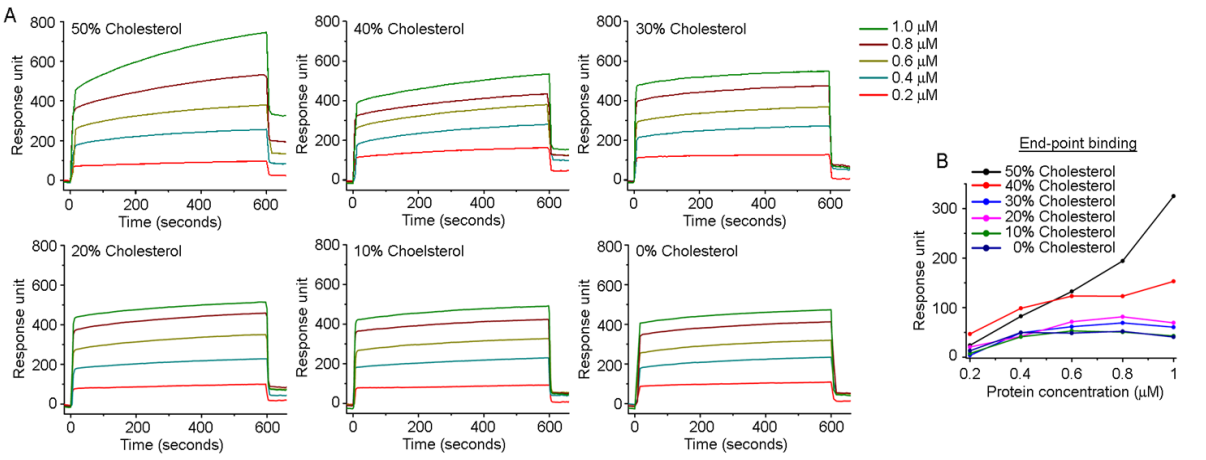

Fig. 21. SPR-based assay to monitor the binding efficacy of VCC towards different asolectin liposomes containing varying cholesterol levels. (A) Overlayed real-time binding sensograms demonstrated the steady-state binding of the VCC to the different liposomes. (B) End-point response analysis showed the increase in irreversible association of VCC with gradual increase in the cholesterol levels in the liposome membrane.

3.6 Enzyme-linked immunosorbent assay (ELISA) for the determination of VCC binding to the liposomes having varying cholesterol content.

ELISA-based assay also demonstrated gradual increase in the binding ability of VCC to the liposomes containing increasing levels of cholesterol. In the liposome membranes lacking cholesterol, or liposomes having limited cholesterol content, VCC displayed low basal level interaction, indicating inefficient binding to the liposomes. Though there seemed to be low basal level association of VCC to the asolectin membranes lacking any cholesterol, the extent of association of VCC increased with increasing cholesterol levels in the liposomes. When liposomes had 30% or more cholesterol content (by weight), VCC associated most efficiently with the liposome membranes. Therefore, there was a gradual increase in the binding of VCC to the membrane lipid bilayer of liposomes with increasing cholesterol content, which suggests that presence of cholesterol is necessary for the binding step of the toxin to the membrane lipid bilayer of liposomes (Fig. 22).

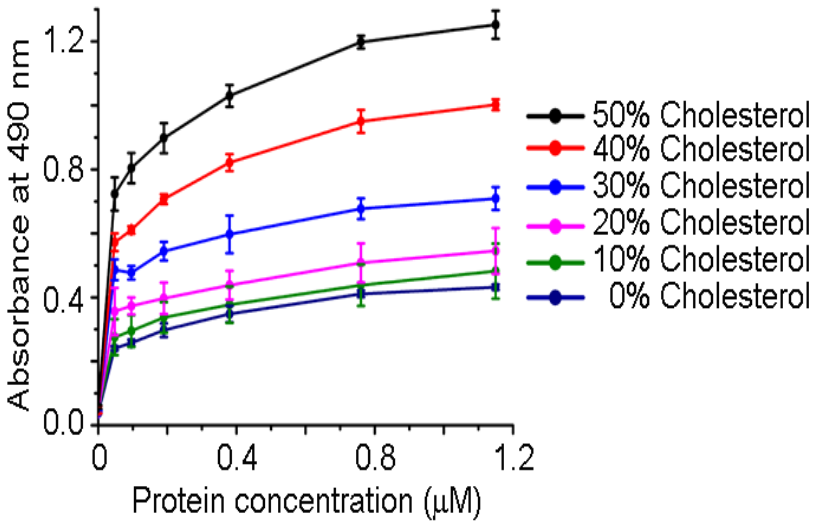

Fig. 22. ELISA-based assay to examine the binding efficacy of VCC with the immobilized asolectin liposomes containing varying cholesterol levels. The extent of association of VCC was monitored by ELISA-based assay which showed progressive increment in the binding of VCC to the asolectin liposomes, containing increasing cholesterol-content.

3.7 Dansyl-FRET-based assay showed that the intimate interaction of VCC with the membrane phospholipid headgroups is critically dependent on the presence of an optimal level of cholesterol in the liposome membranes.

In order to obtain a better understanding of the interaction of VCC with the cholesterol-containing liposomes, we monitored the intimate interaction of VCC with the phospholipid head-groups of the liposomes having varying cholesterol levels. The FRET signal generated from the tryptophan residue(s) in VCC to the dansylated-PE incorporated into the liposome membrane was monitored. VCC displayed time-dependent increase in the FRET signal indicating the intimate interaction and close proximity of the toxin with the phospholipid head-groups of cholesterol-rich liposome membranes. Higher FRET signal was observed in 30% cholesterol, 40% cholesterol and 50% cholesterol-containing asolectin liposomes, suggesting that the intimate interaction tryptophan residues present in the membrane-proximal loop regions of VCC to the dansylated-PE incorporated in the liposome membrane was favoured in the presence of increased membrane cholesterol levels (Fig. 23). The asolectin liposome membranes having less than 30% cholesterol content or the liposome membranes completely lacking cholesterol failed to trigger any detectable FRET signal, indicating that VCC was unable to make close/intimate interactions with such membranes. This result is consistent with the experiments that probed the membrane interaction and binding of the toxin. Hence an optimal level of cholesterol is required in the target membranes for association and intimate interaction of VCC with the phospholipid head-groups of the membrane lipid bilayer of liposomes, as the initial binding step.

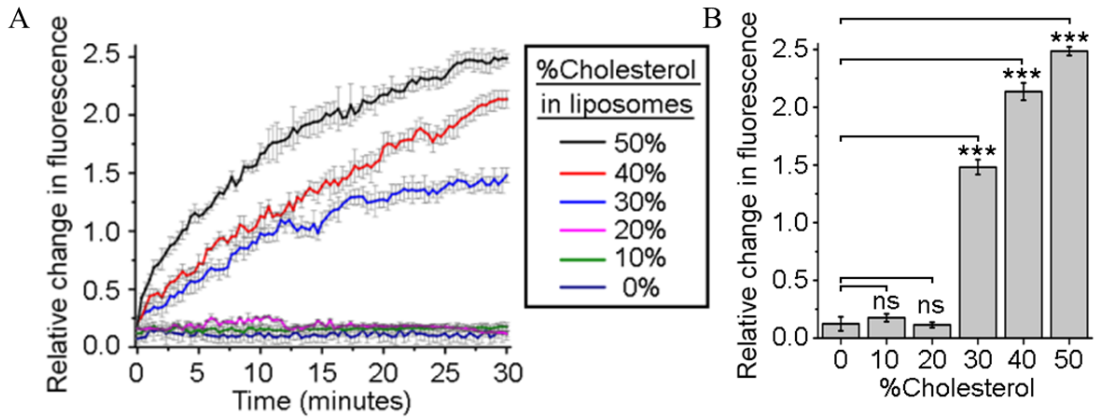

Fig. 23. FRET-based assay for probing the intimate interaction of VCC with the phospholipid head-groups of the membrane lipid bilayer of liposomes. (A) The binding and intimate association of VCC with the phospholipid head-groups of the asolectin liposomes, having varying cholesterol content was probed by monitoring FRET from the tryptophan residue(s) to dansylated-PE FRET incorporated into the membrane lipid bilayer of asolectin liposomes. The assay indicated time-dependent increase in the FRET signal from tryptophan residues in VCC to dansyl-PE incorporated in the asolectin liposomes upon gradual increment in the cholesterol levels. (B) Data represents the average end-point response (±standard deviation) of three independent experiments.

3.8 Oligomerization of VCC in the liposome membranes having varying cholesterol content.

Subsequent to the binding of VCC to the membrane lipid bilayer, oligomerization is the major step required for the formation of functional pore by the toxin. The interaction of monomers within themselves and with the lipid bilayer generates the heat-labile, SDS-stable oligomeric assemblies of VCC on the target lipid membrane. Pull down-based assay was employed to document the oligomerization of VCC in the asolectin liposomes containing varying amount of membrane cholesterol. This assay is similar to the one mentioned above. However, for monitoring the oligomerization step, pellet fraction was taken into consideration only. Here, upon subjecting the reaction mixture to ultracentrifugation, the pellet fraction was collected and incubated under boiled and unboiled conditions in the presence of SDS-PAGE sample buffer. Subsequent SDS-PAGE/Coomassie staining analysis showed that the oligomeric bands were observed prominently in the asolectin liposome

membranes that contained 30%, 40% and 50% cholesterol. In comparison, the liposomes that completely lacked the cholesterol, or had lesser amount of cholesterol (such as 10% and 20% by weight) demonstrated compromised binding. Pull down-based assay clearly revealed reduced binding of VCC to the liposomes having lesser levels of membrane cholesterol, as the boiled fractions indicated very less amount of monomeric form of VCC, and accordingly reduced level of oligomeric bands were observed in such liposomes in the absence of optimal cholesterol levels. However, in the membranes constituted of 30%, 40% and 50% cholesterol (by weight), VCC could efficiently bind to the liposome membranes and these bound fractions of VCC could form the SDS-stable oligomeric assemblies, as observed in the unboiled fractions (Fig. 24). Hence, cholesterol appears to be critical for regulating the initial binding and subsequent oligomerization of VCC in the pore-formation event in the liposome membranes. Absence of optimal levels of cholesterol in the liposome membranes imposed severely compromised binding and thus affected generation of the subsequent oligomer population.

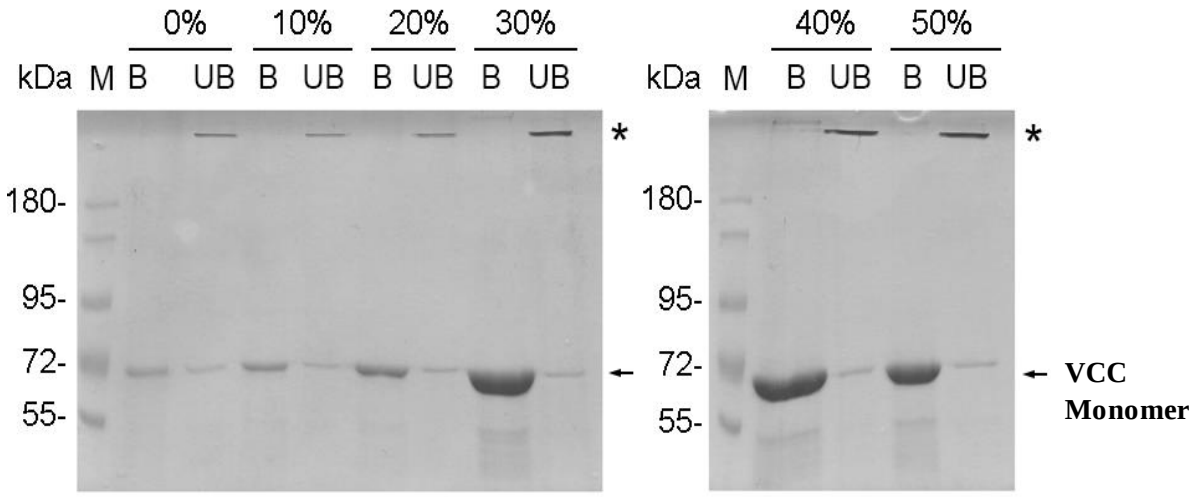

Fig. 24. Pull down-based assay to monitor the ability of VCC to generate SDS-stable oligomeric assemblies in liposomes containing varying amount of cholesterol. SDS-PAGE/Coomassie staining showed the formation of SDS-stable oligomeric species in the UB (unboiled) fractions, indicated by star, in the presence of optimal levels of membrane cholesterol only. B (boiled) fractions represented the monomeric form of VCC associated with the liposome membranes indicated by an arrowhead.

3.9 Membrane insertion of the pore-forming stem loop of VCC into the membrane lipid bilayer of liposomes containing varying level of cholesterol.

After the binding and oligomerization step of VCC, there is insertion of the pre-stem loop of VCC into the membrane which leads to the functional pore-formation. FRET-based assay was employed in order to examine the insertion of the pore-forming pre-stem loop. FRET signal was monitored from Trp318 located within the pre-stem motif to DPH fluorophore which is incorporated into the hydrophobic core of the membrane lipid bilayer. Only upon the insertion of pre-stem loop, Trp318 could effectively form FRET pair with the DPH fluorophore embedded in the liposomes, leading to the prominent FRET signal. Here, the time-dependent increase in FRET signal was observed only when VCC was incubated with the liposomes containing 30% or more cholesterol level. However, in the liposomes devoid of cholesterol or having 10% or 20% cholesterol level, no noticeable Trp-to-DPH FRET signal could be observed upon the addition of VCC (Fig. 25). The significant increase in Trp-to-DPH FRET signal in the presence of optimal levels of cholesterol in the asolectin liposome membranes indicated an efficient membrane-insertion process. In contrast, when the optimal level cholesterol was not present in the liposome membranes, the initial binding step was compromised, further leading to the inefficient oligomer generation and therefore compromised membrane-insertion process was noticed. Gradual increase in the membrane cholesterol levels in the liposomes favoured efficient binding, leading to the subsequent oligomerization as well as insertion of the pre-stem motif of VCC in an efficient manner.

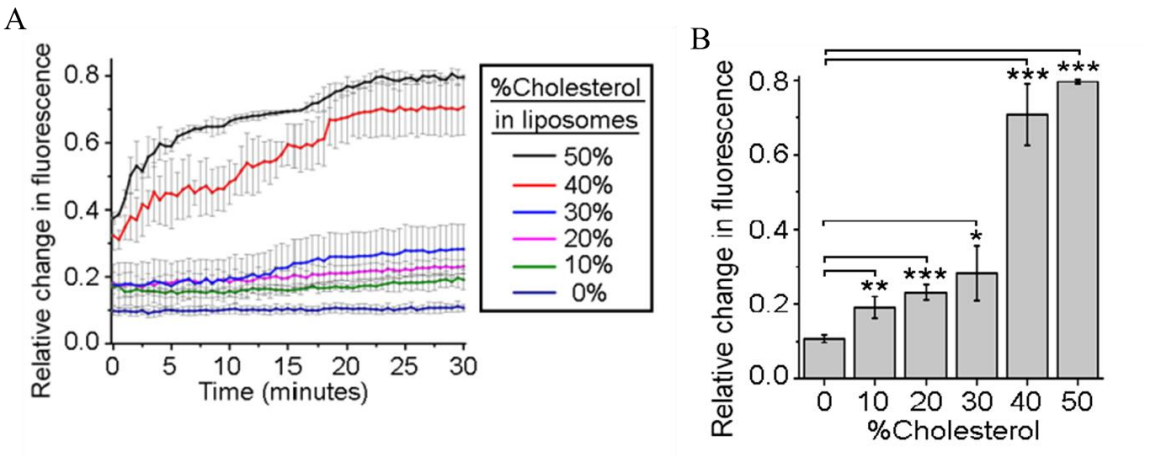

Fig. 25. Tryptophan-to-DPH FRET to probe the insertion of the pre-stem motif of VCC into the membrane lipid bilayer of liposome having varying cholesterol content. (A) FRET from the tryptophan residue (Trp318) within the pore-forming pre-stem region of VCC to DPH in the asolectin liposomes containing varying amount of cholesterol, thus showing the efficacy of the membrane insertion of the pore-forming region of the toxin. (B) Data shown here are the average end-point response (± standard deviation) from three experimental treatments.

3.10 Further insights into the binding process of VCC with the membrane lipid bilayer of liposomes with varying cholesterol levels.

To understand the molecular details of the regulatory mechanism of cholesterol in the binding process of VCC with the liposome membranes, more detailed fluorescence-based studies were performed. There are eleven tryptophan residues in the primary structure of VCC, and these tryptophan residues are distributed, more-or-less uniformly, throughout the molecular structure of the toxin. Therefore, tryptophan fluorescence-based studies were employed to probe the details of the membrane-binding step of VCC, where changes in the tryptophan fluorescence parameters of VCC were monitored upon binding with the asolectin liposome membranes having varying level of membrane cholesterol.

3.10.1 VCC showed increase in the steady-state tryptophan fluorescence anisotropy upon interaction with the membrane lipid bilayer of liposomes containing increased levels of cholesterol.

The steady-state tryptophan fluorescence anisotropy value of any protein is an indicator of the motion (rotational diffusion, in particular) of the tryptophan residues within the protein

molecule. This in turn provided valuable information regarding the shape/size/dynamics of the protein molecule under the specific physicochemical condition. Based on such notion, we explored the changes in the tryptophan fluorescence anisotropy values of VCC in the presence of asolectin liposomes containing varying amount of cholesterol. When VCC interacts efficiently with the liposome membrane, then partitioning of the toxin molecule from the bulk aqueous phase to the two-dimensional plane of the membrane lipid bilayer would be expected to restrict its mobility. This, in turn, would be expected to restrict the fluctuation of the tryptophan residues within the protein structure, thus possibly resulting into the increased tryptophan fluorescence anisotropy values. Consistent with such notion, the tryptophan fluorescence anisotropy values gradually increased with the increasing levels of cholesterol in the asolectin liposomes. Thus, this result confirmed that upon increasing the cholesterol levels in liposome membranes, the interaction ability and binding efficacy of VCC with the liposomes increased progressively that, in turn, presumably resulted into decreased mobility/fluctuation of the membrane-bound toxin molecule(s) (Fig. 26).

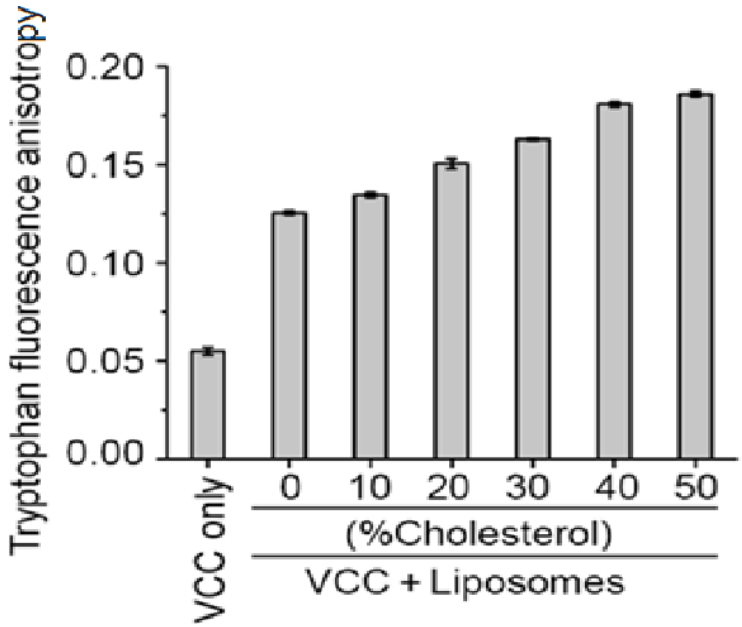

Fig. 26. Tryptophan fluorescence anisotropy of VCC upon interaction with the liposome membranes. The anisotropy values of tryptophan residues in VCC increased with the increasing level of membrane cholesterol in the liposome membrane. This result suggests restricted mobility of the protein intrinsic fluorophore with increasing levels of the membrane cholesterol, indicating efficient interaction of VCC with the liposomes membranes.

3.10.2 Acrylamide quenching of tryptophan fluorescence showed altered solvent exposure of the tryptophan residues in VCC upon association with the cholesterol-rich liposome membranes.

Fluorescence quenching experiment was performed to obtain detailed insights regarding the mode of association of VCC with the membrane lipid bilayer of liposomes. Here, collisional quenching experiment was employed using acrylamide, which can quench the fluorescence of the solvent-accessible tryptophan residues in the protein molecule. Acrylamide quenching experiments were carried out for VCC present in the aqueous buffer, as well as for VCC upon incubation with the asolectin liposomes, with or without cholesterol. Upon comparing the tryptophan fluorescence emission profile in the presence and absence of acrylamide, and calculating the Stern-Volmer constant, we observed that the tryptophan fluorescence of free VCC in the buffer was more strongly quenched in the complete absence of the liposomes. This was presumably due to the solvent-accessibility of the tryptophan residues in the free protein that could be quenched by the acrylamide. However, when VCC was incubated with the asolectin liposomes, there was reduction in the extent of quenching of tryptophan fluorescence. This was possibly due to the basal level association of VCC with the liposome membranes that caused reduction in the solvent-accessibility of the tryptophan residues in VCC. Interestingly, in the case of VCC interaction with 50% cholesterol-containing liposomes, we observed further reduction in the quenching of tryptophan fluorescence. This result suggested that the presence of cholesterol in the liposomes allowed VCC to interact with the membranes in a more intimate manner that possibly resulted into the inaccessibility of the tryptophan residues in VCC for acrylamide quenching.

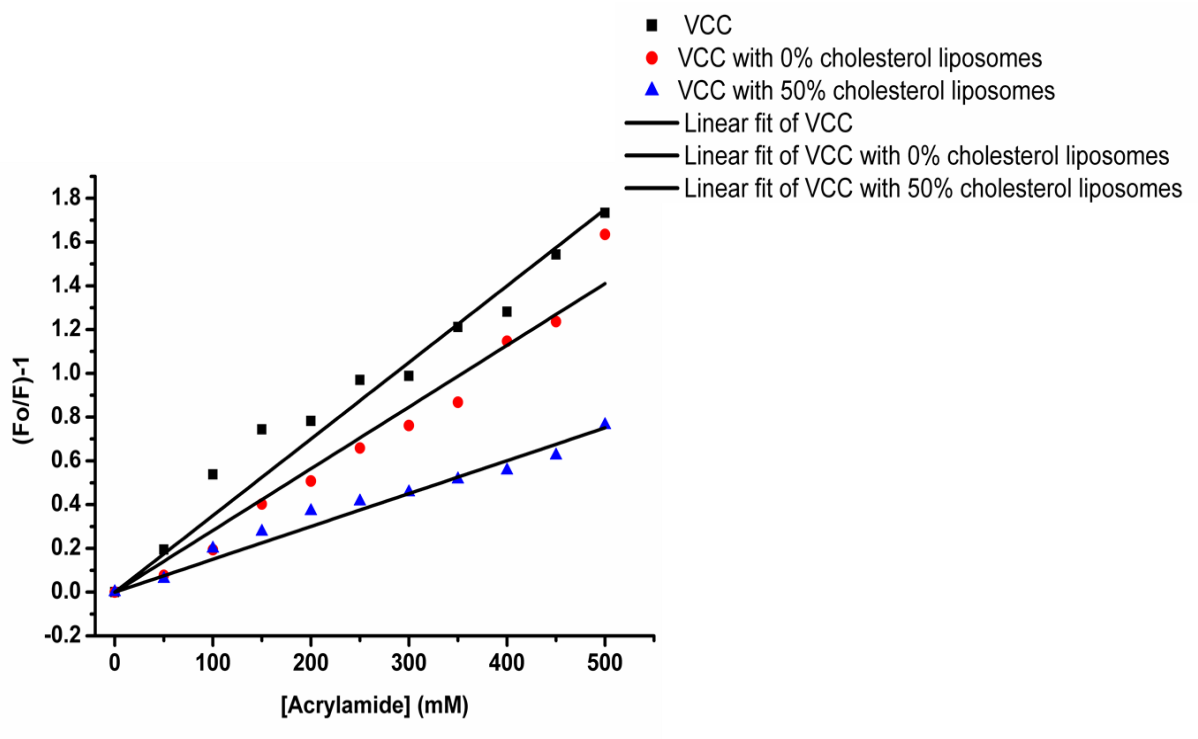

Fig. 27. Stern-Volmer plots for acrylamide quenching of free VCC, and VCC incubated with the liposomes containing cholesterol. Acrylamide prepared in aqueous buffer was added to VCC in buffer, and to VCC incubated with the asolectin liposomes, having no cholesterol and 50% cholesterol (by weight). Here, F_o represents fluorescence intensity in the absence of quencher, while F is the intensity in the presence of quencher, acrylamide. Slope of the graph represents the Stern-Volmer constant.

Representative results from the acrylamide quenching of tryptophan fluorescence in free and liposome-bound form of VCC were analysed in the form of the Stern-Volmer plots. The slope of the Stern-Volmer plot depends on the degree of exposure or accessibility of the tryptophan residues in a protein to the aqueous phase containing acrylamide. Larger value of the slope indicates the larger degree of exposure to the soluble quencher. The Stern-Volmer constant values, calculated for different samples are shown in the table 4. 50% cholesterol-containing liposomes showed more intimate association of VCC as compared to the asolectin liposomes lacking cholesterol, presumably due to differential accessibility of the quencher to the liposome-bound VCC, in the absence or the presence of cholesterol.

Table 4. Stern-Volmer constant determined for free form of VCC and upon incubation with the asolectin liposomes with (50%, by weight) or without cholesterol.

Samples	Stern-Volmer Constant
Free VCC	0.0035
VCC incubated with asolectin liposomes	0.00282
VCC incubated with 50% cholesterol-containing liposomes	0.0015

3.10.3 Time-Correlated Single Photon Counting (TCSPC)-based assay shows an increased tryptophan fluorescence lifetime of VCC in the presence of cholesterol-containing liposomes, presumably due to enhanced binding of the toxin to the membranes.

The mean fluorescence lifetime of the free protein would be expected to be lower than that of the liposome-bound form of VCC. Fitting of the fluorescence decay was performed using the tri-exponential function. The obtained fluorescence intensity decay curves were de-convoluted with the instrument response function (IRS) and the analysis was done as:

$$F(t) = \sum_i \alpha_i \exp(-t/\tau i)$$

F (t) represents fluorescence intensity at time t, and α_i is the pre-exponential factor that represents the fractional contribution for time-resolved decay. When χ^2 value is minimum, preferably less than 1.4 and plots of the weighted residuals along with an auto-correlation function exhibit random deviation about zero, then the fit is acceptable.

The mean fluorescence lifetime of tryptophan residues of VCC is mentioned in the table and calculated using the following equation using the decay times and pre-exponential factors:

$$\langle\tau\rangle = \frac{\alpha_1\tau_1^2 + \alpha_2\tau_2^2 + \alpha_3\tau_3^2}{\alpha_1\tau_{1+} \alpha_2\tau_{2+} \alpha_3\tau_3}$$

Measurement of the fluorescence lifetime imparts information of the local environment and polarity where the specific fluorophore is confined. The fluorescence lifetime decay profile of VCC upon incubation with 0% and 50% cholesterol-containing liposomes, with tri-exponential fitting and calculated goodness of fit are shown in figure 28.There was increase in the mean fluorescence lifetime of VCC in the presence of the 50% cholesterol-containing asolectin liposomes, as compared to that in the presence of liposomes lacking any cholesterol. This can be attributed to the increased non-polar environment surrounding the tryptophan residues, presumably due to more efficient binding /interaction of the protein with 50% cholesterol-containing liposomes. Thus more fluorescence lifetime in the presence of the 50% cholesterol-containing (by weight) liposomes suggests enhanced binding and lesser solvent accessibility toward the tryptophan residues in VCC.

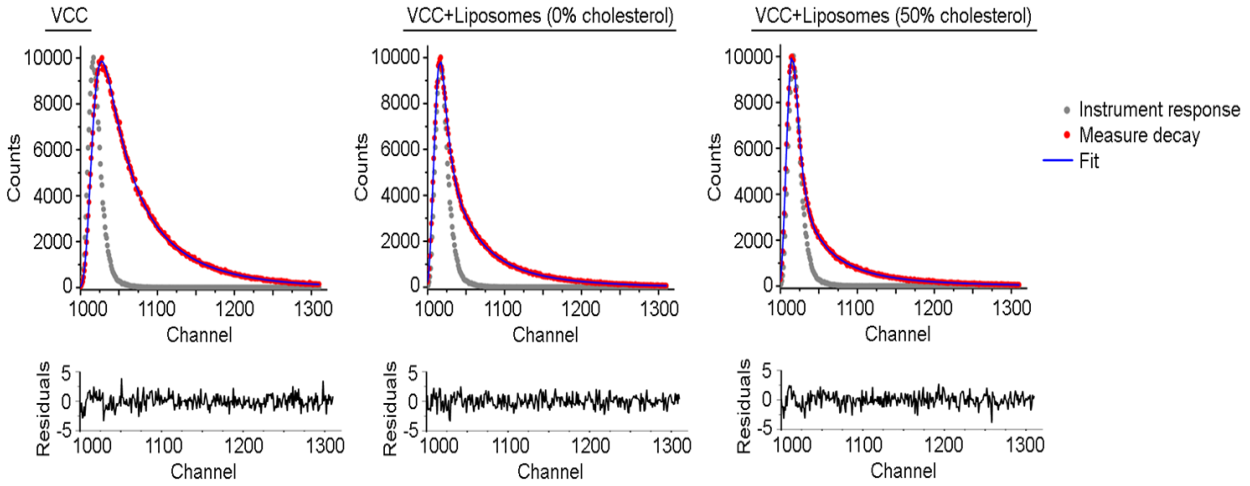

	α_1	τ_1*	α_2	τ_2*	α_3	τ_3*	<τ>*	χ^2
VCC	0.3287	1.48	0.6713	4.059	-	-	3.67	1.137
VCC+Liposomes (0% cholesterol)	0.1678	1.915	0.1675	5.007	0.6647	0.02248	4.09	1.056
VCC+Liposomes (50% cholesterol)	0.1474	2.159	0.7467	0.02378	0.1058	6.486	5.027	1.128

*in nanoseconds

Fig. 28. TCSPC showing mean fluorescence lifetime of VCC in the free form, and upon incubation with the asolectin liposomes with (50%, by weight) or without cholesterol. Excitation wavelength of 295 nm with pulsed diode laser source was used. The left-sided sharp peak defines the profile of pulsed laser emitting diode (LED), while the right-sided broad peak represents the decay profile of VCC, upon fitting the equation to obtained data.The averaged calculated τ values indicated in the table represent the mean lifetimes of all the three samples.

3.11 VCC exhibits direct interaction with cholesterol even in the absence of membrane lipid bilayer.

We wanted to examine whether VCC could interact with free cholesterol in the absence of the membrane lipid bilayer. To examine the interaction of VCC with pure cholesterol in the absence of membrane lipid bilayer, we performed pull-down-based assay and lipid dot blot assay. These results showed the ability of VCC to bind to free cholesterol in suspension, even in the absence of membrane lipid bilayer. Varying levels of cholesterol and VCC were incubated together in suspension, the reaction mixture was centrifuged and the pellet was subjected to SDS-PAGE/Coomassie staining analysis. This result suggested direct binding of VCC to pure cholesterol in suspension (Fig. 29A). Further, in the lipid dot blot assay, different amounts of cholesterol were immobilized by spotting onto the nitrocellulose membrane. Subsequently, it was incubated with VCC, which indicated direct interaction of VCC with immobilized cholesterol. VCC interacting with the spotted cholesterol was probed by immunoblotting using Anti-VCC antiserum (Fig. 29 B).

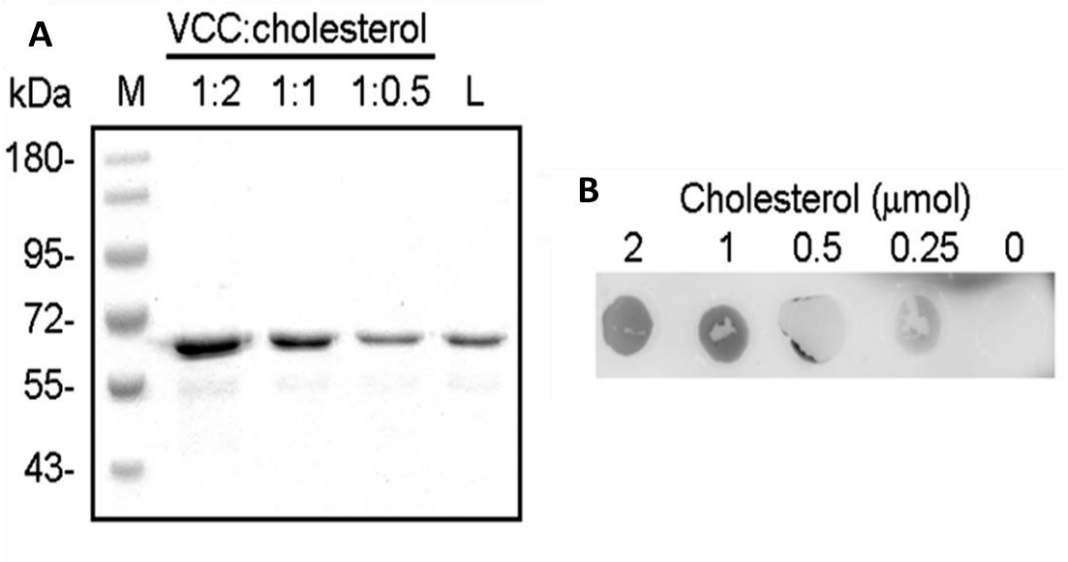

Fig. 29. Monitoring direct association and binding ability of VCC with cholesterol. VCC is capable of interacting with pure cholesterol in solution as indicated by SDS-PAGE/ Coomassie staining analysis (shown in A), and even when cholesterol is immobilized onto the nitrocellulose membrane (shown in B).

Next, in order to test the functional implications of the direct interaction of VCC with cholesterol, we checked whether pre-incubation of VCC with cholesterol in suspension could block the hemolytic activity of VCC against the human erythrocytes. The hemolytic activity profile indicated complete inhibition of the pore-forming activity of VCC against human erythrocytes, when VCC was incubated with twice the amount of cholesterol (by weight). A dose-dependent reduction in the hemolytic activity of VCC could be observed upon pre-incubation of the toxin with gradually increasing amount of cholesterol. This data confirmed that the direct interaction of VCC with cholesterol could possibly act to block subsequent membrane-damaging pore-forming hemolytic activity of the toxin (Fig. 30).

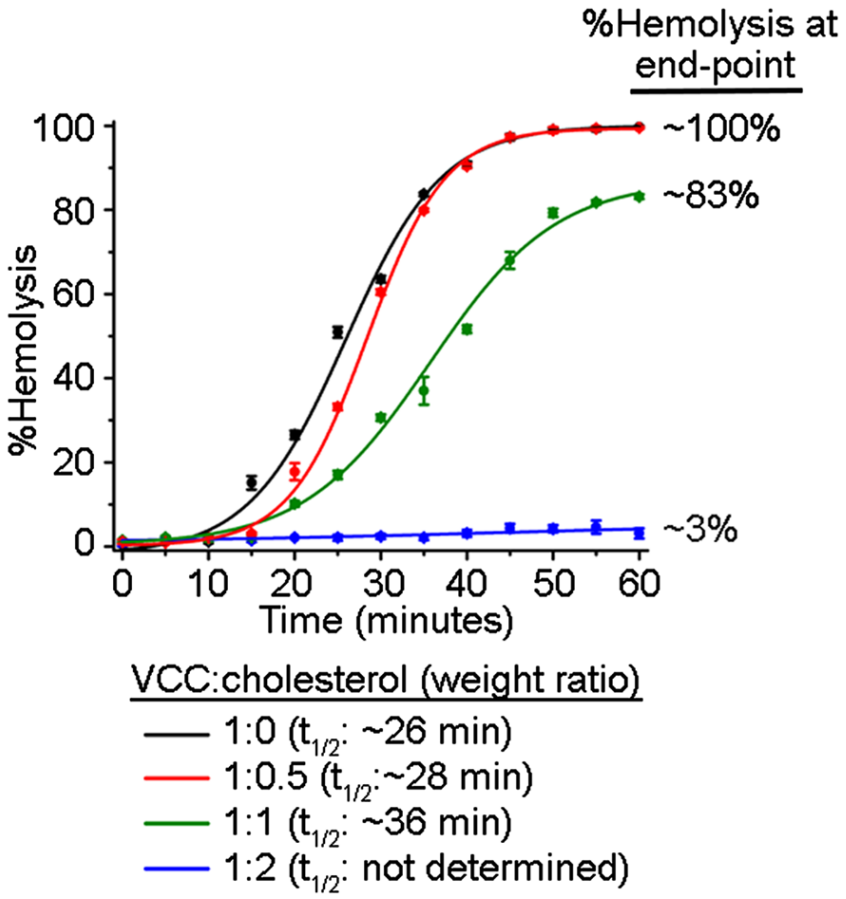

Fig. 30. Inhibition of hemolytic activity of VCC upon prior interaction with cholesterol in suspension. The decrease in hemolytic activity was confirmed by the increase in the $t_{1/2}$ of the rate of hemolysis upon increasing the amount of cholesterol employed. VCC was pre-incubated with varying amount of cholesterol in suspension (with varying VCC:cholesterol weight ratio). Subsequently, hemolytic activity of VCC was monitored against the human erythrocytes. Data shown here are the average %hemolysis (± standard deviation) from three independent experimental treatments.

3.12 Exploring the physiological significance of membrane cholesterol in regulating the pore-formation mechanism of VCC.

3.12.1 Cholesterol-depletion from the human erythrocyte membranes critically impairs the functional pore-formation mechanism of VCC.

In order to explore the physiological relevance of the membrane cholesterol for the pore-formation mechanism of VCC against the biomembranes, the membrane-damaging hemolytic activity of VCC against the human erythrocytes was monitored upon depletion of cholesterol from human erythrocytes membranes. Methyl-β-cyclodextrin (mβCD), a well-characterized cholesterol-sequestering agent, was employed to deplete erythrocytes membrane cholesterol. The human erythrocytes, upon pre-treatment with mβCD, were treated with VCC in order to examine how the different steps of pore-formation event are being regulated by the membrane cholesterol.

The cell-type, the concentration of mβCD used, and the time of its incubation determine the extent of cholesterol-depletion by mβCD. To ensure and estimate the depletion of cholesterol from the membranes, cholesterol levels were estimated upon mβCD treatment. Also the cholesterol-content in the erythrocytes membranes was estimated upon replenishing back the cholesterol. Cholesterol levels were estimated in the replenished cells to monitor the replenishment efficacy of the mβCD:cholesterol complex (Fig. 31).

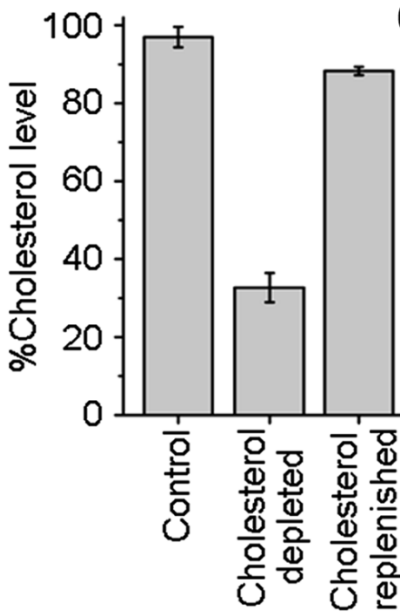

Fig. 31. Monitoring the effect of 5 mM mβCD treatment on the cholesterol levels of the human erythrocytes membranes. Estimating the cholesterol levels of human erythrocyte membranes revealed that 5 mM mβCD was capable of depleting nearly 65% of cholesterol, compared to the control untreated erythrocytes. Also the cholesterol level was restored to the near-normal level upon replenishment with mβCD:cholesterol complex. The control here represents human erythrocytes without any pre-treatment. Data shown here is the representative of two independent experiments.

Pre-treatment of human erythocytes with 1 mM mβCD did not result in any noticeable changes in the hemolytic activity of VCC. The treatment of erythrocytes with 2.5 mM mβCD, prior to VCC treatment, resulted in noticeable inhibition in the hemolytic activity. Upon incubating human erythrocytes with 5 mM mβCD, where nearly 65% cholesterol was depleted from the membranes compared to the control, the hemolytic activity was severely compromised (Fig. 32).

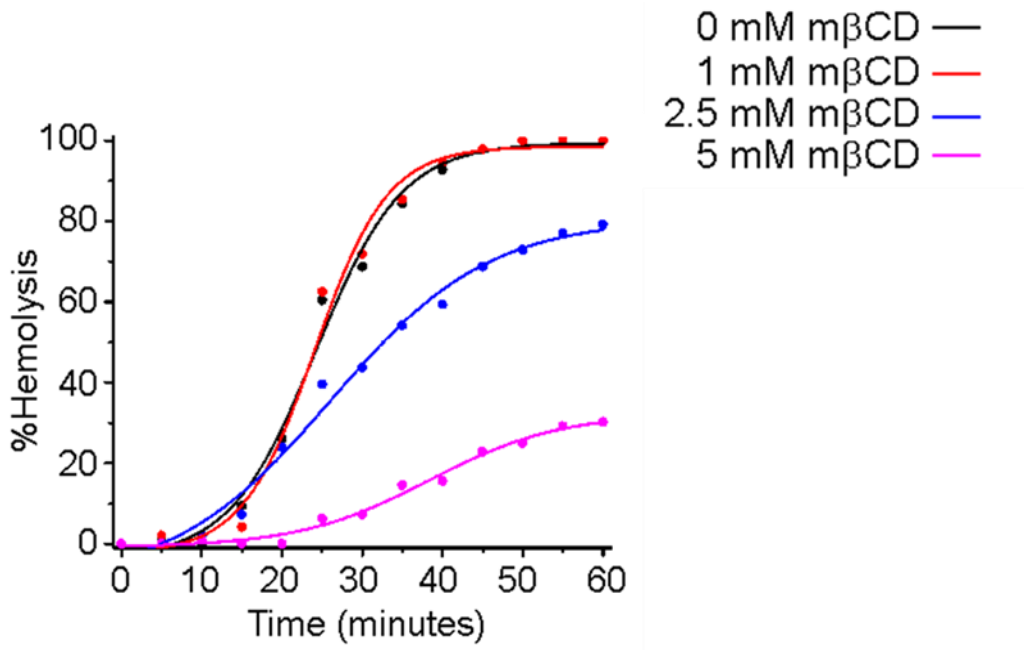

Fig. 32. Hemolytic activity of VCC upon depletion of membrane cholesterol from the human erythrocytes. Human erythrocytes were pre-incubated with the indicated concentrations of mβCD, and then subsequently hemolytic activity of VCC was monitored. The result clearly indicates that the depletion of membrane cholesterol in erythrocytes severely affects the hemolytic activity of VCC.

Further we monitored the hemolytic activity of VCC in human erythrocytes upon replenishment of cholesterol back to the erythrocytes membrane, using mβCD:cholesterol complex. The hemolytic activity appeared to be regained to the similar extent as observed with the control. This data clearly indicates that the hemolytic ability of VCC could be regained back to the normal level if the cholesterol levels are replenished in the target membranes. Altogether, these results suggest that cholesterol plays a crucial role for the pore-forming hemolytic activity of VCC in the erythrocytes membranes (Fig. 33).

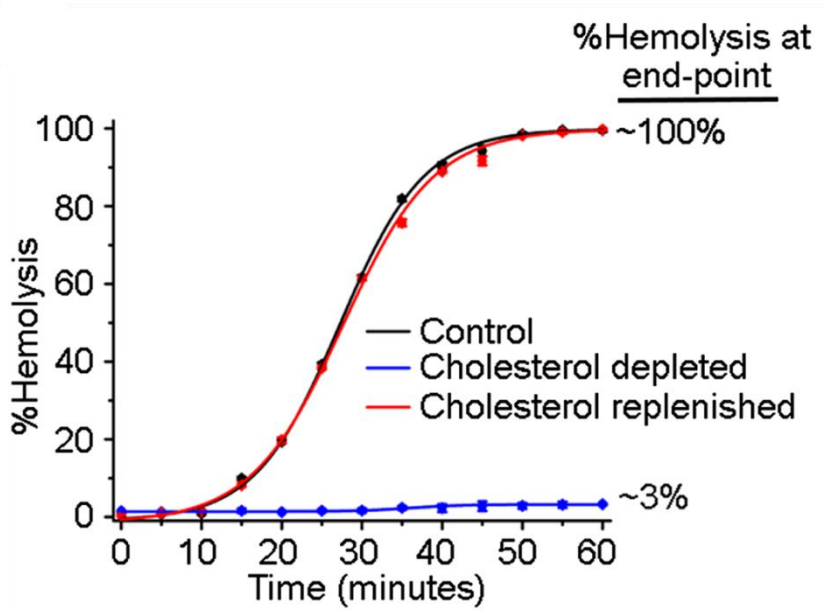

Fig. 33. Hemolytic activity of VCC upon pre-treatment of human erythrocytes with 5 mM mβCD, and after cholesterol replenishment. Pre-treatment of human erythrocytes with 5 mM mβCD completely abrogated the hemolytic activity of VCC due to depletion of the membrane cholesterol. Further, replenishment back of the membrane cholesterol in the human erythrocytes leads to regaining of the hemolytic activity of VCC to a similar extent as observed for the control.

This data clearly showed that the hemolytic activity of VCC is dictated by the cholesterol content of the erythrocytes membranes. Hence, the presence of optimal level of cholesterol appears to be critical in the biomembranes for the execution of the functional pore-formation. VCC is unable to induce hemolytic activity when cholesterol is depleted from the membranes, as the target membranes lack the required optimum levels of cholesterol.

3.12.2 Depletion of membrane cholesterol leads to compromised binding efficacy of VCC toward the human erythrocytes cell surface.

We wanted to examine the effect of depletion of membrane cholesterol on the membrane-binding ability of VCC. For this, we employed the flow cytometry-based assay, where human erythrocytes were subjected to 5 mM mβCD pre-treatment for the depletion of membrane cholesterol, and then subsequently examined the binding efficacy of VCC toward these cells.

Binding assay was performed at 4 °C, as VCC only exhibits binding at this low temperature, and the subsequent oligomerization and pore-formation steps are arrested. Hence, the binding efficacy of VCC could be specifically monitored upon cholesterol depletion at this lower temperature. The flow-cytometric profile showed a pronounced reduction in the binding ability of VCC to the cholesterol-depleted human erythrocytes cell surface, compared to the erythrocytes without cholesterol depletion serving as control (Fig. 34). This result clearly suggests the requirement of cholesterol for the efficient binding of VCC to the target erythrocytes cell membranes. It is important to note that a nominal basal-level binding was observed in the cholesterol-depleted cell membranes. Such residual binding activity was presumably due to interactions of VCC with the other cell-surface molecules present in the biomembranes, such as cell surface glycans. Such interactions were possibly still operational even in the absence of an optimal level of membrane cholesterol in the erythrocytes membranes. Accordingly, the binding was not completely abolished. Altogether, these observations suggest that the presence of an optimal level of cholesterol in the human erythrocytes cell membranes is crucial for the efficient membrane binding of VCC. However, even in the absence of an optimal level of membrane cholesterol, VCC could display nominal basal level binding suggesting that the presence of cholesterol is not obligatory for the binding of VCC to the human erythrocytes cell surface.

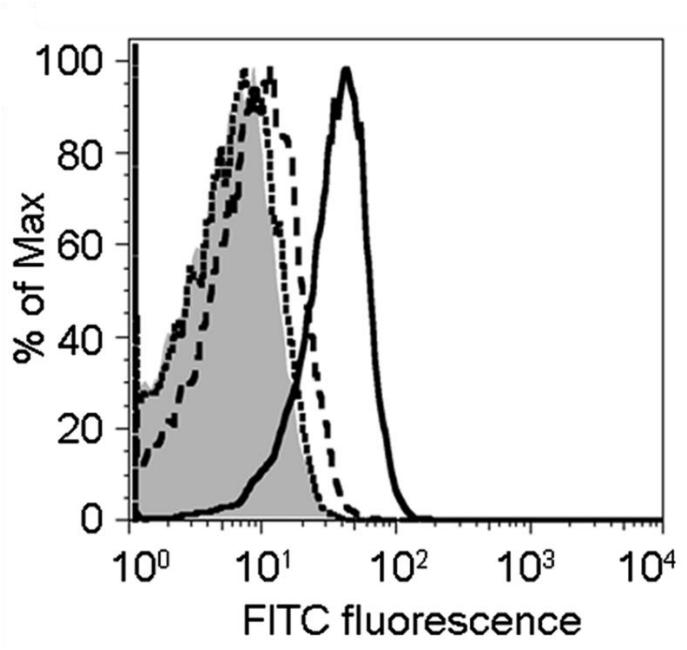

Fig. 34. Flow cytometry-based assay of binding of VCC toward human erythrocytes upon depletion of membrane cholesterol. The binding efficacy of VCC toward the human erythrocytes is compromised upon depletion of membrane cholesterol using 5 mM mβCD, as indicated by the dashed line. The solid line represents binding ability of VCC toward human erythrocytes without any mβCD pre-treatment, acting as a control. Shaded peak represents the buffer control without any protein treatment.

3.12.3 VCC generates non-functional, abortive oligomeric assemblies in the absence of optimal levels of cholesterol in the human erythrocytes membranes.

As indicated by the flow cytometry-based assay, there is reduction in the binding efficacy of VCC upon cholesterol depletion from the erythrocyte membranes. However, nominal basal level binding of VCC was observed in the cholesterol-depleted membranes. It is possible that the pre-treatment with 5 mM mβCD could not completely deplete the membrane cholesterol. Hence, the residual cholesterol in the human erythrocytes membranes could contribute towards the binding of VCC molecules. Also, the erythrocyte membranes harbour several cell surface molecules that could provide the accessory interactions for the binding of VCC. Hence, we wanted to explore whether the membrane-associated fraction of VCC could generate the oligomeric assemblies on the cholesterol-depleted erythrocytes membranes. For

this, the human erythrocytes, upon treatment with 5 mM mβCD, were subjected to pull down-based assay. At 25 °C, the cholesterol-depleted human erythrocytes were incubated with VCC and then the reaction mixture was ultracentrifiged. The pellet fraction obtained by ultracentrifugation was probed by SDS-PAGE and immunoblotting under unboiled condition in the presence of SDS-PAGE sample buffer. The result showed that the fraction of VCC bound to the erythrocytes membranes could undergo oligomerization and form SDS-stable oligomeric assemblies, to a similar extent to that of the control (Fig. 35). This assay was carried out at 25 °C. Thus the reduced binding ability of VCC upon cholesterol-depletion could be compensated by multiple accessory interactions that come into play at this temperature. The result of this assay demonstrated that VCC was capable of binding to the cholesterol-depleted erythrocytes membranes, presumably with the help of the cholesterol-independent multiple accessory interactions provided by the cell-surface molecules, and the membrane-associated fractions of VCC formed oligomeric assemblies generating SDS-stable oligomers. However, the oligomeric assemblies appear to be abortive in nature in the absence of optimal levels of cholesterol. Cholesterol is thus appearing to be critical for the formation of functional pores which leads to functional hemolytic activity. This result also indicates that cholesterol is presumably critical for the membrane-insertion of the pore-forming motif and functional pore-formation step, in the case of biomembrane of human erythrocytes.

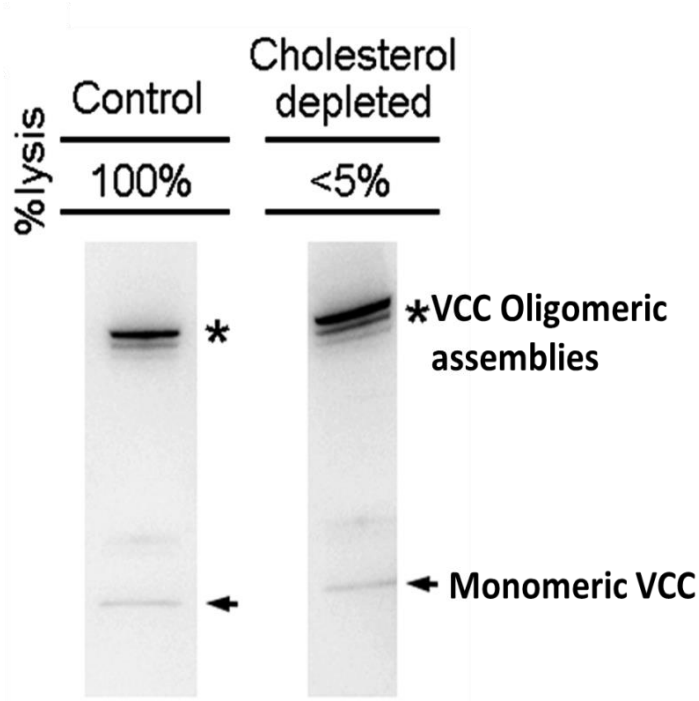

Fig. 35. Oligomerization propensity of VCC upon cholesterol depletion in the human erythrocytes membranes. VCC forms non-functional, abortive, SDS-stable oligomeric assemblies in the human erythrocytes membranes upon the depletion of the membrane cholesterol by 5 mM mβCD, as shown by the the pull down-based assay followed by SDS-PAGE/immunoblotting. Here, the oligomers are represented by * and VCC monomers are indicated by an arrow. Data shown here is the representative of two independent experiments.

Surprisingly, the non-functional abortive oligomers generated upon cholesterol-depletion in the human erythrocytes could revert back to the functional form of transmembrane pores upon replenishment of the cholesterol levels in the human erythrocytes cell membranes. This was confirmed by the regain of hemolytic activity of VCC upon the replenishment of cholesterol back after the depletion. VCC could exhibit hemolytic activity upon supplementing back the membrane cholesterol, confirming further the obligatory requirement of cholesterol in the pore-formation mechanism of VCC in human erythrocytes (Fig. 36).

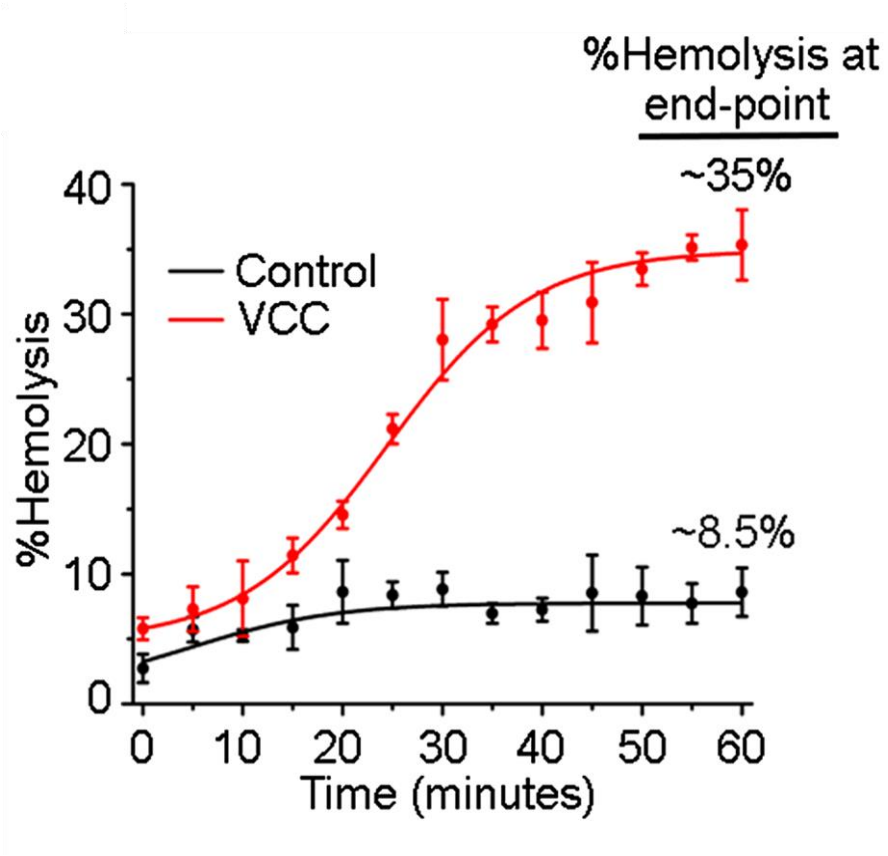

Fig. 36. Hemolytic activity of VCC upon replenishment of the membrane cholesterol, subsequent to VCC-binding with the cholesterol-depeleted erythrocytes membranes. The ability of VCC to cause the lysis of human erythrocytes is regained to some notable extent, upon replenishing back the cholesterol levels in the human erythrocytes membranes. Human erythrocytes were subjected to cholesterol-depletion by treatment with 5 mM mβCD, and then treated with VCC. Cells upon washing with PBS were subjected to cholesterol replenishment using mβCD: cholesterol complex. Then the cells were washed with PBS, resuspended in PBS and monitored for hemolysis. The control here represents cells pre-treated with 5 mM mβCD, followed by treatment with mβCD: cholesterol complex, without any VCC treatment, which was also monitored for hemolysis. An equivalent amount of cells with VCC treatment only were used to obtain the maximum 100% hemolysis. Profile shown here is the representative of average %hemolysis ± standard deviation from three independent experimental treatments.

3.13 VCC exhibits marked tendency to sequester into the cholesterol-rich fractions in the human erythrocytes membranes.

Altogether, our results so far suggest that the presence of membrane cholesterol is critical in governing the pore-formation mechanism of VCC in human erythrocytes cell membranes. Interaction of VCC with cholesterol is an obligatory requirement for its pore-formation mechanism. Exploring further in this direction, we wanted to investigate whether VCC

displays any propensity to interact with the cholesterol-rich membrane micro-domains, commonly designated as the lipid rafts in the human erythrocytes membranes. VCC was incubated with human erythrocytes at 4 °C. Subsequently, cell lysate was prepared by detergent-solubilisation, and subjected to the density-gradient ultracentrifugation that allows the efficient separation and isolation of lipid-raft micro-domains in the form of lighter, buoyant fractions. To confirm the presence of cholesterol-rich lipid rafts in the isolated fractions, cholesterol-content of all the isolated fractions was estimated (Fig. 37). The result of this estimation showed that the cholesterol content was significantly higher, mainly in the fractions 8-12, representing the cholesterol-rich membrane fractions.

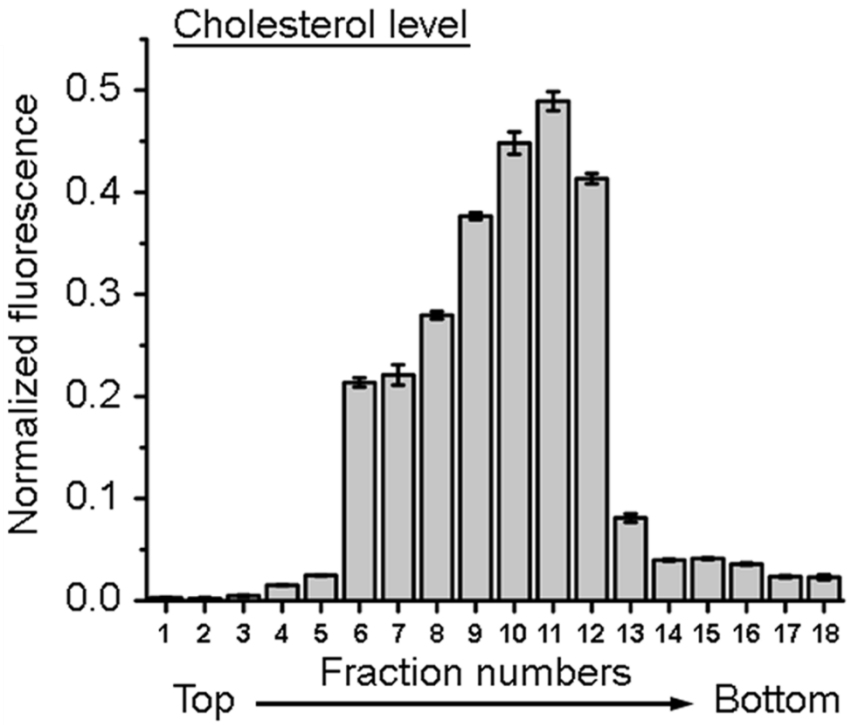

Fig. 37. Estimation of the cholesterol content in the isolated membrane fractions from the human erythrocytes upon VCC incubation. Upon subjecting human erythrocytes to detergent solubilisation and fractionation via density-gradient ultracentrifugation, subsequent to treatment with VCC or CtxB, cholesterol content of the isolated fractions was estimated. Higher cholesterol content was found majorly in the fractions 7-12, thus indicating these fractions to be the probable raft-containing fractions. Profile shown is the representative of two independent experiments.

The isolated membrane fractions were then probed for the presence of VCC, a raft-specific protein Flotillin-1, and a non-raft marker, transferrin receptor (TfR), using the dot-blot assay. The assay showed that significant fraction of VCC was segregated into the fractions 10-11 out of the total 18 fractions. Similarly, flotilin-1 was also segregated into the fractions 10-12. These fractions represented lighter, detergent-resistant fractions, which are rich in cholesterol-content, precisely representing the so-called membrane lipid raft-like fractions. To confirm, an additional raft-marker protein, Cholera Toxin B subunit (CtxB) was also probed. Human erythrocytes were treated with CtxB and then subjected to the membrane fractionation, as described above. The dot-blot assay showed the presence of CtxB in the fractions 10-11, which represent the cholesterol-rich fractions. Hence the lighter, cholesterol-rich fractions 10-11 represented the cholesterol-rich membrane fractions where VCC, Flotillin-1 and CtxB tend to seggregate. Thus, VCC exhibited marked propensity to associate with the cholesterol-enriched membrane lipid micro-domains as the prominent fraction of VCC appeared to be present in the fractions 10-11. However, TfR was mainly observed to be present in the heavier, detergent-soluble non-raft fractions 14-18, having nominal levels of cholesterol (Fig. 38). Thus, these results indicated that the major fraction of VCC tends to migrate to the cholesterol-rich membrane fractions, where the so-called raft markers are also segregated. The immunoblot analysis of the isolated fractions also displayed significant amount of VCC in the lighter, cholesterol-rich membrane fractions, represented mainly by the fraction number 10-12 (Fig. 39)

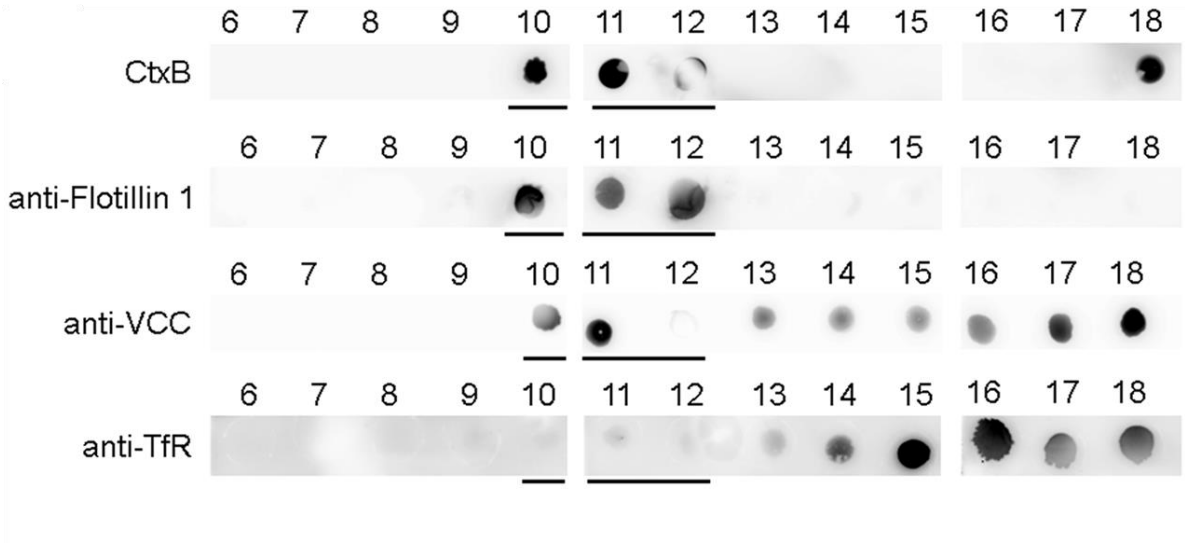

Fig. 38. Dot-blot assay demonstrating association of VCC with the cholesterol-rich membrane fractions in human erythrocytes. The analysis of isolated membrane fractions from the human erythrocytes upon VCC treatment depicts VCC to partition to the cholesterol-rich lipid raft domains, indicated by fractions 10 and 11 (underlined). Raft markers CtxB and Flotillin-1 are also found in these fractions mostly. Transferrin receptor (TfR), a non-raft marker, however is migrating towards the lower detergent-soluble fractions, indicating the non-raft fractions. The lighter detergent-insoluble fractions 10-12 are marked with 'underline'.

.

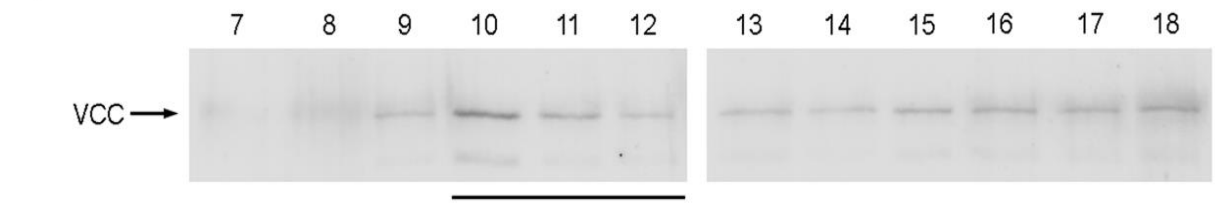

Fig. 39. Immunoblot analysis of the isolated membrane fractions from human erythrocytes upon treatment of VCC. The SDS-PAGE/immunoblot analysis suggests prominent fraction of VCC to be segregated into the cholesterol-rich membrane fraction of human erythrocytes. Presence of VCC in the fractions 10-12 is marked with 'underline'.

The binding and partitioning of VCC with the raft-like membrane micro-domains on human erythrocytes was further confirmed by confocal microscopy-based colocalization assay. Here, VCC demonstrated marked tendency to colocalize with CtxB, which is a conventional raft marker. CtxB exhibits binding towards GM1-ganglioside enriched within the membrane lipid rafts. Significant colocalization of VCC with CtxB confirmed the propensity of VCC to

associate with the cholesterol-rich membrane lipid rafts in the erythrocytes membranes (Fig. 40). (Courtesy: Dr. Samarjit Bhattacharyya, Rohan Sharma and Anish Kumar Mondal).

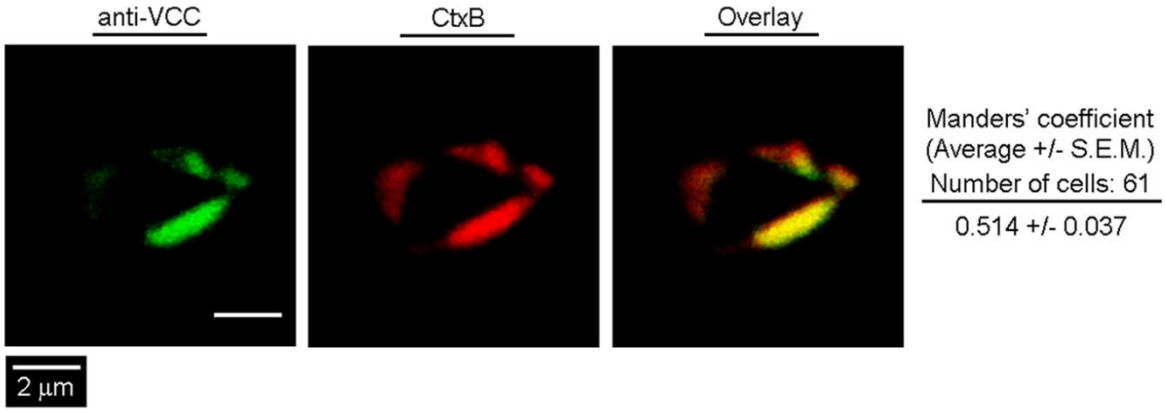

Fig. 40. Colocalization of VCC with CtxB indicates marked propensity of the toxin to associate with the cholesterol-rich lipid raft fractions in the erythrocytes membranes. Confocal microscopy images show marked tendency of VCC to colocalize with the raft-specific marker protein CtxB. The calculation of Mander's coefficient was done based on the analysis of 61 cells, from three independent experiments. S. E. M., standard error of mean.

In the same direction, we wanted explore the effect of cholesterol depletion (upon treatment with 5 mM mβCD) on the distribution of VCC in the human erythrocytes membrane fractions. The human erythrocytes were pre-treated with 5 mM mβCD, then were treated with VCC, and then the prepared cell lysates were subjected to the density-gradient ultracentrifugation, as described above. Cholesterol estimation of the isolated membrane fractions showed that mβCD treatment resulted into drastic reduction in the cholesterol levels in the lighter, detergent-insoluble fractions. Only a nominal basal level cholesterol was detected in the range of fractions from 6-18, presumably due to the disruption of cholesterol-rich raft-like membrane microdomains. The sequestration of membrane cholesterol by mβCD seems to perturb the integrity of raft domains, generating the low basal level distribution of cholesterol over these fractions (Fig. 41).

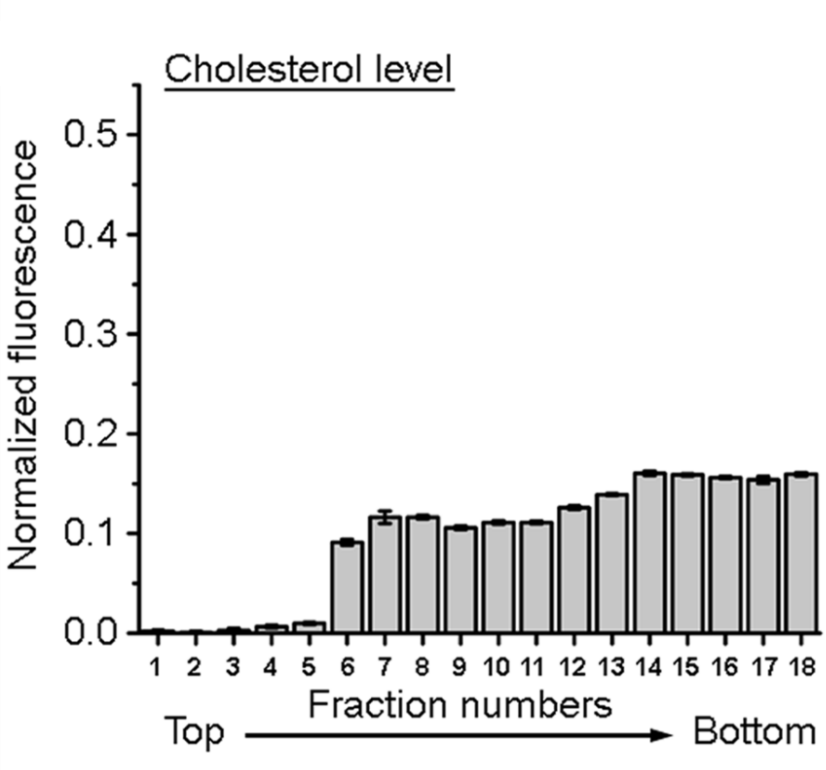

Fig. 41. Determination of the cholesterol content in the isolated membrane fractions from human erythrocytes, upon pre-treatment with 5 mM mβCD. The membrane cholesterol level was decreased, and low basal level cholesterol was detected throughout the fractions 6-18. Prior treatment of human erythrocytes with 5 mM mβCD seems to have disrupted the distribution of cholesterol in the lighter detergent-resistant membranes fractions.

The membrane fractions that were isolated upon pre-treatment of human erythrocytes with 5 mM mβCD, were subsequently probed for the presence of VCC, raft marker Flotillin-1 and the non-raft marker Transferrin receptor, by the dot-blot assay. VCC, CtxB and Flotillin-1 appeared to be equally distributed among the various isolated fractions, rather than being confined to the specific lighter, detergent-resistant membrane fractions. Hence, cholesterol depletion by mβCD resulted into VCC and raft-specific markers flotillin-1 and CtxB to get distributed over the range of membrane fractions, as observed in the dot-blot profile (Fig. 42).

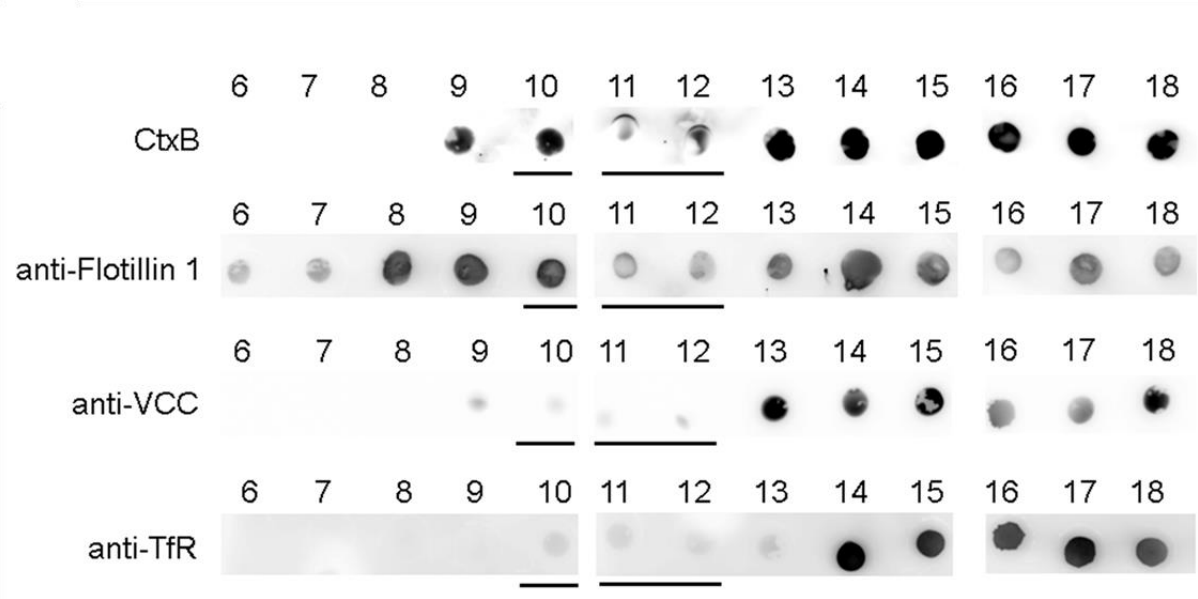

Fig. 42. Dot-blot profile of the isolated membrane fractions upon treatment of human erythrocytes with 5 mM mβCD. Human erythrocytes were treated initially with 5 mM mβCD for the depletion of the membrane cholesterol, and then upon incubation with VCC, isolated membrane fractions were probed for the association of VCC with the detergent-resistant, lighter membrane fractions. VCC, as well as the raft markers were found to be distributed over a range of detergent-soluble and detergent-resistant membrane fractions. VCC is found to be present mostly in the detergent-soluble fractions, where the non-raft protein TfR is enriched.

The immunoblot analysis of the isolated membrane fractions after cholesterol-depletion of human erythrocytes also demonstrated that VCC was associated with the detergent-soluble fractions, predominantly in fractions 13-18 with major fraction of protein being sequestered in fractions 16-18. (Fig. 43).

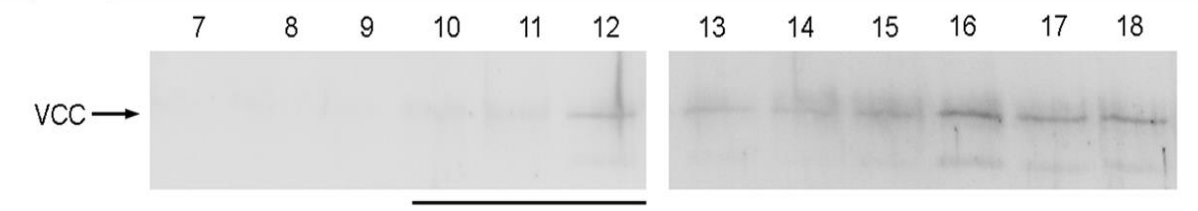

Fig. 43. Immunoblot analysis showing the pattern of association of VCC in the isolated membrane fractions upon cholesterol depletion. The pre-treatment of human erythrocytes with 5 mM mβCD resulted into association of VCC mostly in the detergent-soluble fractions.

In sum, these results suggest a marked propensity of VCC to associate with the cholesterol-rich lipid raft-like membrane micro-domains in human erythrocytes. The mβCD treatment, which leads to the efficient depletion of the membrane cholesterol, can cause the disruption of cholesterol-enriched membrane micro-domains in human erythrocytes. This disruption leads to the re-distribution of VCC to the non-raft fractions.

3.14 Mutation of the cholesterol-dependent membrane-interaction ability of VCC exhibits compromised association of VCC with cholesterol in suspension, without affecting its association with the cholesterol-rich membrane micro-domains in human erythrocyte membranes.

A mutant variant of VCC, harbouring the point mutation of Ala425Val in the membrane-proximal loop region of the toxin has been shown earlier to abrogate the functional pore-formation ability, by compromising the cholesterol-dependent membrane interaction mechanism (14). This mutant variant of VCC, when tested for the direct interaction with cholesterol in suspension in the absence of any membrane lipid bilayer, showed its inability to associate and bind to the cholesterol, as depicted by the pull down-based assay (Fig. 44A). When this mutant variant of VCC was tested for its association propensity with the cholesterol-rich fractions in the human erythrocytes membranes, it displayed nearly similar tendency to sequester into the lipid raft-like membrane micro-domains, as observed with the wild type toxin. Hence, disruption of the cholesterol-dependent interactions, via Ala425Val mutation in VCC, did not affect the association of mutant with the cholesterol-rich membrane micro-domains in human erythrocytes (Fig. 44B).

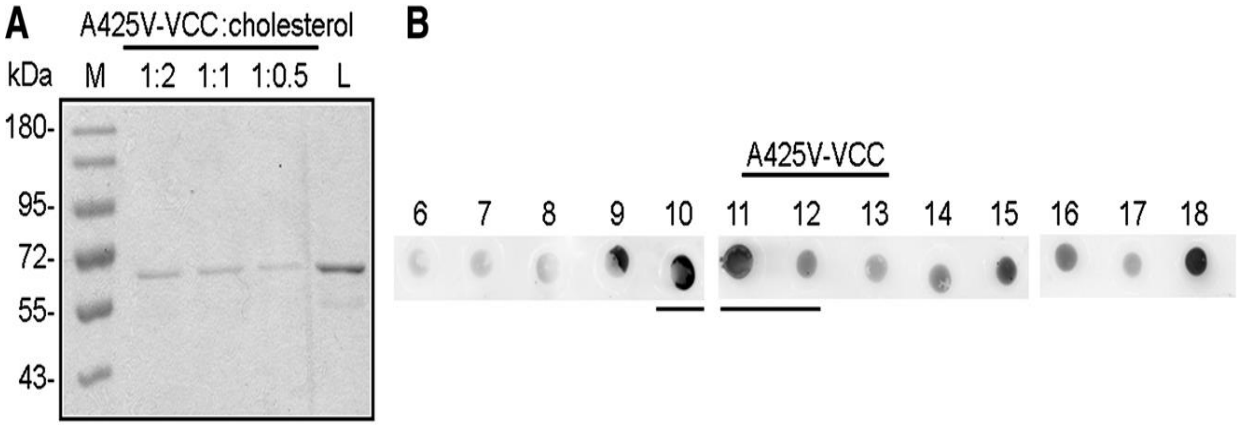

Fig. 44. The mutation of Ala425Val (A425V) in VCC compromised interaction with cholesterol in suspension, without affecting the association of VCC with cholesterol-rich lipid rafts in human erythrocytes. (A) A425V mutant has been earlier reported to have compromised cholesterol-dependent membrane-interaction. This mutant exhibits compromised interaction with cholesterol in suspension, as indicated by the pull down-based assay. (B) This mutant of VCC exhibits preferential distribution in the cholesterol-rich membrane micro-domains of human erythrocytes, shown in the fractions 10-12 marked with 'underlined'.

3.15 Exploring the possible structural determinant(s) that might dictate the association of VCC with the cholesterol-rich membrane micro-domains in human erythrocytes.

3.15.1 Mutation of the lectin-dependent membrane-interaction in VCC does not affect the association of the toxin with the cholesterol-rich membrane micro-domains in human erythrocytes.

VCC exhibits strong propensity to associate to the cholesterol-rich membrane fractions in human erythrocytes membranes, as observed in our results so far. However, the detailed insights defining its association with the lipid rafts in the target human erythrocytes still remain unclear. Earlier studies have shown that the introduction of D617A point mutation in VCC leads to the abrogated lectin-like activity of the toxin, and compromises binding to erythrocytes, and subsequent oligomeric pore formation and hemolytic activity (96). This clearly shows that the mutation of D617A critically affects the lectin-activity-dependent membrane pore-formation mechanism of VCC. We wanted to explore if the lectin-activity-

dependent interaction of VCC with the erythrocytes membranes play any role in its association with the cholesterol-rich membrane micro-domains in human erythrocytes. Interestingly, membrane-bound fraction of the D617A mutant of VCC showed similar propensity to segregate into the cholesterol-rich membrane fractions in human erythrocytes, as observed with the wild type VCC (Fig. 45).

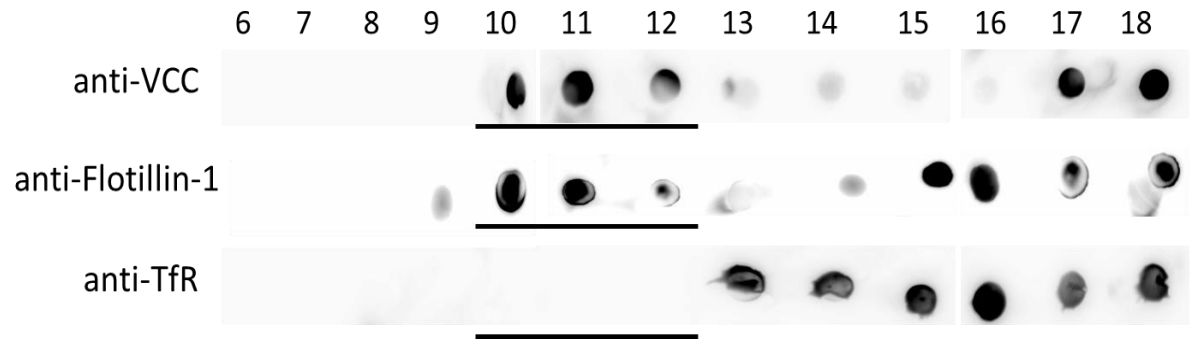

Fig. 45. Dot-blot analysis of the isolated membrane fractions upon treatment of human erythrocytes with the D617A mutant of VCC. The membrane fractions isolated from human erythrocytes, upon treatment with D617A mutant of VCC, show that the mutant protein associates with the cholesterol-rich membrane fractions, fraction numbers 10-12. The data shown here is the representative of three independent experiments.

3.15.2 Mutation that traps VCC in the membrane-associated monomeric form does not affect the partitioning of VCC into the cholesterol-rich membrane fractions in human erythrocytes.

Earlier studies have shown that the mutation R330A in VCC arrests oligomerization of the membrane-bound toxin molecules, and blocks oligomeric pore formation (219). Interestingly, the R330A mutant of VCC shows wild type-like propensity to associate with the cholesterol-rich, detergent-insoluble membrane fractions of human erythrocytes, as observed mainly in the fractions 10, 11 and 12. These fractions also clearly indicate the presence of Flotillin-1, a marker for the lipid rafts (Fig. 46). Despite being incapable of generating the oligomers in the

erythrocytes membranes, the R330A mutant is still capable of associating with the lipid rafts in the human erythrocytes membranes.

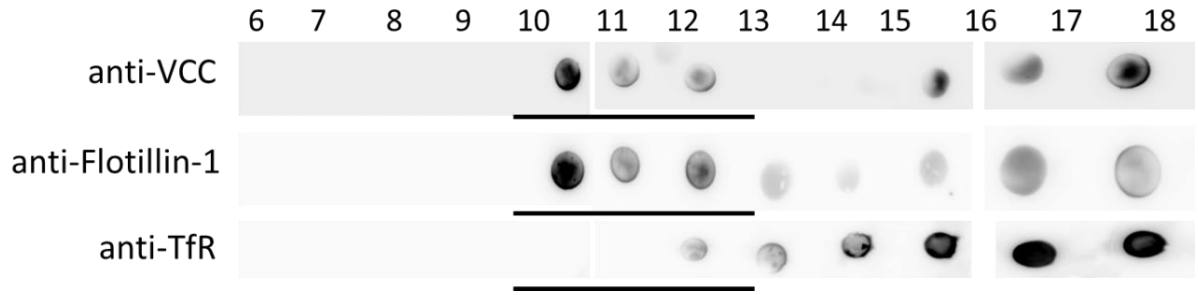

Fig. 46. Mutation in VCC that arrests oligomerization of the membrane-bound toxin molecule retains its ability to associate with the cholesterol-rich membrane fractions in human erythrocytes. The R330A mutant of VCC was incubated with human erythrocytes, and the membrane fractions were isolated, as described above. The R330A mutant associated with the lighter, detergent-insoluble, cholesterol-rich membrane fractions in a similar way as observed with the wild type VCC, in the dot-blot assay. The data shown here is the representative of three independent experiments.

3.15.3 Mutation that arrests the membrane-bound fraction of VCC into the non-functional oligomeric intermediate(s) does not affect its propensity to associate with the cholesterol-rich membrane fractions in human erythrocytes.

We wanted to further explore whether the propensity of VCC to associate with the cholesterol-rich membrane fractions in human erythrocytes is dependent on the ability of the toxin to form the membrane-inserted functional oligomeric pores. It is known that the pre-stem motif of VCC undergoes structural rearrangement during the pore-formation process, and finally inserts into the target membrane leading to the formation of functional transmembrane β-barrel pores. The β-barrel scaffold of the functional pore is generated by this pre-stem motifs contributed from the seven protomers of the membrane-bound VCC. We wanted to explore whether the membrane-insertion of this pore-forming pre-stem loop possibly governs the propensity of VCC to associate with the cholesterol-rich membrane fractions of human erythrocytes. For this, we employed a mutant variant of VCC having

truncation of the pre-stem motif (Δpre-stem (ΔPS)) that has been reported in an earlier study. We examined the propensity of this mutant, lacking the pore-forming pre-stem motif, to associate with the cholesterol-rich membrane fractions of human erythrocytes following the method described above. Interestingly, ΔPS mutant showed similar tendency to associate with the cholesterol-rich, detergent-insoluble, lighter membrane fractions of human erythrocytes, as observed with the wild type VCC protein. This truncated variant of VCC lacking the pre-stem motif is unable to generate the functional pores, due to the absence of the pore-forming motif, and remains arrested in the form of pre-pore oligomeric intermediate in the target membranes (226). Nevertheless, our results suggest that it is still capable of associating with the raft-like cholesterol-rich membrane fractions.

Altogether, these data clearly suggest that the abrogation of the cholesterol-dependent and lectin-dependent interactions, oligomerization, as well as the deletion of the critical pore-forming motif have no effect on the partitioning of VCC to the cholesterol-rich membrane lipid microdomains in human erythrocytes. Based on these results, it appears that the propensity of VCC to associate with the cholesterol-rich membrane fractions of human erythrocytes is possibly an inherent property of the toxin molecule, and/or possibly governed by the physicochemical environment of such specialized membrane micro-domains. Thus, the exact molecular description, and underlying mechanistic basis of this process still remains unclear. Future research efforts would be required to unravel the mechanism and physiological implication of such property of VCC, in the context of its cell-killing pore-formation mechanism.

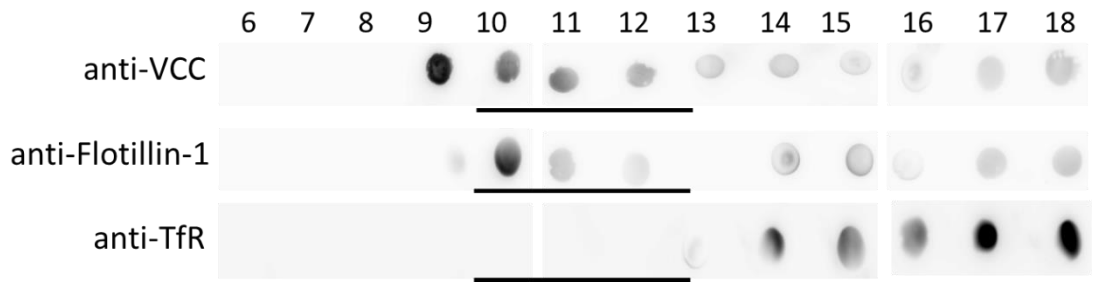

Fig. 47. Dot-blot analysis of the isolated membrane fractions of human erythrocytes to probe association of the ΔPS mutant variant of VCC with the cholesterol-rich membrane lipid microdomains in human erythrocytes. Human erythrocytes were incubated with the VCC mutant, having the deletion of the pre-stem region, and were subjected to the isolation of membrane fractions. The result clearly reveals the tendency of this mutant to associate with the cholesterol-rich raft-like fractions of human erythrocytes, despite being incapable of generating the functional transmembrane pores. The mutant is segregated into the cholesterol-rich membrane fractions, indicated by the fractions 10-12, that also contained Flotillin-1, the raft marker.

CHAPTER 4
Discussion

Chapter 4

Discussion

A large number of different kinds of lipids constitute the bacterial as well as the animal cellular membranes, where the presence of cholesterol forms the distinct feature of the latter (242). These cholesterol-containing membranes are selectively favoured by the microbial pathogenic toxins that attack the animal membranes, where the membrane could either act as an initial prime target as observed in the membrane-damaging toxins or there might be some intracellular target for which, the membrane forms a barrier that needs to be overcome by endocytosis or by the toxin's inbuilt protein translocation activity (243).

Biological membranes are actually complex mixtures comprised of an array of proteins and lipids. The intricate details of the mammalian membrane lipids define them as Sphingolipids, glycerol-based lipids and cholesterol, which further consists of numerous lipid species based on the differences in chemical structures (244). The presence/distribution of a particular lipid in a membrane is determined by the tissue, species and the original subcellular location. The example being ergosterol in yeast membranes and sitosterol in the membranes of plant cells, which are the structural analogous of cholesterol. Cholesterol is present particularly in the mammalian plasma membrane. It exhibits the distinct structure of four-fused rings and a small hydroxyl group, which is significantly different from the polar lipids having hydrocarbon chains and huge polar head-groups (245). Hence, the proteins tend to exhibit quite different extent of interaction with phospholipids and cholesterol that leads to the lateral phase separation of the constituting lipids.

The assembly and pore-formation mechanism of PFTs form an interesting area of investigation to decipher and understand the formation of membrane-damaging oligomeric

assemblies that cause the lysis of target cells. These membrane-integrated structures are formed in the host membranes, endowed with multiple components/determinants critical for the functioning of these membranes. The targeting of the PFTs to the host membranes is mediated by numerous factors. Hence, the molecular components of membranes, association of the PFTs to specific domains and the overall physicochemical properties of the target membranes govern the membrane specificity for execution of pore-formation event by several PFTs. For instance, the toxins that share the structural similarity to *Vibrio* haemolysins harbour the carbohydrate-interacting lectin domain that binds to the cell-surface glycosylated proteins. Cholesterol forms another indispensable constituent of the animal cell membrane that has been shown to be utilized by several PFTs for generation of the lesions in target membranes, inflicting the host cell damage. Cholesterol has been shown to greatly assist the cellular damage, mainly by a class of toxins, known as CDCs and these CDCs have been shown to possess the specific structural motifs for interacting with cholesterol (246).

VCC, an archetypical β-barrel PFT, secreted from the non-cholera-toxigenic strains of *Vibrio cholerae* has been shown to generate heptameric anion-selective pores in the target membrane, leading to the dissipation of ionic gradient, hence inducing the lysis of the target cell. The structural mechanism of pore-formation by VCC is well-defined, where monomeric subunits upon encountering the target membrane generate metastable pre-pore structure and then the concerted insertion of pre-stem motif forms the functional pore (219). Previous studies have indicated an absolute requirement of cholesterol in the host membrane by VCC for channel formation. In the membranes completely lacking cholesterol, pore formation has been shown to be completely compromised by VCC. However, the detailed information on how the membrane cholesterol regulates the activity of VCC has not yet been described in great detail. The mechanistic details of host cellular membrane cholesterol modulating the defined steps in VCC mode of action has not been elucidated so far. In particular, the role of

cholesterol in bio-membranes on the functional pore-forming activity of VCC has remained obscure. Hence, in view of earlier studies, it is of considerable interest to decipher the critical requirement of cholesterol in host membranes for pore-forming activity of VCC. We employed a number of biochemical and biophysical assays for this study. We have extensively monitored the regulatory role of cholesterol on the pore-formation mechanism of VCC by employing liposomes, having a stepwise increment in the cholesterol content. We have monitored the physiological relevance of membrane cholesterol by examining the binding efficacy, oligomerization propensity and the functional pore-forming activity of VCC by depleting cholesterol from the target cell membranes using mβCD, a well-characterized cholesterol-sequestering agent. Recent studies have indicated that the cholesterol defines and regulates many functions by generating the specialized liquid-ordered domain structures, known as lipid rafts. As raft domains are enriched in cholesterol and sphingolipids, a number of experiments were performed in this study to examine the partitioning of VCC in the lipid rafts.

The results reported in this study show that the initial interaction and the subsequent pore-forming capability of VCC are enhanced upon increasing the cholesterol concentration in the liposomes. This could be attributed to the increased availability of cholesterol in the liposomes, which would allow the strong, intimate association of VCC to the lipid membranes. VCC has been demonstrated to display the basal level binding towards asolectin only liposomes, devoid of cholesterol. The association of VCC has been shown to gradually increase with increasing levels of cholesterol in the liposome membrane as indicated by various experiments. This is further reinforced by the FRET-based assay that displays intimate interaction of VCC with the cholesterol-enriched membranes. Thus, with gradually higher levels of cholesterol in the liposome membranes, the association of VCC is enhanced progressively, which leads to the concomitant enhancement of the subsequent steps of pore-

formation viz. oligomerization event and the insertion of pore-forming stem loop that leads to the functional pore-formation. Our findings suggest that the binding of VCC is increased with the increasing levels of cholesterol in the liposome membranes.

To investigate whether the binding and pore-forming activity of VCC is governed by the cholesterol content of bio-membranes, several experiments to probe different steps in the mode of action of VCC were performed, upon depletion of the membrane cholesterol with mβCD. The results in this study indicate the complete abrogation of haemolytic activity, even upon depleting half of the total cholesterol content in the human erythrocytes membrane, suggesting the critical requirement of membrane cholesterol for the formation of functional pores in human erythrocytes. Upon interacting with the membrane lipid bilayer, VCC could form SDS-stable oligomers. In this study, VCC has been shown to generate non-functional, abortive oligomers in biomembranes devoid of cholesterol. These non-functional oligomers formed by VCC do not appear to represent the functional pore assembly of the toxin; rather such assembly represents VCC being trapped in an abortive oligomeric state. Here, the toxin protein was not defective in terms of forming the oligomeric assemblies in the membrane. However, formation of such an oligomeric assembly could not permeabilize the target membrane, hence cannot trigger any cytolytic activity. This could be due to undefined, structural alteration in VCC that hindered the formation of the functional β-barrel pore, leading to the colloid-osmotic lysis of the target cells. The oligomers being non-functional in nature can be due to following reasons:

a) There could have been formation of membrane-bound oligomeric pores with a constricted pore diameter that couldn't generate functional pore.

b) There might be inefficient/abortive membrane insertion of the channel-forming 'stem loop', arresting the oligomer in non-functional state.

The flow-cytometric data suggests significant reduction in the binding efficacy of VCC towards the cholesterol-depleted erythrocytes; however the basal level association of VCC could be observed in these erythrocyte membranes due to the accessory interactions, provided by various other cell-surface components. Surprisingly, in the erythrocyte membranes where the optimal amount of cholesterol is absent, VCC forms abortive oligomers on the membranes, devoid of pore-forming activity. This is supported by our observation that in the erythrocyte membranes, where cholesterol is sequestered using mβCD, VCC fails to execute the functional pore-formation, as haemolytic activity is completely compromised, while the non-functional oligomeric assemblies could be clearly observed.

The existence of raft domains in human erythrocytes has been reported earlier, that forms the preferential interaction sites for various toxins. The involvement of lipid rafts in the PFT mode of action has recently attracted much attention. As lipid rafts are the membrane microdomains rich in cholesterol, we assumed that VCC might exhibit a preferential binding towards these lipid rafts. Membrane rafts were isolated from human erythrocytes as Triton-insoluble fractions at 4 $^{\circ}$C. The results in this study show that a significant amount of VCC migrates towards the Triton-insoluble raft fractions, suggesting the favoured sequestering of VCC to raft domains. Upon employing mβCD, that selectively sequesters membrane cholesterol, there appears to be the disruption of clustered raft domains that inhibit the association of VCC to detergent-resistant membranes (DRMs) of human erythrocytes. Surprisingly, the variant of VCC, Ala425Val that specifically inhibited the cholesterol-dependent membrane-interaction mechanism, also exhibited the propensity to migrate towards cholesterol-rich raft domains.

It is not known whether any particular step in the pore-formation mechanism of VCC governs its segregation into the lipid rafts. We find that the mutations in VCC as shown in Fig. 48 that

affect distinct steps of pore-formation are associating with the DRMs. These variants exhibit the same efficacy of interaction with DRMs as wild-type VCC.

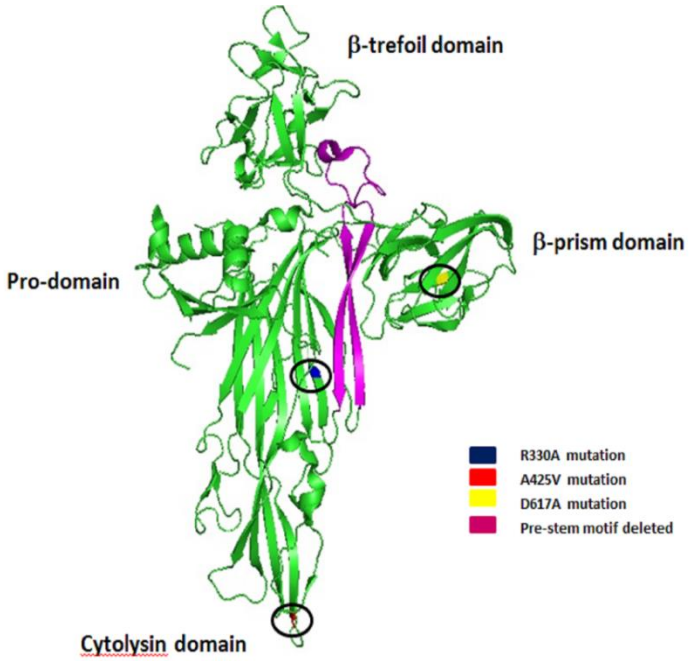

Fig. 48. VCC monomer indicating position of mutations incorporated. Monomeric form of VCC showing the position of residues for which mutational studies have been done. These mutations arrest the toxin at different steps of pore-formation mechanism.

This could possibly be attributed to the fact that no particular residue or step is driving the migration of VCC to cholesterol-rich lipid rafts. Rather, VCC could be segregating in the ordered raft regions due to physicochemical environment of these domains or there could be presence of some probable potential receptor of VCC in these lipid rafts (Fig.49). These potential receptors might get accumulated and appear in substantial amount in these raft domains. Hence, when VCC interacts with the target membrane, the higher local concentration of these potential receptors in the coalesced platforms, provided by lipid rafts may drive the segregation of VCC in these domains (Fig.50).

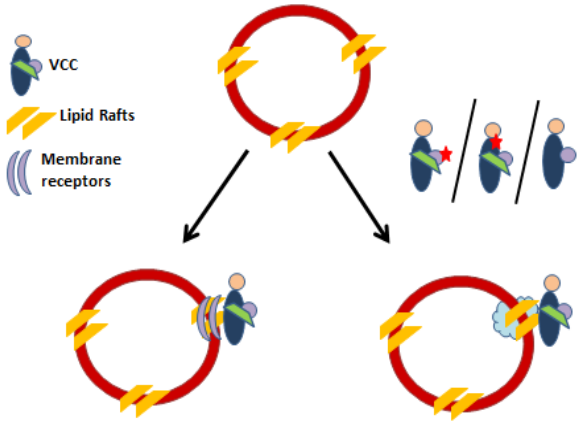

Fig. 49. VCC and variants of VCC having mutations that arrest the toxin at various stages of pore-formation mechanism, exhibit the tendency to associate with lipid rafts. The mutants of VCC that could not execute functional pore-formation by affecting the specific steps of pore-forming ability of VCC have been demonstrated to migrate and partition to cholesterol-rich lipid raft domains to the same extent as wild type VCC. This could be attributed to the presence of some specific receptors, being accumulated in these raft domains or could be due to the microenvironment of cholesterol-rich raft domains.

The collective results in this study forms the first documentation elaborately defining the implications of membrane cholesterol in governing the pore-formation mechanism of VCC. This study provides the comprehensive insights into mechanistic details of how the cholesterol in target lipid bilayer regulates the pore-formation event. Overall, these findings are relevant in deciphering the role of cholesterol in pore-formation mechanism of VCC in the host membranes. Future studies will be required for detailed characterization of the role of cholesterol in more complex nucleated cellular membranes and to further explore the interacting partners that might be localized in the specific regions of host membrane.

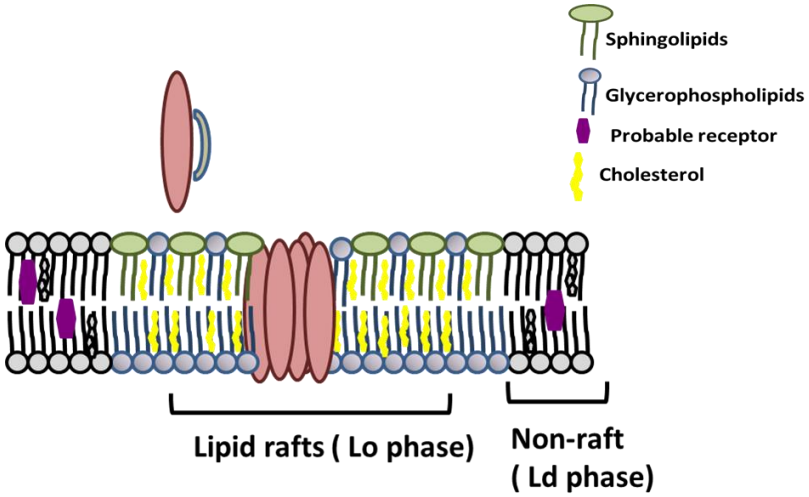

Fig. 50. Graphical representation of VCC favouring association to lipid rafts in the cellular membranes of human erythrocytes.VCC has been shown to translocate to the highly-ordered, cholesterol-enriched lipid raft domains, examined in the case of human erythrocytes. Lo represents the liquid-ordered raft domains, while Ld represents the non-raft disordered phase in membranes.

References

1. Shi, Y., Cai, M., Zhou, L., and Wang, H. (2018) The structure and function of cell membranes studied by atomic force microscopy. in *Seminars in cell & developmental biology*, Elsevier

2. Pohorille, A., and Deamer, D. (2009) *Research in microbiology* **160**, 449-456

3. Coskun, Ü., and Simons, K. (2011) *Structure* **19**, 1543-1548

4. Ohanian, J., and Ohanian, V. (2001) *Cellular and Molecular Life Sciences CMLS* **58**, 2053-2068

5. McAuley, K. E., Fyfe, P. K., Ridge, J. P., Isaacs, N. W., Cogdell, R. J., and Jones, M. R. (1999) *Proceedings of the National Academy of Sciences* **96**, 14706-14711

6. Sharon, N., and Lis, H. (1993) *Scientific American* **268**, 82-89

7. Rand, R. P., and Burton, A. (1964) *Biophysical journal* **4**, 115-135

8. Gilbert, R. (2002) *Cellular and Molecular Life Sciences CMLS* **59**, 832-844

9. Gonzalez, M., Bischofberger, M., Pernot, L., Van Der Goot, F., and Freche, B. (2008) *Cellular and molecular life sciences* **65**, 493-507

10. Dal Peraro, M., and Van Der Goot, F. G. (2016) *Nature reviews microbiology* **14**, 77

11. Los, F. C., Randis, T. M., Aroian, R. V., and Ratner, A. J. (2013) *Microbiol. Mol. Biol. Rev.* **77**, 173-207

12. Tilley, S. J., and Saibil, H. R. (2006) *Current opinion in structural biology* **16**, 230-236

13. Kao, C.-Y., Los, F. C., Huffman, D. L., Wachi, S., Kloft, N., Husmann, M., Karabrahimi, V., Schwartz, J.-L., Bellier, A., and Ha, C. (2011) *PLoS pathogens* **7**

14. Geny, B., and Popoff, M. R. (2006) *Biology of the Cell* **98**, 667-678

15. Ojcius, D. M., and Young, J. D. E. (1991) *Trends in biochemical sciences* **16**, 225-229

16. Rosado, C. J., Kondos, S., Bull, T. E., Kuiper, M. J., Law, R. H., Buckle, A. M., Voskoboinik, I., Bird, P. I., Trapani, J. A., and Whisstock, J. C. (2008) *Cellular microbiology* **10**, 1765-1774

17. Bashford, C. L. (2001) *Cellular and Molecular Biology Letters* **6**, 328-333

18. Bayley, H., and Jayasinghe, L. (2004) *Molecular membrane biology* **21**, 209-220

19. Alouf, J. (2003) *Folia microbiologica* **48**, 5

20. Tanaka, K., Caaveiro, J. M., Morante, K., González-Mañas, J. M., and Tsumoto, K. (2015) *Nature communications* **6**, 1-11

21. Dalla Serra, M., and Tejuca Martínez, M. (2001) *e LS*

22. Heuck, A. P., Tweten, R. K., and Johnson, A. E. (2001) *Biochemistry* **40**, 9065-9073

23. Nomura, M. (1967) *Annual Reviews in Microbiology* **21**, 257-284

24. Lakey, J., Gonzalez-Manas, J., Van der Goot, F., and Pattus, F. (1992) *FEBS letters* **307**, 26-29

25. Lakey, J. H., van der Goot, F. G., and Pattus, F. (1994) *Toxicology* **87**, 85-108

26. Stroud, R. (1995) *Current opinion in structural biology* **5**, 514-520

27. Braun, V., Pilsl, H., and Groß, P. (1994) *Archives of microbiology* **161**, 199-206

28. Lakey, J. H., Duche, D., Gonzáles-Mañas, J.-M., Baty, D., and Pattus, F. (1993) *Journal of molecular biology* **230**, 1055-1067

29. Pattus, F., Massotte, D., Wilmsen, H., Lakey, J., Tsernoglou, D., Tucker, A., and Parker, M. (1990) *Experientia. Basel* **46**, 180-192

30. Xu, C., Wang, B.-C., Yu, Z., and Sun, M. (2014) *Toxins* **6**, 2732-2770

31. Wu, Z., Jakes, K. S., Samelson-Jones, B. S., Lai, B., Zhao, G., London, E., and Finkelstein, A. (2006) *Biophysical journal* **91**, 3249-3256

32. Reed, J. (2006) *Cell death & differentiation* **13**, 1378-1386

33. Mueller, M., Grauschopf, U., Maier, T., Glockshuber, R., and Ban, N. (2009) *Nature* **459**, 726-730

34. Andrews, N. W., and Portnoy, D. A. (1994) *Trends in microbiology* **2**, 261-263

35. Vaidyanathan, M., Sathyanarayana, P., Maiti, P. K., Visweswariah, S. S., and Ayappa, K. (2014) *RSC Advances* **4**, 4930-4942

36. Fahie, M., Romano, F. B., Chisholm, C., Heuck, A. P., Zbinden, M., and Chen, M. (2013) *Journal of Biological Chemistry* **288**, 31042-31051

37. Bravo, A., Gómez, I., Porta, H., García-Gómez, B. I., Rodriguez-Almazan, C., Pardo, L., and Soberón, M. (2013) *Microbial biotechnology* **6**, 17-26

38. Grochulski, P., Masson, L., Borisova, S., Pusztai-Carey, M., Schwartz, J.-L., Brousseau, R., and Cygler, M. (1995) *Journal of molecular biology* **254**, 447-464

39. Gómez, I., Pardo-López, L., Munoz-Garay, C., Fernandez, L., Pérez, C., Sánchez, J., Soberón, M., and Bravo, A. (2007) *Peptides* **28**, 169-173

40. Pardo-Lopez, L., Soberon, M., and Bravo, A. (2013) *FEMS microbiology reviews* **37**, 3-22

41. Buckley, J. T., and Howard, S. P. (1999) *Infection and immunity* **67**, 466-467

42. Szczesny, P., Iacovache, I., Muszewska, A., Ginalski, K., Van Der Goot, F. G., and Grynberg, M. (2011) *PLoS One* **6**

43. Diep, D. B., Nelson, K. L., Raja, S. M., Pleshak, E. N., and Buckley, J. T. (1998) *Journal of Biological Chemistry* **273**, 2355-2360

44. Degiacomi, M. T., Iacovache, I., Pernot, L., Chami, M., Kudryashev, M., Stahlberg, H., Van Der Goot, F. G., and Dal Peraro, M. (2013) *Nature chemical biology* **9**, 623

45. Iacovache, I., De Carlo, S., Cirauqui, N., Dal Peraro, M., Van Der Goot, F. G., and Zuber, B. (2016) *Nature communications* **7**, 1-8

46. Iacovache, I., Paumard, P., Scheib, H., Lesieur, C., Sakai, N., Matile, S., Parker, M. W., and Van der Goot, F. G. (2006) *The EMBO journal* **25**, 457-466

47. Cabiaux, V., Buckley, J. T., Wattiez, R., Ruysschaert, J.-M., Parker, M. W., and van der Goot, F. G. (1997) *Biochemistry* **36**, 15224-15232

48. Podobnik, M., Kisovec, M., and Anderluh, G. (2017) *Philosophical Transactions of the Royal Society B: Biological Sciences* **372**, 20160209

49. Holland, I., Kenny, B., and Blight, M. (1990) *Biochimie* **72**, 131-141

50. Mackman, N., Nicaud, J.-M., Gray, L., and Holland, I. (1986) Secretion of haemolysin by Escherichia coli. in *Protein Secretion and Export in Bacteria*, Springer. pp 159-181

51. Song, L., Hobaugh, M. R., Shustak, C., Cheley, S., Bayley, H., and Gouaux, J. E. (1996) *Science* **274**, 1859-1865

52. Miles, G., Movileanu, L., and Bayley, H. (2002) *Protein science* **11**, 894-902

53. Benz, R., Schmid, A., Wagner, W., and Goebel, W. (1989) *Infection and immunity* **57**, 887-895

54. Kawate, T., and Gouaux, E. (2003) *Protein science* **12**, 997-1006

55. Heuck, A. P., Moe, P. C., and Johnson, B. B. (2010) The cholesterol-dependent cytolysin family of gram-positive bacterial toxins. in *Cholesterol Binding and Cholesterol Transport Proteins: *, Springer. pp 551-577

56. Hotze, E. M., and Tweten, R. K. (2012) *Biochimica Et Biophysica Acta (BBA)-Biomembranes* **1818**, 1028-1038

57. Giddings, K. S., Zhao, J., Sims, P. J., and Tweten, R. K. (2004) *Nature structural & molecular biology* **11**, 1173-1178

58. Tweten, R., Parker, M., and Johnson, A. (2001) The cholesterol-dependent cytolysins. in *Pore-forming toxins*, Springer. pp 15-33

59. Alouf, J. (2000) *International journal of medical microbiology* **290**, 351-356

60. Gilbert, R. J. (2010) Cholesterol-dependent cytolysins. in *Proteins Membrane Binding and Pore Formation*, Springer. pp 56-66

61. Heuck, A. P., Hotze, E. M., Tweten, R. K., and Johnson, A. E. (2000) *Molecular cell* **6**, 1233-1242

62. Giddings, K. S., Johnson, A. E., and Tweten, R. K. (2003) *Proceedings of the National Academy of Sciences* **100**, 11315-11320

63. Hotze, E. M., Wilson-Kubalek, E., Farrand, A. J., Bentsen, L., Parker, M. W., Johnson, A. E., and Tweten, R. K. (2012) *Journal of Biological Chemistry* **287**, 24534-24543

64. Reboul, C. F., Whisstock, J. C., and Dunstone, M. A. (2014) *PLoS computational biology* **10**

65. Dunstone, M. A., and Tweten, R. K. (2012) *Current opinion in structural biology* **22**, 342-349

66. Heuck, A. P., Tweten, R. K., and Johnson, A. E. (2003) *Journal of Biological Chemistry* **278**, 31218-31225

67. Tweten, R. K., Hotze, E. M., and Wade, K. R. (2015) *Annual review of microbiology* **69**, 323-340

68. Cassidy, S. K., and O'Riordan, M. X. (2013) *Toxins* **5**, 618-636

69. van der Goot, G. (2001) *Pore-forming toxins*, Springer Science & Business Media

70. Ros, U., and García-Sáez, A. J. (2015) *The Journal of membrane biology* **248**, 545-561

71. Peitsch, M. C., and Tschopp, J. (1991) *Current opinion in cell biology* **3**, 710-716

72. Anderluh, G., and Lakey, J. H. (2011) *Proteins: membrane binding and pore formation*, Springer Science & Business Media

73. Nguyen, V. T., and Kamio, Y. (2004) *Journal of biochemistry* **136**, 563-567

74. Gonzalez, M. R., Bischofberger, M., Frêche, B., Ho, S., Parton, R. G., and van der Goot, F. G. (2011) *Cellular microbiology* **13**, 1026-1043

75. Bischofberger, M., Gonzalez, M. R., and van der Goot, F. G. (2009) *Current opinion in cell biology* **21**, 589-595

76. Gouaux, E. (1997) *Current opinion in structural biology* **7**, 566-573

77. Montoya, M., and Gouaux, E. (2003) *Biochimica Et Biophysica Acta (BBA)-Biomembranes* **1609**, 19-27

78. Tam, K., Schultz, M., Reyes-Robles, T., Vanwalscappel, B., Horton, J., Alonzo, F., Wu, B., Landau, N. R., and Torres, V. J. (2016) *MBio* **7**, e02024-02016

79. Reyes-Robles, T., Alonzo III, F., Kozhaya, L., Lacy, D. B., Unutmaz, D., and Torres, V. J. (2013) *Cell host & microbe* **14**, 453-459

80. DuMont, A. L., and Torres, V. J. (2014) *Trends in microbiology* **22**, 21-27

81. Wilke, G. A., and Wardenburg, J. B. (2010) *Proceedings of the National Academy of Sciences* **107**, 13473-13478

82. DiFranco, K. M., Gupta, A., Galusha, L. E., Perez, J., Nguyen, T.-V. K., Fineza, C. D., and Kachlany, S. C. (2012) *Journal of Biological Chemistry* **287**, 17618-17627

83. Spaan, A. N., Henry, T., Van Rooijen, W. J., Perret, M., Badiou, C., Aerts, P. C., Kemmink, J., de Haas, C. J., Van Kessel, K. P., and Vandenesch, F. (2013) *Cell host & microbe* **13**, 584-594

84. Spaan, A. N., van Strijp, J. A., and Torres, V. J. (2017) *Nature reviews microbiology* **15**, 435

85. Zhang, D., Takahashi, J., Seno, T., Tani, Y., and Honda, T. (1999) *Infection and immunity* **67**, 5332-5337

86. Jenkins, J. L., and Dean, D. H. (2001) *BMC biochemistry* **2**, 12

87. Polekhina, G., Giddings, K. S., Tweten, R. K., and Parker, M. W. (2005) *Proceedings of the National Academy of Sciences* **102**, 600-605

88. Johnson, S., Brooks, N. J., Smith, R. A., Lea, S. M., and Bubeck, D. (2013) *Cell reports* **3**, 1369-1377

89. Hughes, T. R., Ross, K. S., Cowan, G. J., Sivasankar, B., Harris, C. L., Mitchell, T. J., and Morgan, B. P. (2009) *Molecular immunology* **46**, 1561-1567

90. Imberty, A., Mitchell, E. P., and Wimmerová, M. (2005) *Current opinion in structural biology* **15**, 525-534

91. Johnson, C. L., Ridley, H., Marchetti, R., Silipo, A., Griffin, D. C., Crawford, L., Bonev, B., Molinaro, A., and Lakey, J. H. (2014) *Molecular microbiology* **92**, 440-452

92. Lehotzky, R. E., Partch, C. L., Mukherjee, S., Cash, H. L., Goldman, W. E., Gardner, K. H., and Hooper, L. V. (2010) *Proceedings of the National Academy of Sciences* **107**, 7722-7727

93. Shewell, L. K., Harvey, R. M., Higgins, M. A., Day, C. J., Hartley-Tassell, L. E., Chen, A. Y., Gillen, C. M., James, D. B., Alonzo, F., and Torres, V. J. (2014) *Proceedings of the National Academy of Sciences* **111**, E5312-E5320

94. Abrami, L., Velluz, M.-C., Hong, Y., Ohishi, K., Mehlert, A., Ferguson, M., Kinoshita, T., and Gisou van der Goot, F. (2002) *FEBS letters* **512**, 249-254

95. Ivie, S. E., and McClain, M. S. (2012) *Biochemistry* **51**, 7588-7595

96. Rai, A. K., Paul, K., and Chattopadhyay, K. (2013) *Journal of Biological Chemistry* **288**, 1665-1673

97. Kaus, K., Lary, J. W., Cole, J. L., and Olson, R. (2014) *Journal of molecular biology* **426**, 2800-2812

98. Yamaji, A., Sekizawa, Y., Emoto, K., Sakuraba, H., Inoue, K., Kobayashi, H., and Umeda, M. (1998) *Journal of Biological Chemistry* **273**, 5300-5306

99. Kulma, M., Hereć, M., Grudziński, W., Anderluh, G., Gruszecki, W. I., Kwiatkowska, K., and Sobota, A. (2010) *Biochimica Et Biophysica Acta (BBA)-Biomembranes* **1798**, 471-481

100. Bhat, H. B., Kishimoto, T., Abe, M., Makino, A., Inaba, T., Murate, M., Dohmae, N., Kurahashi, A., Nishibori, K., and Fujimori, F. (2013) *Journal of lipid research* **54**, 2933-2943

101. Zakharov, S. D., Kotova, E. A., Antonenko, Y. N., and Cramer, W. A. (2004) *Biochimica Et Biophysica Acta (BBA)-Biomembranes* **1666**, 239-249

102. Young, N. M., Foote, S. J., and Wakarchuk, W. W. (2013) *Molecular immunology* **56**, 563-573

103. Bonev, B. B., Lam, Y.-H., Anderluh, G., Watts, A., Norton, R. S., and Separovic, F. (2003) *Biophysical journal* **84**, 2382-2392

104. Maxfield, F. R., and van Meer, G. (2010) *Current opinion in cell biology* **22**, 422-429

105. Bittman, R. (1997) Has nature designed the cholesterol side chain for optimal interaction with phospholipids? in *Cholesterol*, Springer. pp 145-171

106. Bandara, A., Panahi, A., Pantelopulos, G. A., and Straub, J. E. (2017) *Journal of computational chemistry* **38**, 1479-1488

107. Epand, R. M., and Epand, R. F. (2011) *The Structure of Biological Membranes* **3**, 133-152

108. Palmer, M. (2004) *FEMS microbiology letters* **238**, 281-289

109. Fantini, J., and Barrantes, F. J. (2013) *Frontiers in physiology* **4**, 31

110. Fantini, J., Di Scala, C., Baier, C. J., and Barrantes, F. J. (2016) *Chemistry and physics of lipids* **199**, 52-60

111. Jamin, N., Neumann, J.-M., Ostuni, M. A., Vu, T. K. N., Yao, Z.-X., Murail, S., Robert, J.-C., Giatzakis, C., Papadopoulos, V., and Lacapere, J.-J. (2005) *Molecular endocrinology* **19**, 588-594

112. Posada, I. M., Fantini, J., Contreras, F. X., Barrantes, F., Alonso, A., and Goñi, F. M. (2014) *Biophysical journal* **107**, 1383-1392

113. Gimpl, G. (2010) Cholesterol–protein interaction: methods and cholesterol reporter molecules. in *Cholesterol Binding and Cholesterol Transport Proteins: *, Springer. pp 1-45

114. Di Scala, C., Baier, C. J., Evans, L. S., Williamson, P. T., Fantini, J., and Barrantes, F. J. (2017) Relevance of CARC and CRAC cholesterol-recognition motifs in the nicotinic acetylcholine receptor and other membrane-bound receptors. in *Current topics in membranes*, Elsevier. pp 3-23

115. Charloteaux, B., Lorin, A., Brasseur, R., and Lins, L. (2009) *Protein and peptide letters* **16**, 718-725

116. Marsh, D. (2010) *Biochimica Et Biophysica Acta (BBA)-Biomembranes* **1798**, 688-699

117. Tomita, T., Watanabe, M., and Yasuda, T. (1992) *Journal of Biological Chemistry* **267**, 13391-13397

118. Watanabe, M., Tomita, T., and Yasuda, T. (1987) *Biochimica Et Biophysica Acta (BBA)-Biomembranes* **898**, 257-265

119. Simons, K., and Ikonen, E. (2000) *Science* **290**, 1721-1726

120. Shearman, G., Ces, O., Templer, R., and Seddon, J. (2006) *Journal of Physics: Condensed Matter* **18**, S1105

121. Zitzer, A., Bittman, R., Verbicky, C. A., Erukulla, R. K., Bhakdi, S., Weis, S., Valeva, A., and Palmer, M. (2001) *Journal of Biological Chemistry* **276**, 14628-14633

122. Dowd, K. J., and Tweten, R. K. (2012) *PLoS pathogens* **8**

123. Harris, J. R., Adrian, M., Bhakdi, S., and Palmer, M. (1998) *Journal of structural biology* **121**, 343-355

124. Shimada, Y., Maruya, M., Iwashita, S., and Ohno-Iwashita, Y. (2002) *European journal of biochemistry* **269**, 6195-6203

125. Nöllmann, M., Gilbert, R., Mitchell, T., Sferrazza, M., and Byron, O. (2004) *Biophysical journal* **86**, 3141-3151

126. Seveau, S. (2014) Multifaceted activity of listeriolysin O, the cholesterol-dependent cytolysin of Listeria monocytogenes. in *MACPF/CDC Proteins-Agents of Defence, Attack and Invasion*, Springer. pp 161-195

127. Gelber, S. E., Aguilar, J. L., Lewis, K. L., and Ratner, A. J. (2008) *Journal of bacteriology* **190**, 3896-3903

128. Zilnyte, M., Venclovas, Č., Zvirbliene, A., and Pleckaityte, M. (2015) *Toxins* **7**, 110-128

129. Lawrence, S. L., Gorman, M. A., Feil, S. C., Mulhern, T. D., Kuiper, M. J., Ratner, A. J., Tweten, R. K., Morton, C. J., and Parker, M. W. (2016) *Structure* **24**, 1488-1498

130. Johnson, B. B., Moe, P. C., Wang, D., Rossi, K., Trigatti, B. L., and Heuck, A. P. (2012) *Biochemistry* **51**, 3373-3382

131. Flanagan, J. J., Tweten, R. K., Johnson, A. E., and Heuck, A. P. (2009) *Biochemistry* **48**, 3977-3987

132. Simons, K., and Van Meer, G. (1988) *Biochemistry* **27**, 6197-6202

133. Lingwood, D., and Simons, K. (2010) *Science* **327**, 46-50

134. Simons, K., and Sampaio, J. L. (2011) *Cold Spring Harbor perspectives in biology* **3**, a004697

135. Schäfer, L. V., de Jong, D. H., Holt, A., Rzepiela, A. J., de Vries, A. H., Poolman, B., Killian, J. A., and Marrink, S. J. (2011) *Proceedings of the National Academy of Sciences* **108**, 1343-1348

136. Chamberlain, L. H. (2004) *FEBS letters* **559**, 1-5

137. Ostrom, R. S., and Liu, X. (2007) Detergent and detergent-free methods to define lipid rafts and caveolae. in *Methods in Membrane Lipids*, Springer. pp 459-468

138. Kenworthy, A. (2002) *Trends in biochemical sciences* **27**, 435-438

139. Lillemeier, B. F., Pfeiffer, J. R., Surviladze, Z., Wilson, B. S., and Davis, M. M. (2006) *Proceedings of the National Academy of Sciences* **103**, 18992-18997

140. Magee, A. I., and Parmryd, I. (2003) *Genome biology* **4**, 234

141. FÜLLEKRUG, J., and Simons, K. (2004) *Annals of the New York Academy of Sciences* **1014**, 164-169

142. HAKOMORI, S. I., Yamamura, S., and Handa, K. (1998) *Annals of the New York Academy of Sciences* **845**, 1-10

143. Grassi, S., Prioni, S., Cabitta, L., Aureli, M., Sonnino, S., and Prinetti, A. (2016) *Neurochemical research* **41**, 130-143

144. Munro, S. (2003) *Cell* **115**, 377-388

145. Macdonald, J. L., and Pike, L. J. (2005) *Journal of lipid research* **46**, 1061-1067

146. Persaud-Sawin, D.-A., Lightcap, S., and Harry, G. J. (2009) *Journal of lipid research* **50**, 759-767

147. Shah, M. B., and Sehgal, P. B. (2007) Nondetergent isolation of rafts. in *Lipid Rafts*, Springer. pp 21-28

148. Lewis, R. N., Zhang, Y.-P., and McElhaney, R. N. (2005) *Biochimica Et Biophysica Acta (BBA)-Biomembranes* **1668**, 203-214

149. Simons, K., and Toomre, D. (2000) *Nature reviews Molecular cell biology* **1**, 31-39

150. Yang, S.-T., Kiessling, V., Simmons, J. A., White, J. M., and Tamm, L. K. (2015) *Nature chemical biology* **11**, 424

151. Feron, O., and Kelly, R. A. (2001) The caveolar paradox: suppressing, inducing, and terminating eNOS signaling. Am Heart Assoc

152. Miaczynska, M., Pelkmans, L., and Zerial, M. (2004) *Current opinion in cell biology* **16**, 400-406

153. Rosenberger, C. M., Brumell, J. H., and Finlay, B. B. (2000) *Current Biology* **10**, R823-R825

154. van der Goot, F. G., and Harder, T. (2001) Raft membrane domains: from a liquid-ordered membrane phase to a site of pathogen attack. in *Seminars in immunology*, Elsevier

155. Suzuki, T., and Suzuki, Y. (2006) *Biological and Pharmaceutical Bulletin* **29**, 1538-1541

156. Pietiäinen, V. M., Marjomäki, V., Heino, J., and Hyypiä, T. (2005) *Annals of medicine* **37**, 394-403

157. Norkin, L. C., Anderson, H. A., Wolfrom, S. A., and Oppenheim, A. (2002) *Journal of virology* **76**, 5156-5166

158. Parton, R. G., and Richards, A. A. (2003) *Traffic* **4**, 724-738

159. Takahashi, T., and Suzuki, T. (2011) *Biochemistry research international* **2011**

160. Favoreel, H. W., Mettenleiter, T. C., and Nauwynck, H. J. (2004) *Journal of virology* **78**, 5279-5287

161. Li, G.-M., Li, Y.-G., Yamate, M., Li, S.-M., and Ikuta, K. (2007) *Microbes and infection* **9**, 96-102

162. Maza, P. K., Straus, A. H., Toledo, M. S., Takahashi, H. K., and Suzuki, E. (2008) *Microbes and infection* **10**, 540-547

163. Goldston, A. M., Powell, R. R., and Temesvari, L. A. (2012) *Trends in parasitology* **28**, 417-426

164. Cruz, K. D., Cruz, T. A., Veras de Moraes, G., Paredes-Santos, T. C., Attias, M., and de Souza, W. (2014) *BioMed research international* **2014**

165. Murphy, S. C., Luisa Hiller, N., Harrison, T., Lomasney, J. W., Mohandas, N., and Haldar, K. (2006) *Molecular membrane biology* **23**, 81-88

166. Winberg, M. E., Holm, Å., Särndahl, E., Vinet, A. F., Descoteaux, A., Magnusson, K.-E., Rasmusson, B., and Lerm, M. (2009) *Microbes and infection* **11**, 215-222

167. Seveau, S., Pizarro-Cerda, J., and Cossart, P. (2007) *Microbes and infection* **9**, 1167-1175

168. Tamilselvam, B., and Daefler, S. (2008) *The Journal of Immunology* **180**, 8262-8271

169. Wang, M., and Hajishengallis, G. (2008) *Cellular microbiology* **10**, 2029-2042

170. Sadikot, R. T. (2012) *Cholesterol Regulation of Ion Channels and Receptors*, 273-280

171. Cuschieri, J., Bulger, E., Billgrin, J., Garcia, I., and Maier, R. V. (2007) *Surgical infections* **8**, 91-106

172. Nelson, L. D., Chiantia, S., and London, E. (2010) *Biophysical journal* **99**, 3255-3263

173. Lin, Q., and London, E. (2013) *Biophysical journal* **105**, 2733-2742

174. Matsuda, S., Kodama, T., Okada, N., Okayama, K., Honda, T., and Iida, T. (2010) *Infection and immunity* **78**, 603-610

175. Sugiyama, H., Kashimoto, T., Ueno, S., Ehara, H., Kodama, T., Iida, T., and Susa, N. (2011) *PLoS One* **6**

176. Abrami, L., and Van Der Goot, F. G. (1999) *The Journal of cell biology* **147**, 175-184

177. Rebolj, K., Ulrih, N. P., Maček, P., and Sepčić, K. (2006) *Biochimica Et Biophysica Acta (BBA)-Biomembranes* **1758**, 1662-1670

178. Schlumberger, S., Kristan, K. Č., Ota, K., Frangež, R., Molgó, J., Sepčić, K., Benoit, E., and Maček, P. (2014) *FEBS letters* **588**, 35-40

179. Kovbasnjuk, O., Edidin, M., and Donowitz, M. (2001) *Journal of Cell Science* **114**, 4025-4031

180. Vandenesch, F., Lina, G., and Henry, T. (2012) *Frontiers in cellular and infection microbiology* **2**, 12

181. Kuo, C.-H., and Wang, W.-C. (2003) *Biochemical and biophysical research communications* **303**, 640-644

182. Sanyal, S. C. (2000) *Journal of the Indian Medical Association* **98**, 371-376

183. Saha, D., Rajendran, K., Ramamurthy, T., Nandy, R., and Bhattacharya, S. (2008) *Epidemiology & Infection* **136**, 661-664

184. Finkelstein, R. A. (1996) Cholera, Vibrio cholerae O1 and O139, and other pathogenic vibrios. in *Medical Microbiology. 4th edition*, University of Texas Medical Branch at Galveston. pp

185. Ebrahimizadeh, W., Gargari, S. M., Rajabibazl, M., Ardekani, L. S., Zare, H., and Bakherad, H. (2013) *Applied microbiology and biotechnology* **97**, 4457-4466

186. Sarkar, A., Nandy, R. K., Nair, G. B., and Ghose, A. C. (2002) *Infection and immunity* **70**, 4735-4742

187. Mukhopadhyay, A. K., Chakraborty, S., Takeda, Y., Nair, G. B., and Berg, D. E. (2001) *Journal of bacteriology* **183**, 4737-4746

188. Fasano, A., Baudry, B., Pumplin, D. W., Wasserman, S. S., Tall, B. D., Ketley, J. M., and Kaper, J. (1991) *Proceedings of the National Academy of Sciences* **88**, 5242-5246

189. Rivera, I., Chowdhury, M., Sanchez, P., Sato, M., Huq, A., Colwell, R., and Martins, M. (1995) *World Journal of Microbiology and Biotechnology* **11**, 572-577

190. Liu, J., Fu, K., Wu, C., Qin, K., Li, F., and Zhou, L. (2018) *Frontiers in cellular and infection microbiology* **8**, 139

191. Beddoe, T., Paton, A. W., Le Nours, J., Rossjohn, J., and Paton, J. C. (2010) *Trends in biochemical sciences* **35**, 411-418

192. Lai, C., Mendez, E., and Chang, D. (1976) *Journal of Infectious Diseases* **133**, S23-S30

193. Feng, Y., Jadhav, A. P., Rodighiero, C., Fujinaga, Y., Kirchhausen, T., and Lencer, W. I. (2004) *EMBO reports* **5**, 596-601

194. Gill, D. M., and Meren, R. (1978) *Proceedings of the National Academy of Sciences* **75**, 3050-3054

195. Häse, C. C., and Mekalanos, J. J. (1999) *Proceedings of the National Academy of Sciences* **96**, 3183-3187

196. Kirn, T. J., Bose, N., and Taylor, R. K. (2003) *Molecular microbiology* **49**, 81-92

197. Attridge, S. R., Manning, P. A., Holmgren, J., and Jonson, G. (1996) *Infection and immunity* **64**, 3369-3373

198. Tacket, C. O., Taylor, R. K., Losonsky, G., Lim, Y., Nataro, J. P., Kaper, J. B., and Levine, M. M. (1998) *Infection and immunity* **66**, 692-695

199. Chiavelli, D. A., Marsh, J. W., and Taylor, R. K. (2001) *Appl. Environ. Microbiol.* **67**, 3220-3225

200. Sheahan, K.-L., Cordero, C. L., and Satchell, K. J. F. (2004) *Proceedings of the National Academy of Sciences* **101**, 9798-9803

201. Lin, W., Fullner, K. J., Clayton, R., Sexton, J. A., Rogers, M. B., Calia, K. E., Calderwood, S. B., Fraser, C., and Mekalanos, J. J. (1999) *Proceedings of the National Academy of Sciences* **96**, 1071-1076

202. Yamamoto, K., Ichinose, Y., Shinagawa, H., Makino, K., Nakata, A., Iwanaga, M., Honda, T., and Miwatani, T. (1990) *Infection and immunity* **58**, 4106-4116

203. Nagamune, K., Yamamoto, K., and Honda, T. (1995) *FEMS microbiology letters* **128**, 265-269

204. McCardell, B. A., Madden, J. M., and Shah, D. B. (1985) *Canadian journal of microbiology* **31**, 711-720

205. Krasilnikov, O. V., Muratkhodjaev, J. N., and Zitzer, A. O. (1992) *Biochimica Et Biophysica Acta (BBA)-Biomembranes* **1111**, 7-16

206. Löhner, S., Walev, I., Boukhallouk, F., Palmer, M., Bhakdi, S., and Valeva, A. (2009) *The FASEB Journal* **23**, 2521-2528

207. Zitzer, A., Wassenaar, T. M., Walev, I., and Bhakdi, S. (1997) *Infection and immunity* **65**, 1293-1298

208. Saka, H. A., Bidinost, C., Sola, C., Carranza, P., Collino, C., Ortiz, S., Echenique, J. R., and Bocco, J. L. (2008) *Microbial pathogenesis* **44**, 118-128

209. Cinar, H. N., Kothary, M., Datta, A. R., Tall, B. D., Sprando, R., Bilecen, K., Yildiz, F., and McCardell, B. (2010) *PLoS One* **5**

210. Paul, K., and Chattopadhyay, K. (2011) *Biochemistry* **50**, 3936-3945

211. Nagamune, K., Yamamoto, K., and Honda, T. (1997) *Journal of Biological Chemistry* **272**, 1338-1343

212. Olson, R., and Gouaux, E. (2005) *Journal of molecular biology* **350**, 997-1016

213. Rai, A. K., and Chattopadhyay, K. (2015) Vibrio cholerae cytolysin: Structure–function mechanism of an atypical β-barrel pore-forming toxin. in *Biochemical Roles of Eukaryotic Cell Surface Macromolecules*, Springer. pp 109-125

214. Debellis, L., Diana, A., Arcidiacono, D., Fiorotto, R., Portincasa, P., Altomare, D. F., Spirli, C., and de Bernard, M. (2009) *PLoS One* **4**

215. He, Y., and Olson, R. (2010) *Journal of structural biology* **169**, 6-13

216. Chattopadhyay, K., and Banerjee, K. K. (2003) *Journal of Biological Chemistry* **278**, 38470-38475

217. Rai, A. K., and Chattopadhyay, K. (2015) *Molecular microbiology* **97**, 1051-1062

218. Rai, A. K., and Chattopadhyay, K. (2016) *Biochemical and biophysical research communications* **474**, 421-427

219. Rai, A. K., and Chattopadhyay, K. (2014) *Journal of Biological Chemistry* **289**, 16978-16987

220. Mondal, A. K., and Chattopadhyay, K. (2019) *Biochemistry*

221. Khilwani, B., and Chattopadhyay, K. (2015) *Toxins* **7**, 3344-3358

222. Paul, K., and Chattopadhyay, K. (2014) *Biochemical and biophysical research communications* **443**, 189-193

223. Sankaranarayanan, R., Sekar, K., Banerjee, R., Sharma, V., Surolia, A., and Vijayan, M. (1996) *Nature structural biology* **3**, 596-603

224. Lee, X., Thompson, A., Zhang, Z., Ton-that, H., Biesterfeldt, J., Ogata, C., Xu, L., Johnston, R. A., and Young, N. M. (1998) *Journal of Biological Chemistry* **273**, 6312-6318

225. Rutenber, E., Ready, M., and Robertus, J. D. (1987) *Nature* **326**, 624-626

226. Levan, S., De, S., and Olson, R. (2013) *Journal of molecular biology* **425**, 944-957

227. Ganguly, S., Mukherjee, A., Mazumdar, B., Ghosh, A. N., and Banerjee, K. K. (2014) *Journal of Biological Chemistry* **289**, 4001-4008

228. Rojko, N., and Anderluh, G. (2015) *Accounts of chemical research* **48**, 3073-3079

229. Abrami, L., Fivaz, M., and Van Der Goot, F. G. (2000) *Trends in microbiology* **8**, 168-172

230. Kathuria, R., and Chattopadhyay, K. (2018) *IUBMB life* **70**, 260-266

231. Pantano, S., and Montecucco, C. (2006) *Toxicon* **47**, 35-40

232. Zitzer, A., Harris, J. R., Kemminer, S. E., Zitzer, O., Bhakdi, S., Muething, J., and Palmer, M. (2000) *Biochimica Et Biophysica Acta (BBA)-Biomembranes* **1509**, 264-274

233. Zitzer, A., Zitzer, O., Bhakdi, S., and Palmer, M. (1999) *Journal of Biological Chemistry* **274**, 1375-1380

234. Chattopadhyay, K., Bhattacharyya, D., and Banerjee, K. K. (2002) *European journal of biochemistry* **269**, 4351-4358

235. Saha, N., and Banerjee, K. K. (1997) *Journal of Biological Chemistry* **272**, 162-167

236. Khilwani, B., Mukhopadhaya, A., and Chattopadhyay, K. (2015) *Biochemical Journal* **466**, 147-161

237. Krasilnikov, O. V., Merzlyak, P. G., Lima, V. L., Zitzer, A. O., Valeva, A., and Yuldasheva, L. N. (2007) *Biochimie* **89**, 271-277

238. Zitzer, A., Westover, E. J., Covey, D. F., and Palmer, M. (2003) *FEBS letters* **553**, 229-231

239. Ikigai, H., Otsuru, H., Yamamoto, K., and Shimamura, T. (2006) *Microbiology and immunology* **50**, 751-757

240. Harris, J. R., Bhakdi, S., Meissner, U., Scheffler, D., Bittman, R., Li, G., Zitzer, A., and Palmer, M. (2002) *Journal of structural biology* **139**, 122-135

241. Paul, K., and Chattopadhyay, K. (2012) *The FEBS journal* **279**, 4039-4051

242. Presti, F. T. (1985) *Membrane fluidity in biology* **4**, 97-145

243. van der Goot, F. G. (2003) Membrane-damaging toxins: Pore formation. in *Bacterial protein toxins*, American Society of Microbiology. pp 189-202

244. Cullis, P. t., and Kruijff, B. d. (1979) *Biochimica et Biophysica Acta (BBA)-Reviews on Biomembranes* **559**, 399-420

245. de Meyer, F., and Smit, B. (2009) *Proceedings of the National Academy of Sciences* **106**, 3654-3658

246. Ramachandran, R., Heuck, A. P., Tweten, R. K., and Johnson, A. E. (2002) *Nature structural biology* **9**, 823-827

Synopsis of PhD Thesis

By Reema Kathuria (MP12013)

Exploring the implication of cholesterol in regulating the pore-formation mechanism of *Vibrio cholerae* cytolysin, a β-barrel pore-forming toxin

Pore-forming toxins (PFTs) are the unique class of protein toxins that inflict cellular injury by generating pores in the target cell membranes. PFTs punch holes in the membrane lipid bilayer, that in turn disrupt the integrity of the cell membranes, allowing free diffusion of ions, water and other solutes across the membranes (1). This ultimately leads to the lysis of the target cells. PFTs are produced by wide array of organisms that include bacteria, fungi, plants and humans. These toxins exhibit unique dimorphic nature as they are produced as water-soluble molecules, while upon binding to the target membranes they adopt trans-membrane structures (2). Structure-based classification categorises PFTs into two distinct groups depending on whether they employ α-helical bundles (α-PFTs) or β-barrels (β-PFTs) to create the membrane pores (3). PFTs act as the potent virulence factors for many pathogenic bacteria, and play crucial roles in the bacterial pathogenesis processes.

Vibrio cholerae cytolysin (VCC) is a β-barrel pore-forming toxin that acts as a potent virulence factor of the cholera pathogen *Vibrio cholerae*, particularly in those strains that lack the major toxin Cholera Toxin. VCC is a prominent member in the β-PFT family that exhibits potent cytolytic and cytotoxic activity (4). VCC is secreted as the ~79 kDa inactive precursor (Pro-VCC). Pro-VCC undergoes proteolytic removal of ~15 kDa N-terminal Pro-domain, liberating the functionally active mature form of the toxin that is capable of generating pores in the target membranes (5). Consistent with the β-PFT mode of action, pore-formation by VCC involves binding of the toxin monomers to the target membranes, generating the

intermediate pre-pore structures (6). Subsequently, membrane-insertion of the pore-forming motif (β-strand pair) from each toxin protomer takes place (7). VCC possesses two additional lectin-like domains that have been implicated in the binding of VCC to cellular membranes, mediated primarily via interaction with the cell-surface glycans (8).

The interaction and binding of VCC to the target membranes is a complex interplay of multiple interactions, acting in a concerted manner. VCC exhibits non-specific association towards membrane lipid bilayer (9). The interactions of VCC with membrane phospholipid head-groups and accessory receptor-like entities also play important roles in the binding process (10). Previous reports have also suggested that the presence of cholesterol in the membranes is critically required for the pore-formation mechanism of VCC (11). Cholesterol has been shown to be essential for the action of some of the other PFTs, such as cholesterol-dependent cytolysins (CDCs) like Perfringolysin O, Listeriolysin and Streptolysin (12). Role of cholesterol in the pore-formation mechanism of CDCs has been studied in detail. However, the implication of the membrane cholesterol in governing the pore-formation mechanism of VCC has remained obscure. Furthermore, whether/how cholesterol regulates the mode of action of VCC against the biomembranes has not been studied. Therefore, in this direction, the present thesis work aims to explore the implications of cholesterol in regulating the pore-formation mechanism of VCC (13). Our major objectives are detailed below.

1. To investigate the implications of membrane cholesterol in the distinct steps of the membrane pore-formation mechanism of VCC.
2. To examine the role of cholesterol-rich microdomains in the biomembranes for the mode of action of VCC.

Results

Pore-forming activity of VCC in the membrane lipid bilayer of artificial lipid vesicles or liposomes having varying levels of membrane cholesterol

We wanted to examine how cholesterol in the target membranes regulates different steps of membrane pore-formation by VCC. For this, we prepared liposomes containing varying levels of cholesterol. We first examined pore-forming activity of VCC in the membrane lipid bilayer of liposomes by measuring release of calcein from the liposomes. Our result suggested gradual increment in the pore-forming activity of VCC with increasing levels of cholesterol in the liposome membranes. This data suggested that the functional pore-formation by VCC in the liposome membranes is critically dependent on the presence of an optimal level of membrane cholesterol.

Binding of the VCC molecules to the liposome membranes would act as the first step during pore-formation mechanism. Therefore, an array of experiments has been employed to assess the binding event of VCC with the liposome membranes having varying level of cholesterol. Pull-down based assay with different liposomes having varying cholesterol content suggests gradual increase in the binding efficacy of VCC with the progressive increase in the membrane cholesterol levels. Moreover, ELISA and Surface Plasmon Resonance-based experiments also confirmed efficient binding of VCC with the liposome membranes having increased cholesterol level, while in the absence of cholesterol in the liposome membranes binding was severely affected. FRET-based assay also suggested that only in the presence of an optimal level of membrane cholesterol, VCC establishes an intimate interaction with the membrane phospholipid head-groups.

Consistent with increased binding efficacy, with increasing level of membrane cholesterol, VCC also exhibited increased propensity to form oligomeric assembly, and

execute insertion of its pore-forming motif in the liposome membranes having optimal level of membrane cholesterol.

All these results suggested that the presence of an optimal level of cholesterol in the membrane lipid bilayer of liposomes is crucial for the pore-formation mechanism, where cholesterol appears to play a critical role in the membrane-binding process of the toxin. In the absence of an optimal level of cholesterol, binding step is abrogated that in turn compromises membrane-damaging pore-forming activity of the toxin.

Interaction of VCC with cholesterol in the absence of the membrane lipid bilayer

VCC is capable of directly interacting with cholesterol in suspension, as well as in the immobilized form, even in the absence of membrane lipid bilayer, as observed in the pull-down assay and lipid dot blot assay, respectively. Results from these assays suggest that VCC exhibits propensity to directly interact with cholesterol. A mutant variant of VCC having Ala425Val mutation has been reported earlier to display abrogated membrane pore-formation presumably due to the compromised cholesterol-dependent membrane interaction mechanism (14). In the present study we found that the Ala425Val mutant did not bind to cholesterol, suggesting critical importance of this site to be the potential cholesterol-binding motif in VCC. Pre-incubating VCC with cholesterol in suspension resulted into complete abrogation of the pore-forming activity of VCC against the erythrocytes. This result suggests that the prior interaction of VCC with cholesterol in suspension possibly competes for the membrane interaction process of the toxin, and blocks subsequent membrane pore-formation process.

Role of cholesterol in the pore-formation mechanism of VCC in the biomembranes

In order to assess the role of cholesterol in the pore-formation mechanism of VCC in the biomembranes, human erythrocytes were subjected to prior treatment with 5 mM methyl β-cyclodextrin that depleted more than ~65% of cholesterol from the erythrocytes membranes. These cholesterol-depleted erythrocytes were tested for the distinct steps of pore-formation by VCC. It was observed that there was no significant decrease in the binding efficacy of VCC to these erythrocytes, as accessory cell-surface interactions might have compensated for the binding process. However, the membrane-bound fraction of VCC was found to remain trapped in the form of non-functional and abortive oligomeric assembly in the cholesterol-depleted erythrocytes membranes, and did not exhibit any pore-forming activity. Therefore, it appears that VCC critically requires optimal level of cholesterol to be present in the target erythrocyte membranes for the functional pore-formation.

Partitioning of VCC into cholesterol-enriched lipid rafts of human erythrocytes

To further explore the implications of membrane cholesterol, we examined whether VCC shows any propensity to associate with the cholesterol-rich membrane micro-domains or lipid raft-like regions in human erythrocytes. For this, erythrocytes membranes were fractionated upon cell lysis by density-gradient ultracentrifugation, and isolated fractions were probed for the positive raft markers such as cholera toxin B-subunit (CtxB) and Flotillin-1, and negative raft marker transferrin receptor. Levels of cholesterol were also estimated in the separated membrane fractions. By employing the dot blot and immunoblot assays, we observed that a prominent fraction of membrane-bound VCC sequestered into the detergent-insoluble, cholesterol-rich lipid raft-like membrane fractions. Confocal-microscopy based co-localization assay also confirmed association of

VCC with the lipid raft-like membrane fractions in human erythrocytes. This assay showed the co-localization of VCC with CtxB, the positive marker of rafts. Depletion of membrane cholesterol with methyl β-cyclodextrin caused disruption of the cholesterol-rich membrane fractions, and altered the distribution of VCC in the detergent-insoluble membrane fractions. Notably, the Ala425Val mutant of VCC, which exhibits compromised cholesterol-dependent pore-formation mechanism, partitioned well into the lipid raft-like membrane micro-domains in human erythrocytes. This observation suggests that the cholesterol-dependent interaction of VCC with the membranes is not possibly the driving force for its partitioning into the cholesterol-rich membrane micro-domains. It is possible that the physicochemical properties of the lipid raft-like membrane micro-domains act to mediate the sequestration of VCC into these regions. Future research in this direction would be required to elucidate the molecular basis of this phenomenon.

Conclusion

Present thesis work has explored the role of cholesterol in regulating the membrane-damaging pore-forming functionality of VCC. VCC is not traditionally classified in the group of cholesterol-dependent cytolysins (CDCs), particularly based on the structural features and mechanism of pore formation. Nevertheless, pore-formation mechanism of VCC is critically dependent on the presence of cholesterol in the target membranes. The present study, for the first time, provides detailed insights regarding how cholesterol regulates some of the distinct steps of the pore-formation mechanism of VCC as a prototype small pore-forming β-PFT.

The results of this study have been published in the **Biochemical Journal**. (13)

Publications during PhD research work

1) **Kathuria R**, Mondal AK, Sharma R, Bhattacharyya S, Chattopadhyay K. Revisiting the role of cholesterol in regulating the pore-formation mechanism of *Vibrio cholerae* cytolysin, a membrane-damaging β-barrel pore-forming toxin. Biochemical Journal. 2018 Oct 15; 475 (19):3039-55.
2) **Kathuria R**, Chattopadhyay K. *Vibrio cholerae* cytolysin: Multiple facets of the membrane interaction mechanism of a β-barrel pore-forming toxin. IUBMB life. 2018 Apr; 70 (4):260-6.

References

1. Dal Peraro, M., and Van Der Goot, F. G. (2016) *Nature reviews microbiology* **14**, 77-92
2. Mondal, A. K., and Chattopadhyay, K. (2019) *Biochemistry* **59**, 163-170
3. Gilbert, R. (2002) *Cellular and Molecular Life Sciences CMLS* **59**, 832-844
4. Khilwani, B., and Chattopadhyay, K. (2015) *Toxins* **7**, 3344-3358
5. Paul, K., and Chattopadhyay, K. (2011) *Biochemistry* **50**, 3936-3945
6. Rai, A. K., and Chattopadhyay, K. (2014) *Journal of Biological Chemistry* **289**, 16978-16987
7. Paul, K., and Chattopadhyay, K. (2014) *Biochemical and Biophysical Research Communications* **443**, 189-193
8. Rai, A. K., Paul, K., and Chattopadhyay, K. (2013) *Journal of Biological Chemistry* **288**, 1665-1673
9. Kathuria, R., and Chattopadhyay, K. (2018) *IUBMB life* **70**, 260-266
10. Rai, A. K., and Chattopadhyay, K. (2015) *Molecular microbiology* **97**, 1051-1062
11. Zitzer, A., Westover, E. J., Covey, D. F., and Palmer, M. (2003) *FEBS letters* **553**, 229-231
12. Rosado, C. J., Kondos, S., Bull, T. E., Kuiper, M. J., Law, R. H., Buckle, A. M., Voskoboinik, I., Bird, P. I., Trapani, J. A., and Whisstock, J. C. (2008) *Cellular microbiology* **10**, 1765-1774

13. Kathuria, R., Mondal, A. K., Sharma, R., Bhattacharyya, S., and Chattopadhyay, K. (2018) *Biochemical Journal* **475**, 3039-3055
14. Paul, K., and Chattopadhyay, K. (2012) *The FEBS Journal* **279**, 4039-4051